Light, Photophobia and Headache: an Investigation of Visually-induced Migraine

Chi-ieong Lau

Nuffield Department of Clinical Neurosciences

Thesis submitted for the degree of
Master of Science by Research in Clinical Neurosciences
University of Oxford

words: 23975

October, 2012

FMRIB Centre
Nuffield Department of Clinical Neurosciences

Abstract

Exacerbation of headache by light is a major symptom in migraine. A recent study unraveled the non-image forming (NIF) visual pathway to be a key component underlying photophobia in migraine. Several lines of evidence also indicate that an altered cortical excitability may render migraineurs more susceptible to attacks, although it is unclear whether the cortex is more or less excitable. Accordingly, this thesis investigated the link between migraine, visual systems and brain responsiveness using three complementary approaches. To begin with, I assessed the response of the NIF visual system to light of different wavelengths in healthy subjects. My results provided the first neuroimaging evidence that the suprachiasmatic nucleus (SCN) of the NIF system displays a sustained response to blue light but not to other wavelengths. This highlights the unique property of the SCN for mediating the circadian cycle, which some investigators have suggested drive the periodicity of migraine attacks.

Next, I examined the interictal cortical sensitivity to light and visual stimuli in migraine. The fMRI results revealed a hypo-excitable response to diffuse illumination in migraineurs compared to healthy controls. The response, however, did not differ when subjects were exposed to a more aversive flickering checkerboard stimulus. Furthermore, the phenomenon appeared to be magnified in a group harboring the TRESK variant, who may be considered an extreme form of the migraine spectrum. This suggests that the initial cortical hypo- excitability may serve as a protective mechanism against further attacks. Surprisingly, I found no disturbance of glutamate, GABA and NAA in the visual cortex of interictal migraine subjects, arguing against the notion that these metabolites may mediate the protective mechanism or predispose the brain to migraine attacks. Finally, I optimized the PCR and prepared a DNA pool of 741 migraineurs and 416 controls for sequencing four candidate genes including TRESK and OPN4. Variants identified in these genes that associate with migraine may provide mechanistic insights into how genetic backgrounds alters neuronal and brain responsiveness and how this in turn increases migraine liability.

Taken together, my studies reveal cortical hypo-excitability in patients with migraine between attacks and established a foundation for future studies including the NIF visual system in migraine. Longitudinal studies will also help unravel compensatory from primary changes in the migraine brain.

Contents

Acknowledgements

First of all, I offer my sincerest gratitude to my supervisors, Dr. Holly Bridge and Dr. Zameel Cader, who gave me an opportunity to work in their research groups and supported me throughout my graduate study. Without their attentive guidance, endless support and tremendous patience, it would not have been possible to accomplish this thesis.

A very special thanks goes to Gregory Weir who provided me lots of technical support and constructive suggestions in my research conducting. Besides, I am grateful to Ms. Katie Morrison who kindly taught me the technique of DNA quantification. I must also acknowledge Bolton Chau and Dr. Ming-Tsung Tseng for their valuable comments on my thesis.

Last but not least, I am deeply appreciative of my beloved family and Ms. Frankie Wing See Tam who have always supported me through difficult times. Without their love and support, I would not have survived the frustration during my graduate program.

Chapter 1

General Introduction

1.1 What is Migraine?

Migraine is an episodic and disabling disease that is characterized by a unilateral pulsating headache that lasts 4 to 72 hours, associated with nausea, vomiting, photophobia and phonophobia (table 1)("The International Classification of Headache Disorders: 2nd edition," 2004). It is a common disease affecting 6% of men and 15 to 17% of women (Stewart, Shechter, & Rasmussen, 1994). Migraine has a tremendous impact both on individual and society. The World Health Organization has ranked migraine among the ten most disabling conditions. It results in sufferers being disrupted from work and social activities, hence reducing productivity and causing major impact on society and economy(Mennini, Gitto, & Martelletti, 2008).

There are two major subtypes – migraine with aura (MwA) and migraine without aura (MwoA). About 30% of migraine patients experience reversible neurological symptoms known as auras that mostly involve the visual system either during or prior to attacks, but can also be in the form of sensory or dysphasic symptoms (Launer, Terwindt, & Ferrari, 1999).

Migraine without Aura

Diagnostic criteria:

A. At least 5 attacks fulfilling criteria B-D

B. Headache attacks lasting 4-72 hours (untreated or unsuccessfully treated)

C. Headache has at least two of the following characteristics:

1. unilateral location
2. pulsating quality
3. moderate or severe pain intensity
4. aggravation by or causing avoidance of routine physical activity (**eg**, walking or climbing stairs)

D. During headache at least one of the following:

1. nausea and/or vomiting
2. photophobia and phonophobia

E. Not attributed to another disorder

Migraine with aura

Diagnostic criteria:

A. At least 2 attacks fulfilling criteria B-D

B. Aura consisting of at least one of the following, but no motor weakness:

a. fully reversible visual symptoms including positive features (**eg**, flickering lights, spots or lines) and/or negative features (**ie**, loss of vision)

b. fully reversible sensory symptoms including positive features (**ie**, pins and needles) and/or negative features (**ie**, numbness)

c. fully reversible dysphasic speech disturbance

C. At least two of the following:

a. homonymous visual symptoms[1] and/or unilateral sensory symptoms

b. at least one aura symptom develops gradually over ≥5 minutes and/or different aura symptoms occur in succession over ≥5 minutes

c. each symptom lasts ≥5 and ≤60 minutes

D. Headache fulfilling criteria B-D for 1.1 **Migraine without aura** begins during the aura or follows aura within 60 minutes

E. Not attributed to another disorder

Table. 1 Diagnostic criteria for migraine with aura and migraine without aura.

International Headache Society (IHS) Classification ICHD-II © 2004.

1.2 Migraine as a disease of sensory dysmodulation

Despite the high prevalence of migraine in general population, its pathogenesis is complex and remains elusive. At present, several lines of evidence suggest that migraine is a disease of sensory dysmodulation – an altered cortical sensitivity rendering migraineurs more susceptible to attacks (Coppola, Pierelli, & Schoenen, 2007) (Coppola, Pierelli, & Schoenen, 2009). This can be reflected in several major aspects of the disease including its abnormal sensitivity to light (photophobia), sound (phonophobia), odor (osmophobia) and pain (aggravation of pain by routine physical activity) both during and between attacks ("The International Classification of Headache Disorders: 2nd edition," 2004).

1.3 Cortical spreading depression

Cortical spreading depression (CSD) was discovered by Leão (Leao, 1947). He reported that a needle stab in the cortex of rabbit initiated a self-propagating neural and glial depolarization at a rate of 2 to 5 mm/min. This phenomenon was followed by a prolonged neuronal inactivity with massive release of excitatory amino acids as well as transient loss of brain ionic homeostasis(Leao, 1944). He also reported that the initial CSD caused a transient dilatation of pial arteries (Leao, 1944) which was followed by a spreading oligemia that persisted after the CSD waves. Although Milner suggested the association between CSD and aura(Milner, 1958), CSD has been induced in laboratory animal models and in human hippocampus cells (Tepper,

Rapoport, & Sheftell, 2001). However, some researchers questioned CSD as the electrophysiological correlate of aura due to the resistance to CSD in the highly convoluted human cortex (Dalkara, Zervas, & Moskowitz, 2006). Nevertheless, with the advent of neuroimaging technology, direct observations of human CSD and aura became possible. For example, by using magnetoencephalography (MEG), Barkley et al. found spontaneous depolarization, suppression of spontaneous cortical activity, and large amplitude waves that were considered as parallels of animal CSD(Barkley et al., 1990). This observation was further supported by another study showing that an initial asymmetrical bilateral hyperoxia was followed by spreading oligemia that originated at the occipital region(Welch, Cao, Aurora, Wiggins, & Vikingstad, 1998). An important study using fMRI and retinotopic maps recorded the ongoing visual aura and provided clear evidence supporting the correlate between CSD and visual aura(Hadjikhani et al., 2001). In this study, five episodes of visual aura were recorded in three MwA subjects. They revealed that the fMRI characteristics corresponding to the aura percept resembled to those of CSD observed in experimental animal models. These included an initial cortical hyperfusion at characteristic velocity and duration, followed by hypoperfusion associated with suppressed stimulus-induced response. Recovery of MR signal slowly to baseline was also accompanied with the recovery of stimulus-induced response. Lastly, the spreading BOLD perturbation did not cross the parieto-occipital gyrus. Collectively, these findings provided strong evidence to support the notion that CSD is the electrophysiological correlate of visual aura(Aurora, 2001). Interestingly, CSD-like changes have also been reported in MwoA (Woods, Iacoboni, & Mazziotta, 1994) and is regarded as the result of CSD generated within clinically silent brain regions(Moskowitz, 2007).

1.4 The non-image forming visual system

The past decade has seen a growing body of evidence that a third class of photoreceptor, the intrinsically photosensitive retinal ganglion cell (ipRGC), mediates the light entrainment of circadian rhythms and other non-image forming functions of the eye. The ipRGC of the non-image forming (NIF) pathway responds to light in the absence of input from rods and cones and achieves activation intrinsically by a unique photopigment known as melanopsin (Fu, Liao, Do, & Yau, 2005). These ipRGCs project primarily to the endogenous circadian pacemaker, the suprachiasmatic nucleus (SCN) (Mai, Bartholomaeus, & Jennissen, 1981) and play a role in other non-image forming functions of the visual system including the photoentrainment of circadian cycle(Panda et al., 2002), sustained pupillary light reflex (Lucas et al., 2003), inhibition of pineal melatonin secretion (Jasser, Hanifin, Rollag, & Brainard, 2006) (table 2). Recently, a ground-breaking study shed light on the relationship between the NIF visual system and migraine(Noseda et al., 2010). This study revealed that the photic signals from the melanopsin-containing ipRGCs converged on the nociceptive signals from the dura at the posterior thalamus, suggesting that the NIF visual system may be implicated in the pathophysiology of the exacerbation of migraine by light (Noseda, et al., 2010) (figure 1).

Pathway	Classical(imaging-forming)	Melanopsin(non-imaging-forming)
Photoreceptor cell	Rods and cones	Intrinsic photosensitive retinal ganglion cells
Photopigment	Rhodopsin, cone opsins	Melanopsin
Light sensitivity	All visible wavelengths	Broad band, most sensitive to blue wavelength
Response to light	Hyperpolarization	Depolarization
Receptive fields	Very small	Very large(photosensitive net)
Properties	Fine spatial resolution	Temporal integration of ambient light(irradiance)
Main target of ganglion cells	LGN	Suprachiasmatic nucleus
	Superior colliculus	Subparaventricular zone
	Olivary pretectal nucleus	Ventrolateral preoptic area
		Intrageniculate leaflet of the LGN
		Olivary pretectal nucleus
Function	Image formation	Entrainment of circadian clock
	Pupillary light reflex(early and transient response)	Light-induced sleep regulation and inhibition of melatonin secretion
		Pupillary light reflex(sustained response)
Involvement in disease	Affected in rod-cone dystrophies	Affected in SAD
	Affected in mitochondrial optic neuropathy	Affected in glaucoma
		Relatively spared in mitochondrial optic neuropathy

Table 2. Differential features between the classical IF visual system and the melanopsin-mediated NIF visual system. LGN: lateral geniculate nucleus; SAD: seasonal affective disorder. Adapted from (Benarroch, 2011).

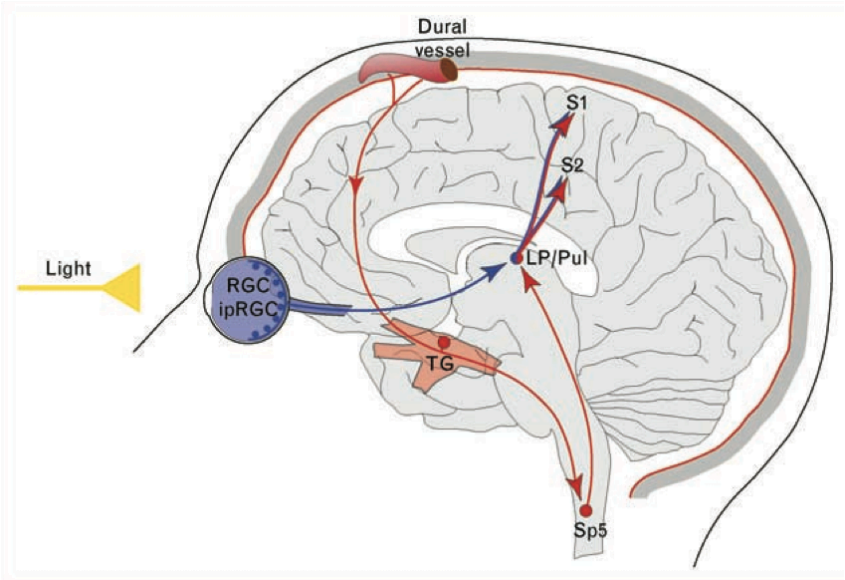

Figure 1. Proposed mechanism for the exacerbation of headache by light. The photic signal from the ipRGCs converge on the dural nonciceptive signals at the thalamus. Red depicts the trigeminovascular pathway. Blue depicts the NIF visual pathway from the retina to the posterior thalamus. ipRGCs, intrinsically photosensitive retinal ganglion cells; LP, lateral posterior nucleus; Pul, pulvinar; RGCs, retinal ganglion cells; S1, primary somatosensory cortex; S2 secondary somatosensory cortex; Sp5, spinal trigeminal nucleus; TG, trigeminal ganglion. Adapted and modified from (Noseda & Burstein, 2011)

1.5 Objectives

Based on the idea that light, the NIF visual system and migraine are closely related to each other, in the following chapters, I investigated the link between them using three complementary approaches. First, since very few studies have managed to investigate the human NIF visual system using functional imaging techniques, I compared the light response of the NIF visual pathway to the image-forming (IF) system at different wavelengths in control subjects. Second, as migraine is a genetically predisposed disease, I investigated the possible genetic variants of four candidate genes that might be implicated in the pathophysiology of migraine, including the melanopsin-encoding OPN4 gene in a large cohort of migraineurs. Finally, I combined both migraine and light to examine the cortical light sensitivity of a group of MwA with visually-induced migraine and a family group of MwA linked to TRESK variant.

My findings showed that the NIF visual system is unique in its sustained response to blue light compared to other wavelengths as well as the IF visual system. Second, MwA subjects exhibited hypo-excitable response to light, suggesting the presence of a compensatory protective mechanism in the interictal visual cortex. This mechanism, however, may not be modulated by the baseline levels of glutamate, gama-aminobutyric acid (GABA) or N-acetylaspartate (NAA). Finally, I optimized the polymerase chain reactions (PCR) and constructed a DNA pool with a large sample of MwA and control for sequencing four candidate genes that may provide insights into the molecular mechanisms of neuronal excitability and the NIF visual system in migraine.

1.6 Reference

Aurora, S. K. (2001). Pathophysiology of migraine headache. *Current pain and headache reports, 5*(2), 179-182.

Barkley, G. L., Tepley, N., Nagel-Leiby, S., Moran, J. E., Simkins, R. T., & Welch, K. M. (1990). Magnetoencephalographic studies of migraine. *Headache, 30*(7), 428-434.

Benarroch, E. E. (2011). The melanopsin system: Phototransduction, projections, functions, and clinical implications. *Neurology, 76*(16), 1422-1427.

Coppola, G., Pierelli, F., & Schoenen, J. (2007). Is the cerebral cortex hyperexcitable or hyperresponsive in migraine? *Cephalalgia : an international journal of headache, 27*(12), 1427-1439.

Coppola, G., Pierelli, F., & Schoenen, J. (2009). Habituation and migraine. *Neurobiology of learning and memory, 92*(2), 249-259.

Dalkara, T., Zervas, N. T., & Moskowitz, M. A. (2006). From spreading depression to the trigeminovascular system. *Neurological sciences : official journal of the Italian Neurological Society and of the Italian Society of Clinical Neurophysiology, 27 Suppl 2*, S86-90.

Fu, Y., Liao, H. W., Do, M. T., & Yau, K. W. (2005). Non-image-forming ocular photoreception in vertebrates. *Current opinion in neurobiology, 15*(4), 415-422.

Hadjikhani, N., Sanchez Del Rio, M., Wu, O., Schwartz, D., Bakker, D., Fischl, B., . . . Moskowitz, M. A. (2001). Mechanisms of migraine aura revealed by functional MRI in human visual cortex. *Proceedings of the National Academy of Sciences of the United States of America, 98*(8), 4687-4692.

The International Classification of Headache Disorders: 2nd edition. (2004). *Cephalalgia : an international journal of headache, 24 Suppl 1*, 9-160.

Jasser, S. A., Hanifin, J. P., Rollag, M. D., & Brainard, G. C. (2006). Dim light adaptation attenuates acute melatonin suppression in humans. *Journal of biological rhythms, 21*(5), 394-404.

Launer, L. J., Terwindt, G. M., & Ferrari, M. D. (1999). The prevalence and characteristics of migraine in a population-based cohort: the GEM study. *Neurology, 53*(3), 537-542.

Leão, A.A. (1944). Spreading depression of activity in cerebral cortex. *Journal of Neurophysiology*, 7, 359–390.

Leao, A. A. (1947). Further observations on the spreading depression of activity in the cerebral cortex. *Journal of neurophysiology, 10*(6), 409-414.

Lucas, R. J., Hattar, S., Takao, M., Berson, D. M., Foster, R. G., & Yau, K. W. (2003). Diminished pupillary light reflex at high irradiances in melanopsin-knockout mice. *Science, 299*(5604), 245-247.

Mai, J. K., Bartholomaeus, I., & Jennissen, J. J. (1981). Evaluation of distribution of retinal afferents within the suprachiasmatic area (ASC): a quantitative approach. *Folia morphologica, 29*(1), 95-99.

Mennini, F. S., Gitto, L., & Martelletti, P. (2008). Improving care through health economics analyses: cost of illness and headache. *The journal of headache and pain, 9*(4), 199-206.

Milner, P. M. (1958). Note on a possible correspondence between the scotomas of migraine and spreading depression of Leao. *Electroencephalography and clinical neurophysiology, 10*(4), 705.

Moskowitz, M. A. (2007). Genes, proteases, cortical spreading depression and migraine: impact on pathophysiology and treatment. *Functional neurology, 22*(3), 133-136.

Noseda, R., & Burstein, R. (2011). Advances in understanding the mechanisms of migraine-type photophobia. *Current opinion in neurology, 24*(3), 197-202.

Noseda, R., Kainz, V., Jakubowski, M., Gooley, J. J., Saper, C. B., Digre, K., & Burstein, R. (2010). A neural mechanism for exacerbation of headache by light. *Nature neuroscience, 13*(2), 239-245.

Panda, S., Sato, T. K., Castrucci, A. M., Rollag, M. D., DeGrip, W. J., Hogenesch, J. B., . . . Kay, S. A. (2002). Melanopsin (Opn4) requirement for normal light-induced circadian phase shifting. *Science, 298*(5601), 2213-2216.

Stewart, W. F., Shechter, A., & Rasmussen, B. K. (1994). Migraine prevalence. A review of population-based studies. *Neurology, 44*(6 Suppl 4), S17-23.

Tepper, S. J., Rapoport, A., & Sheftell, F. (2001). The pathophysiology of migraine. *The neurologist, 7*(5), 279-286.

Welch, K. M., Cao, Y., Aurora, S., Wiggins, G., & Vikingstad, E. M. (1998). MRI of the occipital cortex, red nucleus, and substantia nigra during visual aura of migraine. *Neurology, 51*(5), 1465-1469.

Woods, R. P., Iacoboni, M., & Mazziotta, J. C. (1994). Brief report: bilateral spreading cerebral hypoperfusion during spontaneous migraine headache. *The New England journal of medicine, 331*(25), 1689-1692.

Chapter 2

Non-image Forming Visual System and Migraine

2.1. Introduction

2.1.1 The discovery of melanopsin and the ipRGC

Clyde Keeler discovered in 1927 that blind mice with complete degradation of rod and cone photoreceptors preserved the function of pupillary light responses (Keeler, 1927). Half a century later, a study in the 80s showed that mice response to the shift of light-dark cycles in spite of their outer retinal degeneration mutation (Ebihara & Tsuji, 1980). Since then, a number of studies have demonstrated that animals and patients with loss of rods and cones preserve some NIF functions of the eye such as the photoentrainment of circadian rhythm (Foster et al., 1991) (Czeisler et al., 1995). The discovery of melanopsin by Provencio and his colleagues provide new evidence as to how rodless and coneless blind mice can distinguish day from night (Provencio et al., 2000). This fifth retinal photopigment (also known as OPN4) of human, with one rod and three cone opsins constituting the other four, is an opsin class of G-protein-coupled receptor (GPCR) that is expressed exclusively in 0.2% of retinal ganglion cells in the inner retina (Dacey et al., 2005) (Berson, Dunn, & Takao, 2002). These ipRGCs are referred to as intrinsically photosensitive because they depolarize to light stimulation in the absence of input from rods and cones. Initially they were believed to be a homogeneous group, subsequent work revealed that they are further

classified into 4 subtypes(Tu et al., 2005), figure 1.1. The M1 ipRGCs are characterized by their dendrites in the outer "OFF" lamina of the inner plexiform layer (IPL) of retina (Baver, Pickard, & Sollars, 2008); M2 cells, on the other hand, have dendrites mainly located at the inner lamnia of the IPL. M1 cells project primarily to SCN while M2 cells innervate the olivary pretectal nucleus (OPN) (Baver, et al., 2008). The spectrum of ipRGC subtypes continues to expand with M3, a bistratified type of ipRCs, M4 and a rare type M5 cells recently added to the complexity of the family of ipRGCs (Berson, Castrucci, & Provencio, 2010) (Ecker et al., 2010).

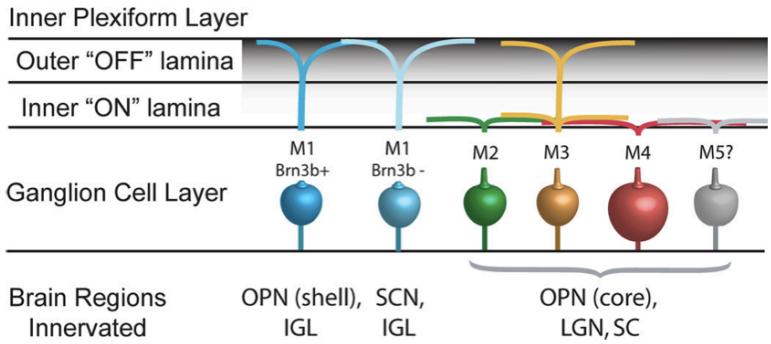

Figure 1.1 ipRGC subtypes. Adapted from (Sexton, Buhr, & Van Gelder, 2012)

2.1.2 Neural innervations of the ipRGCs

The projections of the ipRGCs have been carefully studied and mapped in rodents(Hattar, Liao, Takao, Berson, & Yau, 2002). Unlike the classical IF pathway, the ipRGCs do not project directly to the contralateral brain after crossing the optic chiasma. Instead, ipRGC signals from each eye project primarily and equally to both halves of the SCN(Hatori & Panda, 2010). They also project to other brain regions including the intergeniculate leaflet (IGL) of the lateral geniculate nucleus (LGN), the ventrolateral preoptic area (VPN), subparaventricular zones, the olivary pretectal

nucleus (OPN), habenulla and pineal region. All these structures are responsible for the NIF functions of the visual system (the circadian photoentrainment, the control of pupillary constriction, the regulation of pineal melatonin) as well as other functions related to sleep and behavior (Qu, Dong, Sugioka, & Yamadori, 1996) (Falcon et al., 2009) (Lucas et al., 2003). More recently, projections of the ipRGCs have also been found in the dura-sensitive neurons in the posterior thalamus, suggesting that the NIF visual system may be implicated in the pathophysiology of light-induced migraine (Noseda et al., 2010).

2.1.3 Functions and properties of NIF visual system

As described, the NIF visual system possesses functions that are distinct from the classical IF system. These functions and properties are classified as follow.

2.1.3.1. Photoentrainment of the circadian rhythms

The circadian rhythm is a behavioral, physiological and endocrinological cycle that is governed by the SCN of the anterior hypothalamus(Shibata, Oomura, Kita, & Hattori, 1982). In mammals, the intrinsic periodicity of this pacemaker is close to, but not exactly, 24hours (.Czeisler et al., 1999) (Wright, Hughes, Kronauer, Dijk, & Czeisler, 2001). It is thus crucial to synchronize the intrinsic pacemaker to the environmental dark-light cycle on a daily basis. This circadian photoentrainment in mammals is dependent on a non-rod, non-cone photopigment in the retina. In retinally degenerated mice (*rd/rd*), Foster et al. showed that the magnitude of circadian phase shift caused

by a 15min light pulse was preserved in wild-type controls (Foster, et al., 1991). To determine whether the preserved circadian response was due to surviving cones, the same research group demonstrated that the circadian response to light did not parallel the cone degeneration in aged mice homozygous for retinal degeneration (*rd/rd*)(Provencio, Wong, Lederman, Argamaso, & Foster, 1994). The two studies suggest that there is a non-rod, non-cone retinal photopigment governing the photoentrainment of circadian rhythm. The importance of melanopsin in this role was supported by a number of studies in melanopsin knock-out mice (*Opn4*$^{-/-}$). For example, a marked attenuation in circadian phase resetting caused by a brief pulse of monochromatic light was found in *Opn4*$^{-/-}$ mice compared to wild-type mice (Panda et al., 2002) (Ruby et al., 2002). Further studies revealed that the NIF functions of the retina are not solely supported by melanopsin. *Opn4*-/- mice still retained entrainment to light whereas mice with *Opn4*$^{-/-}$ and *rd/rd* did not (Panda et al., 2003). These studies highlight the contribution of melanopsin in the photoentrainment of the circadian rhythm and indicate that both the visual and non-visual photoreceptors may interplay in this respect.

2.1.3.2 Controlling the pupillary light reflex (PLR)

Despite the fact that both rod and cone photoreceptors are essential for determining the pupil size (Ohba & Alpern, 1972) (Trejo & Cicerone, 1982), PLR is still present in mice with retinal degeneration (Keeler, 1927) (Kovalevsky et al., 1995). Lucas et al. demonstrated that, provided a bright enough stimulus was used, the extent of pupillary constriction in rodless and coneless (*rd/rd cl*) mice was similar to that of wild types (Lucas, Douglas, & Foster, 2001). Further analysis showed that *rd/rd cl*

mice exhibited a significant delay of PLR response compared to wild-type animals. This study opened a new horizon supporting the role of a novel non-rod, non-cone photopigment in PLR. To further address the question of whether the candidate cells, melanopsin-expressing RGCs, are responsible for this function, the same research group retrogradely labeled the RGCs from the SCN in melanopsin-lacking mice and confirmed that the RGCs were not intrinsically photosensitive(Lucas, et al., 2003). In addition, mice lacking melanopsin exhibited a smaller pupil constriction during both the transient and steady phase of the response under a bright monochromatic light when compared to wild-type mice. This discrepancy became indistinguishable under dimmer light, suggesting that melanopsin contributed to PLR only at high irradiances.

The classical and melanopsin photoreceptors are complementary in eliciting PLR. Studies in humans indicate that cones drive the transient phase whereas melanopsin RGCs contribute to the sustained phase of PLR. By varying the excitation of melanopsin-expressing RGCs alone using a novel technique that could stimulate the former independently, Tsujimura et al. demonstrated a significant change in steady-state pupil diameter (Tsujimura, Ukai, Ohama, Nuruki, & Yunokuchi, 2010). The change of pupil diameter under bright steady stimuli contributed by melanopsin-expressing RGCs was three times greater than that of L- and M-cones. The role of ipRGCs in this post-illumination pupil response (PIPR) was further supported by another study showing a significant sustained PIPR in blue light 10 seconds after light offset but not in red light(Kankipati, Girkin, & Gamlin, 2010). Taken together, these studies suggest that classical photoreceptors contribute to PLR under low irradiance of light, whereas melanopsin-expressing ipRGCs is required for sustained pupil constriction at high irradiance.

2.1.3.3 Suppression of pineal melatonin in response to light

Melatonin synthesis occurs in the pineal gland of mammals. Exposure to light reduces synthesis whereas environmental darkness increases the synthesis and secretion of melatonin(Wurtman, Axelrod, & Fischer, 1964). Further studies using transgenic mice (*rd/rd cl*) without rods or cones showed they were capable of suppressing pineal melatonin in response to monochromatic light exposure(Lucas, Freedman, Munoz, Garcia-Fernandez, & Foster, 1999), suggesting that a non-rod, non-cone photoreceptor may be responsible for this function. In humans, studies also showed that the magnitude of melatonin suppression appears to be greatest when exposed to the short wavelength (~460nm) compared to long wavelength (550nm) (Thapan, Arendt, & Skene, 2001) (Lockley, Brainard, & Czeisler, 2003), suggesting that the function of melatonin suppression is mediated by a photopigment distinctive to the three-cones in the IF visual system.

2.1.3.4 Spectral sensitivity of rods, cones and ipRGCs

The peak light sensitivities of human rods, S cones, M cones and L cones are ~500nm, ~420nm, ~530nm and ~560nm respectively(Hatori & Panda, 2010). In contrast to rods and cones, a substantial number of studies, both in animals and human, demonstrated that melanopsin has a distinct maximum spectral sensitivity at 460 to 480nm which lies in the blue range of the visible light, figure 1.2, table 1.1.

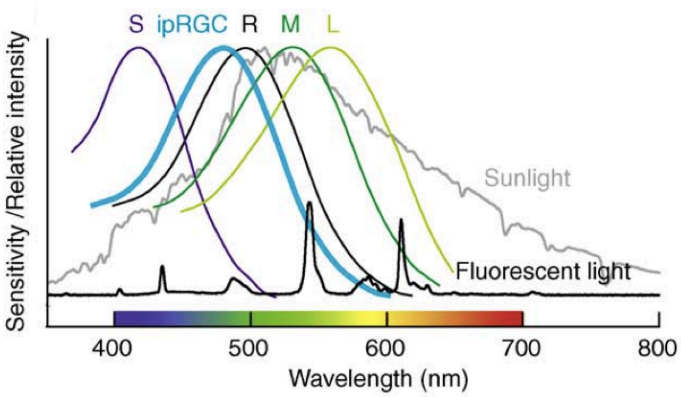

Figure 1.2 Spectral sensitivity of rods, cones and ipRGCs. Adapted from Dacey et al. 2005

Species	Measure	λ_{max}
Mouse *rd cl*	Pupillometry	479 nm
Mouse *rd cl*	Circadian phase shifting	481 nm
Rat WT	pRGC light response	484 nm
Macaque	pRGC light response	482 nm
Macaque	Pupillometry	482 nm
Human	Melatonin suppression	446–477 nm
Human	Melatonin suppression	459 nm
Human	Regulation of cone electroretinogram	483 nm
Human	Heterologous expression	420–440 nm
Mouse	Heterologous expression	420 nm
Mouse	Heterologous expression	479 nm
Mouse	Heterologous expression	480 nm

Table 1.1. Maximum spectral sensitivity for various irradiance detection tasks reported in various species. Adapted from (Hankins, Peirson, & Foster, 2008)

In hamster, the maximum spectral sensitivity responsible for circadian phase shift caused by a 15min pulse of monochromatic light lies near 500nm(Takahashi, DeCoursey, Bauman, & Menaker, 1984). In mice lacking rods and cones, Lucas et al. demonstrated the preservation of pupillary light reflex with a peak sensitivity of response around 479nm(Lucas, et al., 2001). Dacey et al. measured the peak depolarization of macaque giant ganglion cells as a function of wavelength over an illuminance range and revealed a peak at 482nm distinctive from that of rods and cones(Dacey, et al., 2005). In human, Thapan et al. compared the magnitudes of plasma melatonin suppression in 30min pulses of different wavelengths and irradiances of monochromatic light exposure(Thapan, et al., 2001). They found that

an opsin with peak sensitivity around 459nm was most likely to be involved in light-induced melatonin suppression. The degree of melatonin suppression of each wavelength was also irradiance dependent. Another study in human demonstrated higher level of both circadian shift and melatonin suppression induced by 460nm monochromatic light compared to 555nm monochromatic light (Lockley, et al., 2003). Two studies, however, found a peak between 420 and 440nm, suggesting the absolute values may vary according to various experiment environment and cell status. (Newman, Walker, Brown, Cronin, & Robinson, 2003) (Melyan, Tarttelin, Bellingham, Lucas, & Hankins, 2005). Collectively, these studies support the idea of a unique photopigment, presumably melanopsin, which mediates circadian resetting, pupillary reflex response and melatonin suppression has a peak spectral sensitivity at short-wavelength ~480nm.

2.1.4 Light and dark adaptation in the image-forming visual system

Our visual system detects a wide spectrum of light intensity covering over 10 orders of magnitudes. At any time, however, only 2 log unit range of light intensity can be perceived by the human eye. This range can shift upward by light adaptation and downward by dark adaptation to accommodate to the environmental light (Rushton, 1958) . The control of light intensity via adaptation in the classic visual system occurs at multiple levels including the pupils, rods and cones, thalamus, the SCN and the visual cortex, with the photoreceptors at retina contribute most significantly to this phenomenon.

Adaptation of the IF visual system involves many complicated mechanisms and can be categorized into two phenomena, the dark and the light adaptation. Dark adaptation describes the regain of sensitivity to light after returning to darkness from prolonged light exposure(Hecht, 1920). This can be achieved partly by the complementary roles of rods and cones with rods increasing their sensitivity rapidly in the initial 5 minutes and cones after 5 to 10 minutes of light deprivation (Pirenne, 1962). Conversely, light adaptation refers to the gradual reduction of sensitivity of rods and cones upon steady background illumination such that previously saturated photoreceptors regain their ability to response to further increase of light intensity(Fain, Matthews, Cornwall, & Koutalos, 2001). This is presumably due to the bleaching of rod and cone photopigments upon prolonged illumination. As a result, less photopigments are available and generate diminished response to higher intensity of illumination (Cornsweet, 1970). Meanwhile, a decrease of intracellular Ca^{2+} causes a desensitization of the photoreceptors via the modulation of the transduction cascade(Fain, et al., 2001). Adaptation also takes place by means of inhibitory feedback on the photoreceptors from the horizontal cells when they experience a strong and prolonged illumination (Dowling, 1967)

2.1.5 Purpose of the current study

The IF visual system protects its rods and cones from damage upon prolonged illumination by gradually reducing their responsiveness via light adaptation(Rushton, 1958). The NIF visual system, by contrast, needs to maintain a constant responsiveness to light in order to photoentrain the circadian rhythm and to suppress melatonin across the long scale of environmental daylight exposure. Besides, sustained activity of the NIF system is also required for the PIPR(Kankipati, et al., 2010).

Indeed, a substantial number of studies demonstrated that the melanopsin-containing ipRGCs-mediated NIF visual system does not follow the type of light adaptation in the IF system(Berson, et al., 2002) (Warren, Allen, Brown, & Robinson, 2003) (Dacey, et al., 2005). Instead, they are more resistant to prolonged illumination and display a sustained level of photoresponsiveness. This distinct and functional important physiological property of the NIF has, nonetheless, not yet been studied *in vivo.* Although a previous study attempted to investigate the response of the SCN to visual stimuli, they focused on the diurnal signal changes and did not explore this unique property (Vimal et al., 2009). Moreover, investigating this aspect would potentially add value to the recent understanding of the implication of the NIF visual system in light-induced migraine(Noseda, et al., 2010). Therefore, I conducted an fMRI study to compare the light adaptation of the IF and NIF visual systems. I hypothesized that the blue-light induced signal at the SCN would exhibit a distinct pattern of light adaptation compared to other color of light and the response at the primary visual cortex.

2.2 Methods

2.2.1 Subject, ethical approval and informed consent

Thirteen healthy female subjects, aged 20 to 38, without history of migraine or neurological diseases participated in this study. The study has been reviewed and approved by the Staffordshire Research Ethics Committee (11/WM/0088). All subjects gave their written informed consent and were informed of the potential adverse effects of the scans before the scan.

2.2.2 Experimental design, pre-study requirements and preparations

Each study lasted about an hour and was scanned at approximately the same period of time of day, i.e. 14:00 to 18:00. This allowed us to match the fluctuations of cerebral metabolites within a day due to the oscillatory and rhythmical characteristics of the SCN(Reppert & Weaver, 2002). The experiment consisted of 5 individual scans performed sequentially with exposure to 3 different wavelengths of light as shown in figure 2.1. The first 9 subjects received the order of presentation of stimuli in figure 2.2A whereas the remaining 4 subjects were presented to a new order of presentation (figure 2.2B). The new order was scheduled such that one of the blue-lights was not pre-exposed by any other stimulation. Each scan was 9min in total including 3 light-on (60sec each) alternating with 3 light-off periods (120sec each) in an off-on-off pattern, figure 2.3. Light adaptation was defined as the % BOLD change of the initial 30s (light onset) minus that of the remaining 90s (adaptation).

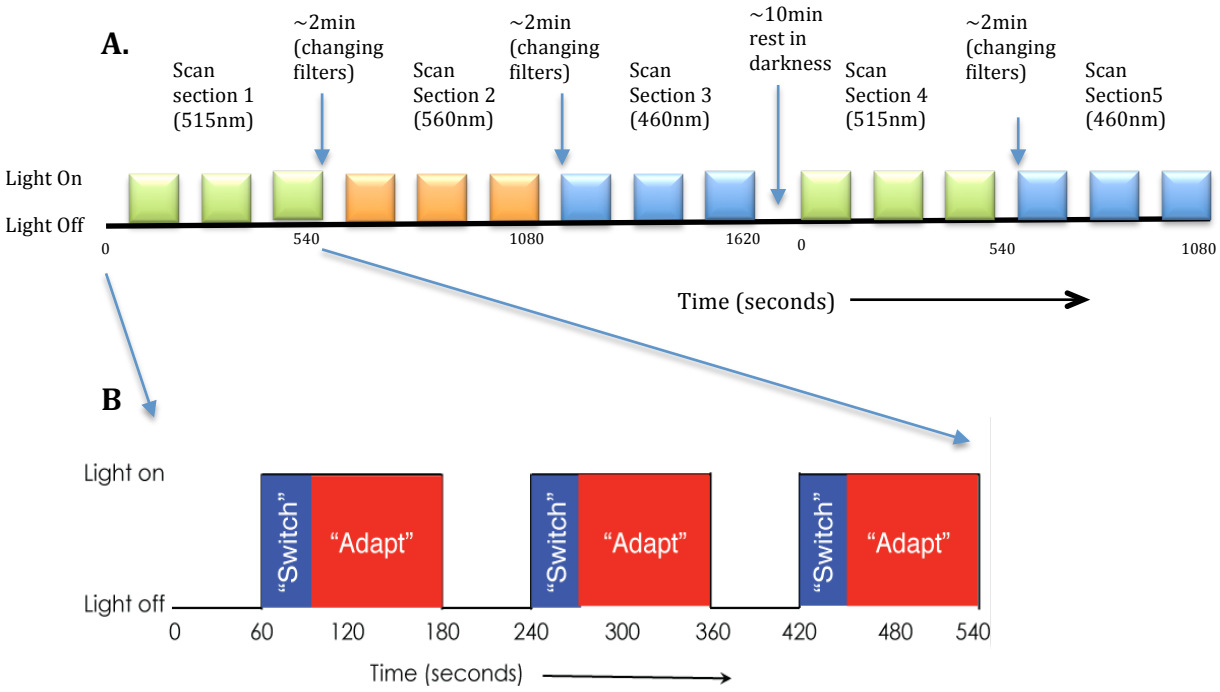

Figure 2.1. A. Model for the entire experiment protocol. B. Example model for one section (colour) of the experiment protocol

A. Stimulus order 1

subject						
1	Green	Yellow	Blue		Green	Blue
2	Green	Yellow	Blue		Green	Blue
3	Green	Yellow	Blue		Green	Blue
4	Green	Yellow	Blue		Green	Blue
5	Green	Yellow	Blue		Green	Blue
6	Green	Yellow	Blue		Green	Blue
7	Green	Yellow	Blue		Green	Blue
8	Green	Yellow	Blue		Green	Blue
9	Green	Yellow	Blue		Green	Blue

B. Stimulus order 2

subject						
10	Blue	Yellow		Green	Blue	Green
11	Blue	Yellow		Green	Blue	Green
12	Blue	Yellow		Green	Blue	Green
13	Blue	Yellow		Green	Blue	Green

Figure 2.2. A. Order of presentation of wavelengths (color) in the stimulus order 1 (subject 1 to 9). B. Modified order in the stimulus order 2 (subjects 10 to 13).

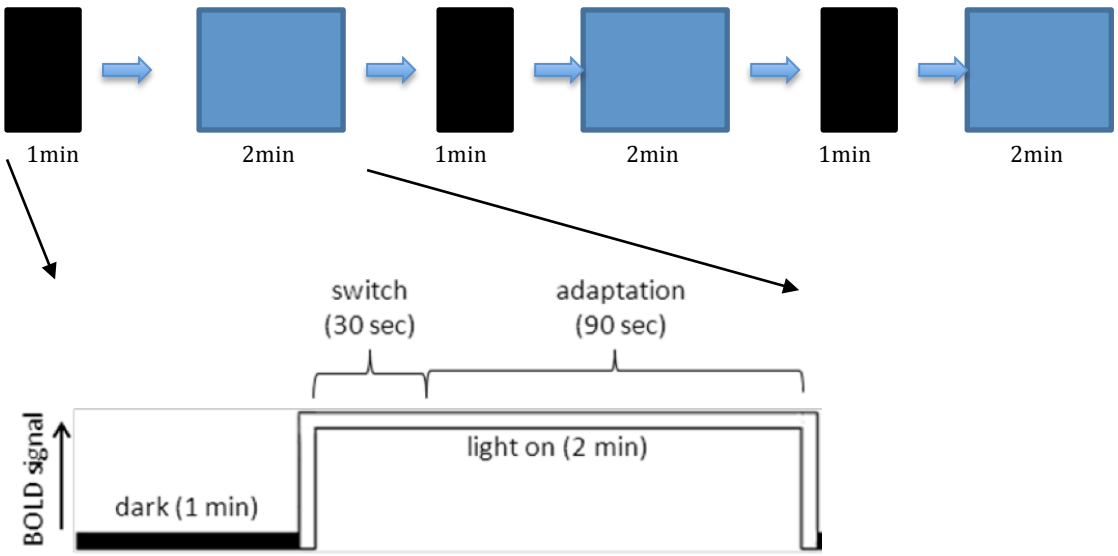

Figure 2.3. Model for one (blue as an example) of the five successive scans. 1-min black screens were alternated with 2-min blue stimuli. Light adaptation is defined as the % BOLD change of the initial 30s (light onset) minus that of the remaining 90s (adaptation).

2.2.3 Protocol Programming and Presentation of Stimuli

The ON/OFF visual stimuli of the experiment was programmed and run by the software *Presentation 2.0* (Neurobehavioral Systems, Inc). A Sony VPL-ES2 projector displayed the program output to an MRI-compatible screen 200cm away from the projector lamp. The three different wavelengths of monochromatic light, namely green (515nm), yellow (560nm) and blue (460nm), were generated by attaching different monochromatic filters to a filter holder in front of the projector lamp. The subjects viewed the visual stimuli on the screen via a mirror on the head coil.

2.2.4 MR imaging acquisition

A Siemens MAGNETOM Tim Trio whole-body 3T scanner (Erlangen, Germany) with a 32-channel head coil was used for image acquisition. All scans were performed at the University of Oxford Centre for Clinical Magnetic Resonance Research (OCMR). Anatomical images were acquired using a T1-weighted sequence (MPRAGE) with isotropic voxels (voxel size 1 x 1 x 1mm^3, repetition time [TR] = 2040ms, echo time[TE] = 4.68ms, field of view[FOV] = 192mm, a slice thickness of 1mm, matrix 192 x 192, 192 slices).

Each fMRI scan consisted of 180 whole-head T2-weighted echo planar images (EPI) acquired at a voxel size of 3.0 x 3.0 x 2.5 mm^3 (TR = 3000ms, TE = 30ms, 44 slices, a thickness of 2.5mm, a flip angle of 90°). Total time for each scan was 9 minute. Filters for generating different monochromatic lights were changed in between the scans and this allowed a ~2min of eye rest between scans.

Subjects were instructed to remain alert, keep their eyes opened and fixated onto the projector screen. Subject head motion was minimized using small cushions either side of the head.

2.2.5 Data Analysis

2.2.5.1 Functional analysis

Pre-processing steps

All fMRI data analysis were carried out using FMRIB Software Library (FSL), version 6.00 (www.fmrib.ox.ac.uk/fsl/). The pre-processing of each subject data consisted of skull stripping with the Brain Extraction Tool (BET) (Smith, 2002) and motion correction using MCFLIRT (Jenkinson & Smith, 2001). Data were spatially smoothed with a 5mm full-width, half maximal 3D Gaussian kernel. A non-linear high-pass filtering was applied and each time series was prewhitened using FILM (FMRIB's Improved Linear Model).

First-level fMRI analysis

First-level fMRI analysis of individual subject data was performed using FEAT (FMRI Expert Analysis Tool) version 6.00. Registration of the data was performed following a 2-stage process. First the initial EPI (echo planar imaging) images were registered to each subject's own T1-weighted structural images using FLIRT (FMRIB's Linear Image Registration Tool). Then the intermediate structural images were registered to the standard space (the Montreal Neurological Institute [MNI] 152 2mm brain). The contrasts used for analysis included the "light onset" which represented the first 30seconds of light exposure compared to baseline, the "constant light" which referred to the last 90seconds of light exposure compared to baseline and the comparisons of activations between the "light onset" and "constant light" periods,

i.e. light onset – constant light and constant light – light onset. Images were threshold using clusters determined by $Z > 2.3$ with a corrected cluster significance threshold of $p = 0.05$.

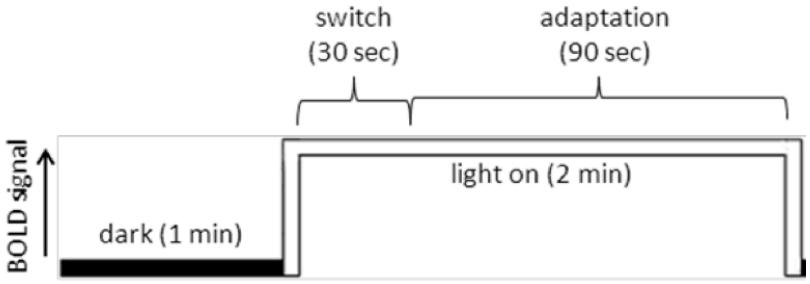

Figure 2.4. Contrasts defined for first-level fMRI analysis. "Light onset" was defined as the activation during the first 30sec of the light-on period subtracting the baseline (darkness). "Adaptation" referred to the activation of the last 90sec of the light-on period compared to baseline. "Light adaptation" is defined as "light onset – adaptation".

2.2.5.2 Localization and creation of the mask (ROI) including the SCN and surrounding anterior hypothalamic region – SCN$^+$

The SCN was localized anatomically on the standard MNI images according to the atlas (Carpenter, 1983; Atlas of the Human Brain, second edition, 2003). It is a cluster of neurons measured about 1.1mm X 1.7mm X 1.1mm (~2mm^3) in size located on either side of the midline of the brain (Vimal, et al., 2009). Using FSLVIEW of FSL, a mask (ROI, Region of interest) of the SCN was carefully drawn according to the following. In coronal section, it lies at the midline adjacent to the third ventricle and superior to the optic chiasm(Mai, Kedziora, Teckhaus, & Sofroniew, 1991). In sagittal section, it is located superiorly and anteriorly to the optic chiasm. Since BOLD change indicates the difference in signal on T2*-weighted images as a function of the amount of deoxygenated hemoglobin (Huettel et al. 2008), I included the adjacent anterior hypothalamic structures in my ROI to reflect the regions of blood supply

during SCN activation(figure 2.5). As a result, the SCN ROI of my study is the summation of SCN as well as surrounding anterior hypothalamic areas (SCN^{+}).

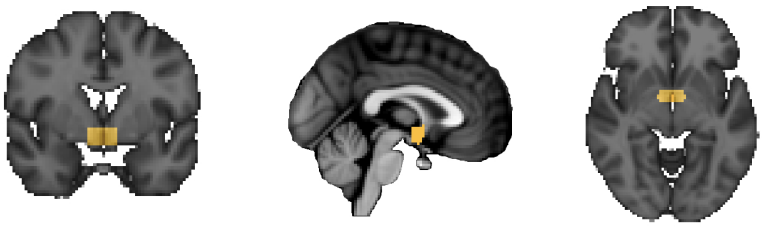

Figure 2.5. SCN^{+} mask (ROI). A. coronal view B. sagittal view C. axial view

2.2.5.3 Calculation of %BOLD change within the visual cortices and the SCN^{+}

Featquery, a tool of FEAT, was used to calculate the mean % signal change associated with my modeled experimental paradigm within the visual cortices. I used the standard space mask "GM visual cortex V1 BA17" in the Juelich Histological Atlas for the left and right visual cortices (figure 2.6) and ran Featquery to obtain the mean % signal changes of (1) light onset, (2) constant light and (3) light onset – constant light within that areas.

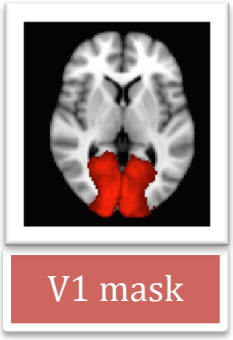

Figure 2.6. Mask of the primary visual cortex V1 (combined left and right) in the Juelich Histological Atlas of Featquery.

The mask image of the SCN^+ created in 2.9.1 was transformed into the space of each individual subject using FLIRT (FMRIB's Linear Image Registration Tool).
The mean % signal change within the SCN^+ areas was then calculated with the transformed mask using Featquery as described above.

2.2.6 Statistical analysis

I used SPSS version 20 to perform the Statistical analysis. Analyses of variance (ANOVA) were used to compare the means of the differences (light onset – constant light) of %BOLD change between the three wavelengths of light. Post-hoc t-statistics was performed. Statistical significance refers to a two-tailed p-value < 0.05.

2.3 Results

2.3.1 Signal activations at V1 of individual and group

An example of the first-level analysis of a subject (no. 2) reveals a higher level of BOLD signal at V1 in the initial “light onset” than the “constant light”, regardless of the color of light presented (figure 3.1).

Figure 3.2 demonstrates the group signal activations at V1. Similar to the findings at individual level, the higher-level analysis showed stronger percentage BOLD signal changes at V1 in the “light onset” than the “constant light” period, across the three different colors, suggesting the presence of light adaptation.

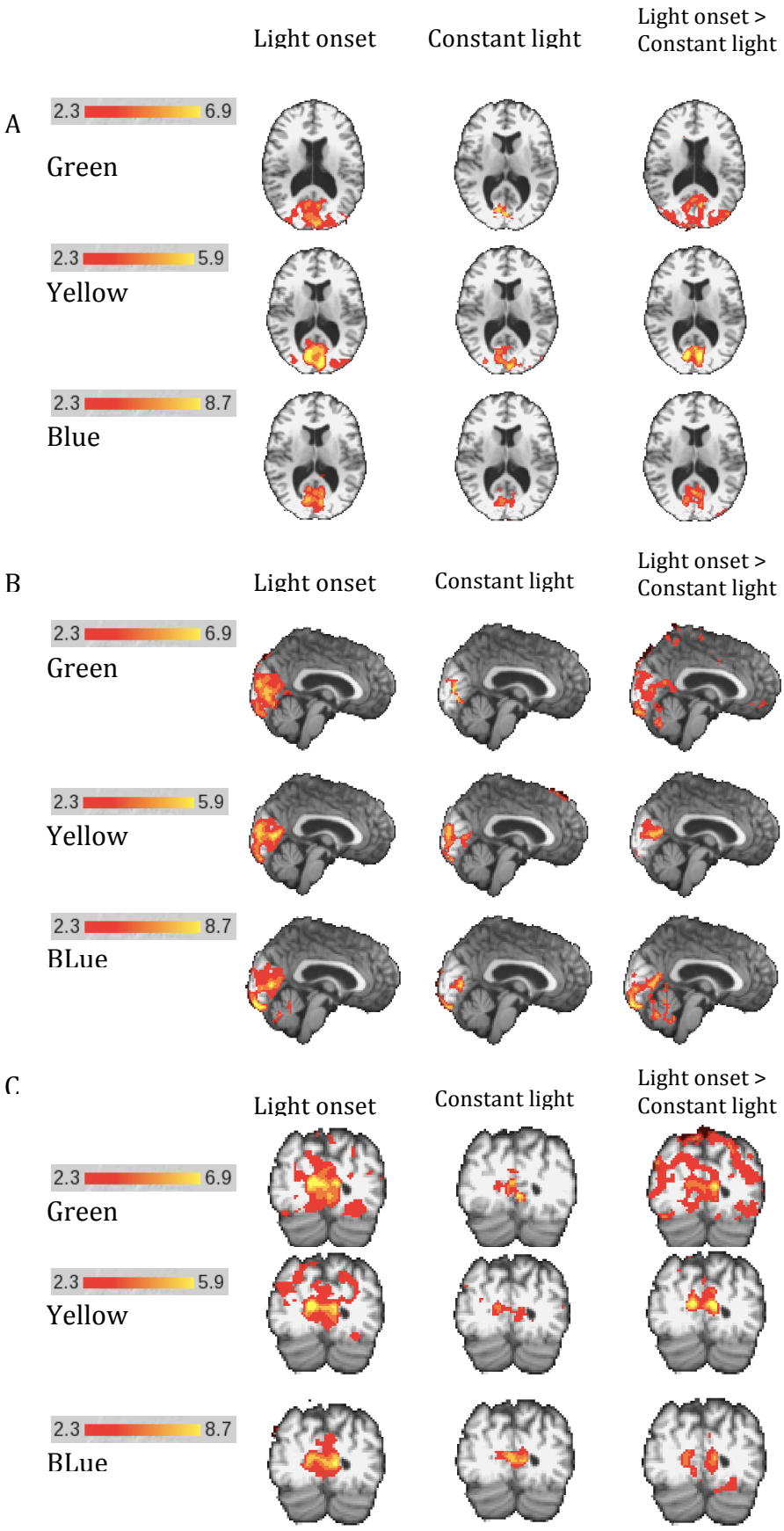

Figure 3.1 Example of individual (subject 2) percentage BOLD change at V1 in response to different wavelengths of light. A. axial view B. sagittal view C. coronal view . Images showing higher occipital signals at Light onset compared to Constant light across three wavelengths of light. Images were threshold using clusters determined by $Z > 2.3$ with a corrected cluster significance threshold of $p = 0.05$.

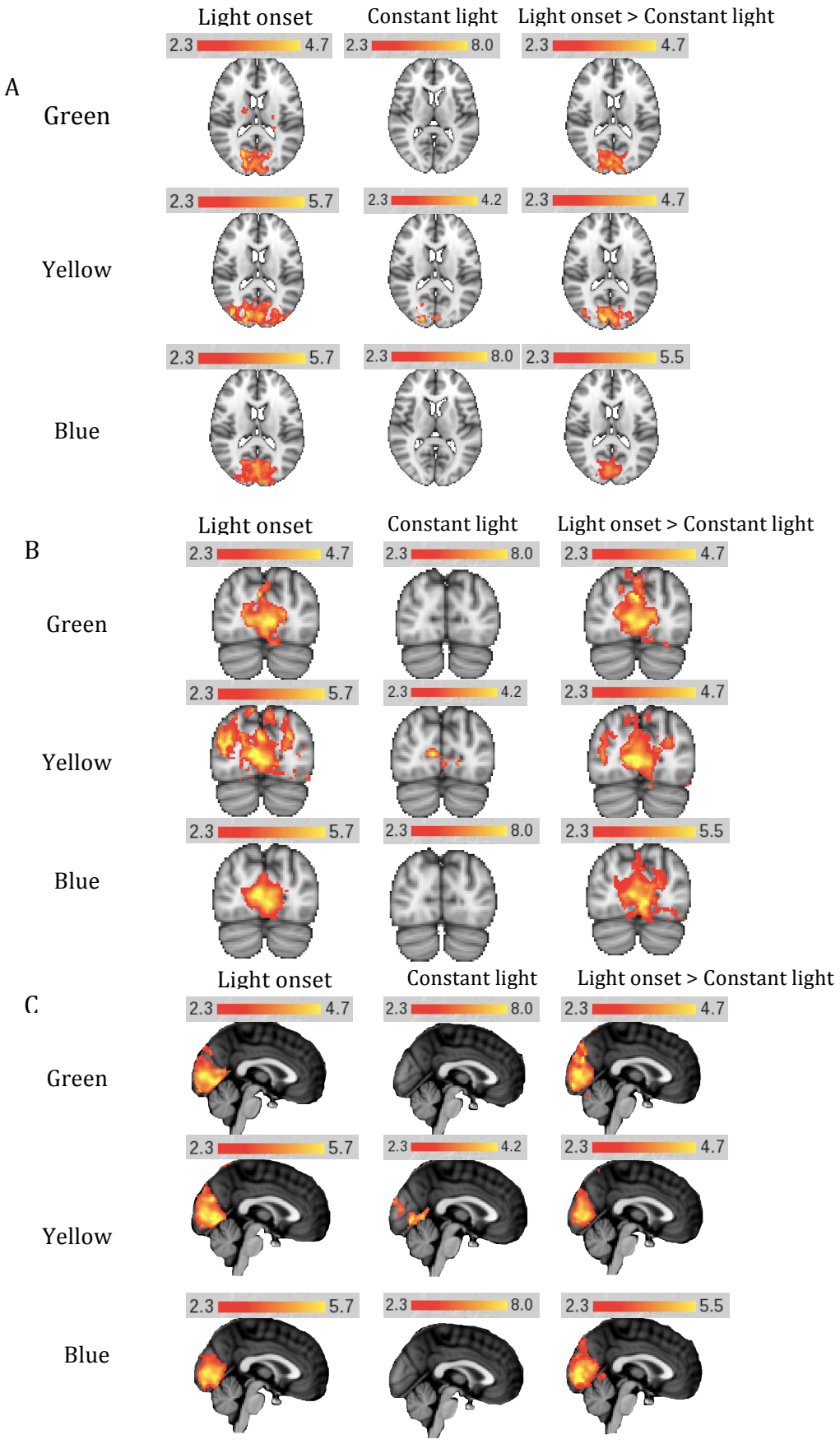

Figure 3.2 Group (n = 13) percentage BOLD change at V1 in response to different wavelengths of light. A. axial view B. coronal view C. sagittal view. Images showing higher occipital signals at Light onset compared to Constant light across three wavelengths of light. Images were threshold using clusters determined by $Z > 2.3$ with a corrected cluster significance threshold of $p = 0.05$.

2.3.2 Quantitative comparison of signal responses between different wavelengths at V1 and SCN^+

Since the SCN+ region is small, it is not suited to whole brain analysis. I applied the SCN+ mask in each subject and extracted the %BOLD change individually to avoid the possibility of non-overlapping of masks due to misregistrations.

Figure 3.3 shows the quantitative analysis of all 13subjects in both orders of stimulation. When comparing the percentage of BOLD change between the initial 30sec "light onset" and the remaining 90sec "constant light" of the light-on period at V1 (figure 3.3B), there was a decline in signal, i.e. "light onset" greater than "constant light", in all wavelengths of light. This indicates that the responses to illumination at the visual cortices declined along the steady light-on period, suggesting the presence of habituation or adaptation to response at V1, regardless of the wavelength of light (460, 515 or 560nm).

Surprisingly, comparing the "light onset" and "constant light" periods at the SCN^+ revealed inconsistent trends among the three wavelengths (figure 3.3A). For longer wavelengths, i.e. green (515nm) and yellow (560nm), the percentages of BOLD change during the light onset period were greater than that of the constant light period, indicating that the same adaptation occurred in the SCN^+ as in V1. However, the most striking finding to emerge from my data is that the shorter wavelength, blue light (460nm), evoked an opposite trend. The signal response did not decline in the latter constant light period but appeared to exhibit an even stronger response.

A one-way between-subject ANOVA was conducted to compare the effect of color (wavelength) on the magnitude of light adaptation(light onset – constant light) at SCN+. Although there was a trend showing that blue-light displayed a lower level of light adaptation, there was no significant effect of color on the magnitude of light adaptation [$F(4, 40) = 1.66$, $p = 0.178$].

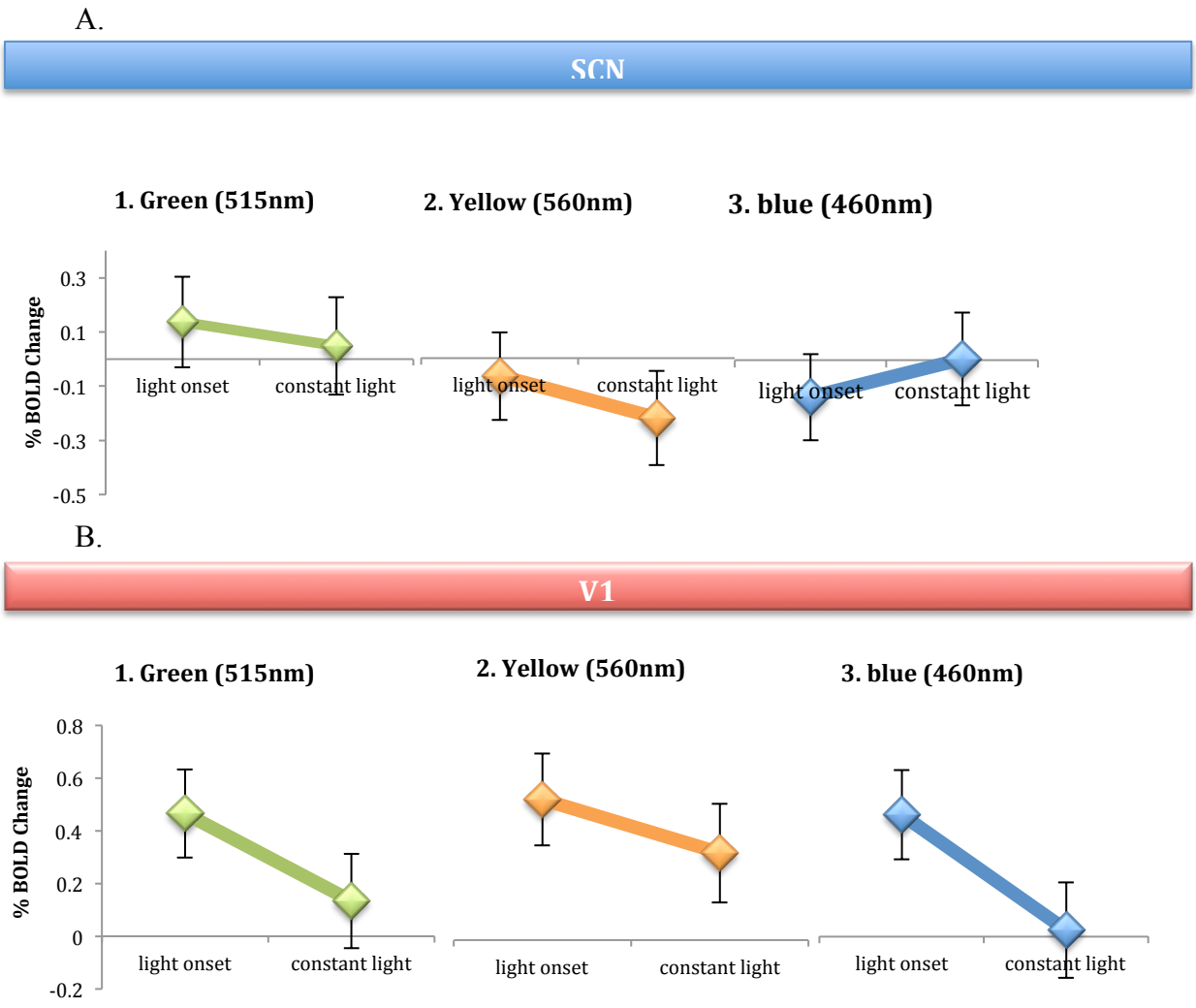

Figure 3.3. Overall results in both orders of stimulation. Signals are shown in percentage of BOLD change (mean ± s.e.m.) averaged across both presentations and all subjects in both orders of stimulation (n = 13). A. SCN+. Both green and yellow light evoked declining responses towards continuous illumination. Only blue light-evoked response showed the opposite trend. B. V1. All wavelengths of light elicited higher responses at light onset compared to that at constant light period.

2.3.3 Effect of stimulus order

Figure 3.4 shows the results of the stimulus order 1 as well as the stimulus order 2. For stimulus order 2, another 4 healthy female subjects received the same experimental protocol but with a new order of stimulus presentation.

Regardless of the order of stimulus presentation, the responses to light at V1 generally decline along continuous illumination in both studies. The responses at the SCN+ in the stimulus order 2 were also similar to that of the stimulus order 1, i.e. yellow and green light evoked stronger responses in “light onset” than “constant light”, whereas blue-light elicited stronger signals in the latter “constant light” than “light onset” periods. Nevertheless, the second green-light exhibited an opposite trend of response compared to the first green-light and was inconsistent to the stimulus order 1.

A. Stimulus order 1 (n =9)

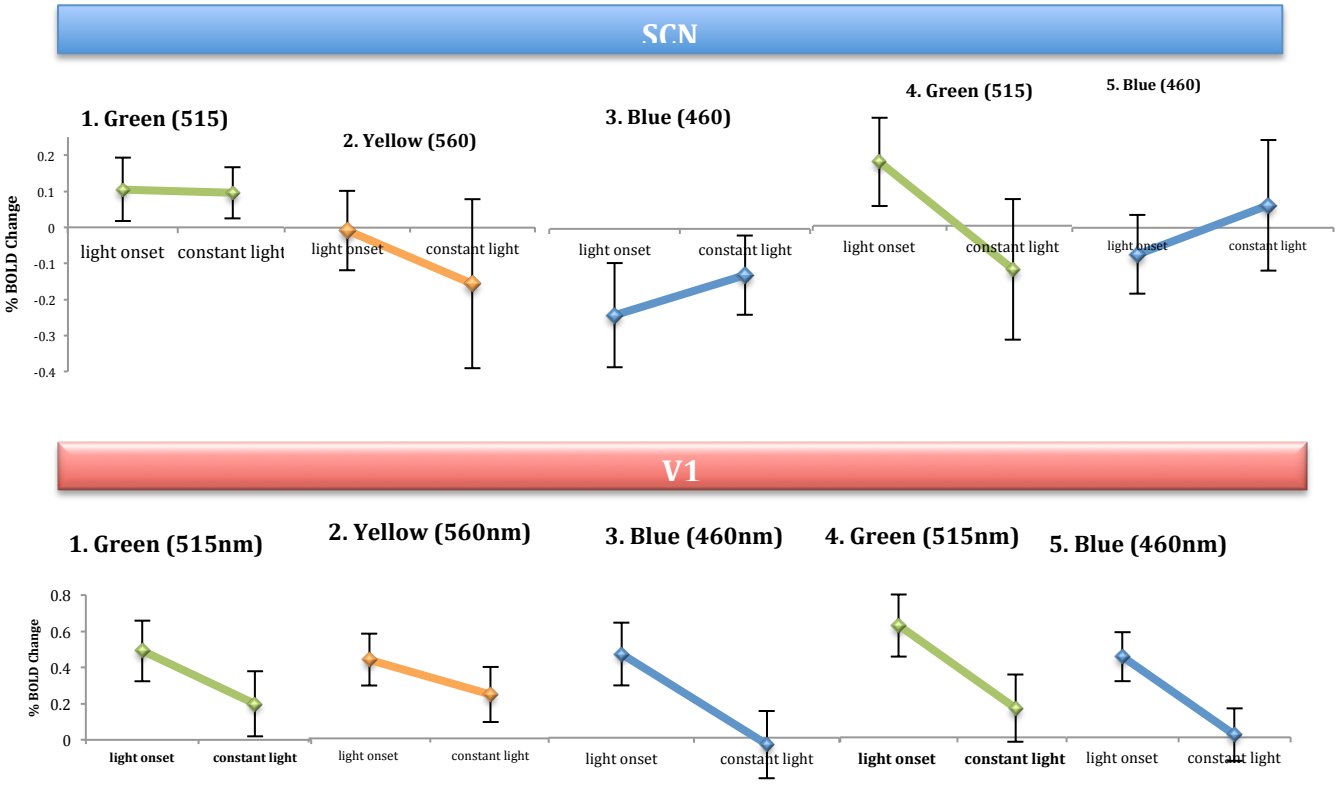

B. Stimulus order 2 (n = 4)

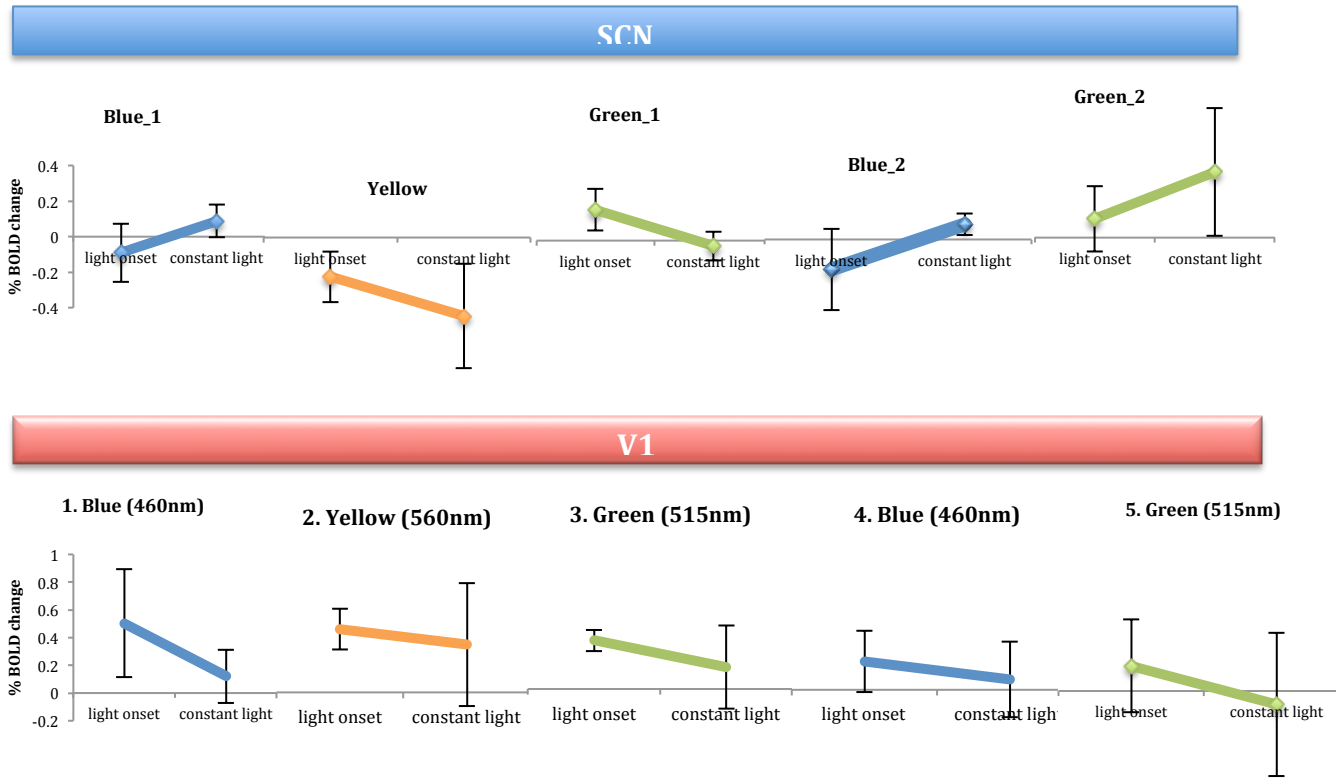

Figure 3.4. Effect of stimulus order. **A**. Stimulus order 1. At V1, all wavelengths of light elicited higher responses at onset of light than constant light. At SCN+, green and yellow followed the same pattern of signal changes at V1 except for blue which evoked an opposite trend. **B.** Stimulus order 2. Another four subjects (no. 10, 11, 12 and 13) received the same scans with the new order of stimulus presentation (Green/Yellow/Blue/Green/Blue). All trends of signal changes were similar to that of the stimulus order 1. Only the second green light evoked a different pattern at SCN+. Signals are shown as mean percentage of BOLD change with error bars representing s.e.m.

Figure 3.5 shows the difference of % BOLD signal change between "light onset" and "constant light" at the SCN+ and V1. Presumably, this difference in signal (light onset – constant light) reflects the magnitude of light adaptation towards prolonged constant light exposure. At V1, all wavelengths of light exhibited "positive" light adaptation, i.e. light onset > constant light(figure 3.5A). At the SCN+, positive light adaptation only exists in green and yellow but not in blue (figure 3.5B). Although t test showed significant difference between blue and green ($t = 2.37$, $df = 4$, $p = 0.026$) at SCN+ , ANOVA revealed no significant effect of color (wavelength) on the magnitude of light adaptation (light onset-constant light) [$F(2, 36) = 2.423$, $p = 0.103$].

A.

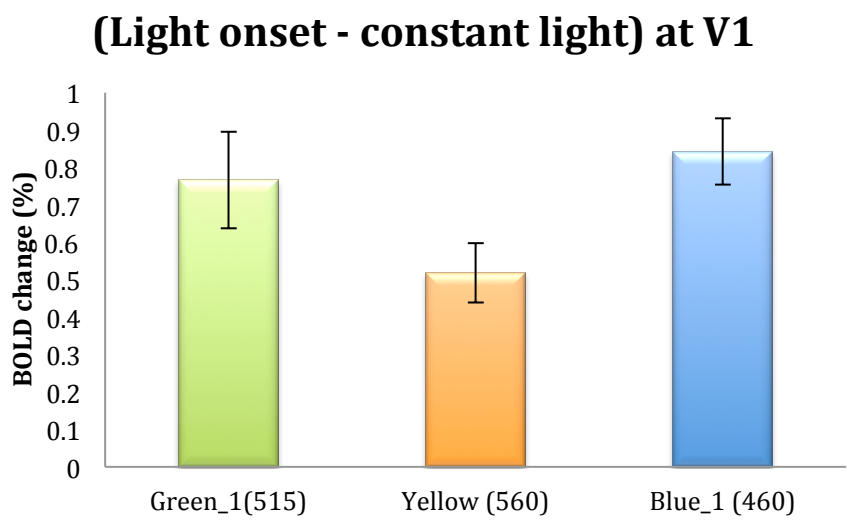

B.

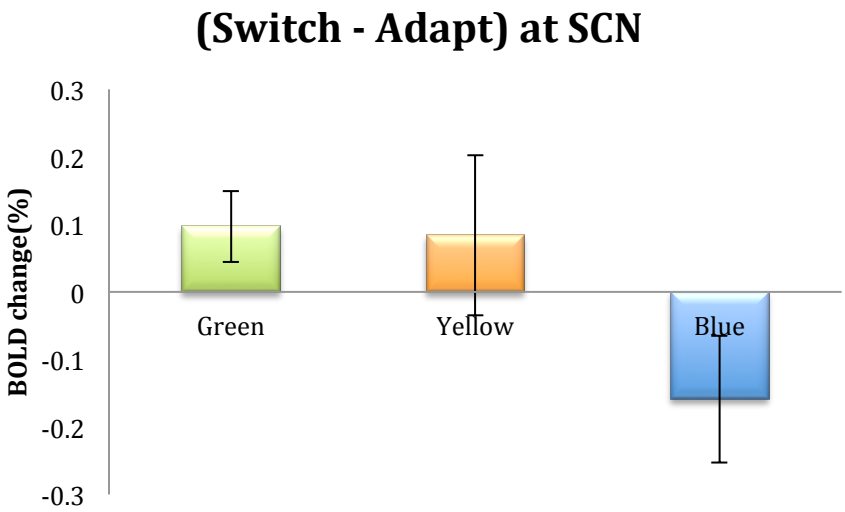

Figure 3.5. Comparison of light adaptation (light onset – constant light) between wavelengths at V1 and the SCN+. A. V1. All wavelengths of light elicited a positive light onset – constant light, suggesting the presence of light adaptation. B. SCN+. Both green and yellow lights evoked positive light adaptation, whereas blue light induced a "negative" light adaptation, suggesting that the SCN+ might be more resistant to blue-light induced light adaptation. Signals are shown in percentage of BOLD change (mean ± s.e.m.) averaged across both presentations and all subjects in both orders of stimulation (n = 13).

2.4 Discussion

The major finding in this study is that short wavelength blue (460nm) light appears to evoke a qualitatively different pattern of response in the SCN compared to green (515nm) and yellow (560nm) light. Specifically the response to prolonged light is greater than that to the onset of light. In contrast the primary visual cortex response did not differ between wavelengths. This is in line with the notion that the IF visual system responds rapidly to generate transient but robust visual information whereas the NIF visual system exhibits a maintained response for circadian phase resetting and is thus more resistant to light adaptation(Nelson & Takahashi, 1991).

2.4.1. Sustained response of the NIF visual system to steady illumination

2.4.1.1 Neuroimaging and electrophysiological evidence

The current findings support the electrophysiological studies that the rod-and-cone-mediated IF visual system adapts to constant illumination, as demonstrated by a decline in %BOLD change at V1 (figure 3.4B). On the contrary, the ipRGCs-governed NIF visual system, as demonstrated by the remarkable distinct response to blue-light at the SCN+, did not display this type of adaptation (figure 3.4A). This observation was further strengthened by the opposite finding of the other two non-blue light at the SCN+ showing a decline in %BOLD change upon prolonged light exposure (figure 3.4A).

To my knowledge, no studies have been performed using neuroimaging methods to compare the patterns of light adaptation in the IF and NIF visual systems. Only one study attempted to compare the BOLD change of the SCN and V1 and found that their signals varied with time of day(Vimal, et al., 2009). Nevertheless, they did not address the question of whether the two regions respond differently towards steady and prolonged illumination. My findings provide the first neuroimaging evidence that the rapid light adaptation in the classic IF visual system may not exist in the melanopsin-containing ipRGCs-driven NIF visual system. In contrast, ipRGCs of the NIF visual system display sustained response to constant illumination. This notion is supported by a number of electrophysiological studies. For example, using whole-cell patch-clamp techniques in rat retina, Berson et al. showed that ipRGCs (SCN-projecting RGCs) evoked a tonic and maintained depolarization during a 20-min constant illumination (Berson, et al., 2002) (figure 4.1). The response latency of the depolarization was found to be prolonged, suggesting that the depolarization was mediated by an intracellular signaling pathway.

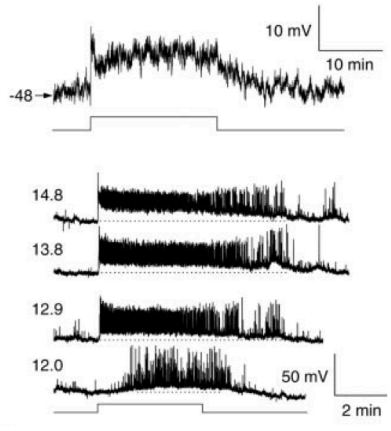

Figure 4.1. Sustained depolarization in ipRGCs evoked by 20min of constant illumination (3 x 10^{13} photons s^{-1} cm^2). Maintained spiking during the entire stimulation as well as a long response latency were observed. (adapted from (Berson, et al., 2002)

Another study also recorded the current in rat ipRGCs evoked by a bright illumination. They found that the light-activated current developed slowly to a peak at 5.35±2.7 s and declined slowly to a plateau in 10.9±4.2 s (Warren, et al., 2003). Likewise, in human retina, intracellular recording of ipRGCs showed that these "giant" ganglion cells had a slow onset of depolarizing response towards light (Dacey, et al., 2005). The response grew slowly to a peak which continued to fire for a prolonged period after light offset. These studies support the idea that the type of rapid light adaptation in the IF visual system may not be present in the NIF system. By contrast, ipRGCs of the NIF system tend to react sustainedly upon steady illumination.

2.4.1.2 Functional & physiological evidence

Parallel findings have also been reported in studies investigating the functions of the NIF visual system. A recent study clearly dissected the roles of cones and melanopsin in responding to long light exposure (Gooley et al., 2010). The effects of melanopsin and cones in melantonin-suppression were initially indistinguishable during a 6.5hour bright light exposure. However, the contribution of cones decayed exponentially over time relative to melanopsin, suggesting that cones are responsible for transient suppression of melatonin whereas melanopsin responses tonically during long exposure to light.

Similar findings have also been reported for the pupillary light reflex in human and primates. The initial pupillary constriction is mediated by photoreceptors of the classic IF visual system, whereas the melanopsin-containing ipRGCs contribute to the

latter sustained pupillary constriction(Gamlin et al., 2007). This sustained pupillary response, referred to as the post-illumination pupillary response (PIPR) of the pupillary light reflex, is the 10 seconds of redilatation of pupils mediated by the ipRGCs after the cessation of light exposure (Kankipati, et al., 2010).

Taken together, these electrophysiological and functional studies provide evidence to support my findings in the current study that the blue-light specific, melanopsin-driven NIF visual system displays a more prolonged and endurable response. This remarkable property of the ipRGCs allows the NIF visual system 1) to reset the circadian rhythms over a long scale of daylight exposure 2) to maintain sustained post-stimulus pupil constriction and 3) to suppress pineal melatonin in a continuous manner during constant illumination.

2.4.2 Molecular mechanism underlying the sustained responsiveness of ipRGCs

In addition, my findings that the ipRGC-driven NIF visual system is more resistant to continuous illumination can be explained by the "bistable" nature of the ipRGCs (Nayak, Jegla, & Panda, 2007). Rods and cones are transducin mediated ciliary photoreceptors that follow the vertebrate-type regeneration of chromophone after light exposure. Upon light exposure, 11-cis retinaldehyde is photoisomerized to all-trans retinal and released from the opsin(Pepe & Cugnoli, 1992). This light activated state is thermally unstable and requires another cell type to re-isomerize the all-trans-retinal back to 11-cis for restoring photo-responsiveness(Hardie & Raghu, 2001). In ipRGCs,

however, all-trans retinal is not released from the opsin but re-isomerizes back to 11-cis-retinal via the absorption of a specific second wavelength, i.e. blue light (Lucas, 2006). As such, unlike the rods and cones, ipRGCs are "bistable" and possess two photosensitive states, i.e. the ground state and the thermally stable activated state(Mure et al., 2009). This unique bistability allows the ipRGCs to regenerate their chromophore via the blue light wavelength and resist photic bleaching, providing plausible molecular mechanism to explain the sustained responsiveness observed in the present study(Panda et al., 2005) (Zhu et al., 2007) (Mure, Rieux, Hattar, & Cooper, 2007) (Rollag, 2008) (Sexton, et al., 2012).

2.4.3 Justification for selected parameters

2.4.3.1 Thirty seconds as a cutting point for comparison

My study compared the initial 30sec to the remaining 90sec of the steady illumination. I chose to use 30s as the cutting point for the following reasons. First, the duration must be long enough for light adaptation to occur in the IF visual system. Rushton et al. showed that the bleaching of rods and cones occurred rapidly and exponentially in the first 30s during light adaptation (Rushton, 1958) (Rushton & Henry, 1968). Second, as described above, the onset of activation of ipRGCs is typically prolonged after a very long latency. Berson et al. showed that the latency of onset was typically 10 to 20s after illumination, depending on the intensity of the light (Berson, 2003). Another study showed that the voltage of ipRGCs peaked at 5.35±2.7s and declined to a plateau in 10.9±4.2 s (Warren, Allen, Brown, & Robinson, 2003).

In order to allow sufficient time for the ipRGCs to reach their steady activation after the prolonged latency, it appeared that 30s might be reasonable and sufficient, given that I also took into account the additional time required for BOLD change in fMRI to take place.

2.4.4 Time of scan

The responsiveness of the two light-sensitive areas, the SCN+ and the V1, depend on the time of day. In vivo recordings of single SCN units in rats showed higher response to light at night comparing to day, suggesting a change of sensitivity to light of the SCN neurons with higher responsiveness at night. (Meijer, Watanabe, Detari, & Schaap, 1996) (Meijer, Watanabe, Schaap, Albus, & Detari, 1998).

In human studies, using melatonin-plotted phase response curves (PRC), maximum phase delay in response to light exposure was found to occur at approximately 24:00 hours, suggesting that the maximum response of the SCN may be at about midnight (Khalsa, Jewett, Cajochen, & Czeisler, 2003). Moreover, the only in vivo fMRI study in human showed that the BOLD signal at midday (14:00 to 16:00 hours) was significantly lower than that at night (22:00 to 24:00 hours) (Vimal, et al., 2009). Taken together, these studies support the notion that the light-induced response of the SCN fluctuates with time of day and generally elicits a maximum response at midnight and a minimum response in the afternoon. I decided to control this

confounding factor by limiting my scans between 14:00 to 18:00 in which the SCN appeared to response at a relatively constant but minimum level.

2.4.5 Sexual dimorphism and orientation of the SCN

In my study, all 13 subjects were female. Morphometrical studies in rats showed that the volume of the SCN was larger in males(Robinson, Fox, Dikkes, & Pearlstein, 1986). In the human SCN, the shape of the SCN is elongated in women and more spherical in men(Swaab, Fliers, & Partiman, 1985). Vasoactive intestinal polypeptide (VIP) neurons in males were twice as many as that in females(Swaab, Chung, Kruijver, Hofman, & Hestiantoro, 2003). Interestingly, even within the same sex, the size of the SCN in homosexual men was larger than that of heterosexual men(Swaab & Hofman, 1990). This rendered us to study only female subjects to control for the sexual dimorphism and orientation of the SCN. Future studies are required to establish whether the sustained responsiveness of the SCN also exist in heterosexual and homosexual men.

2.4.6 Limitations

2.4.6.1 Small sample size and inconsistent luminances

The current study has some limitations that can be considered in future studies. First, although my study provides evidence that the SCN may response differently to melanopsin-specific blue-light compared to other wavelengths of light, the sample size may be too small to yield a statistically significant difference. Second, the

monochromatic light sources were generated by using filters that attached to the projector lamp. I tested and verified the monochromaticities of the filter-generated light by spectrometer but failed to control the luminances of the different wavelengths. The luminances of blue (460nm), green (515nm) and yellow (560nm) light were 2.30 ± 0.08cd/m^2, 18.58 ± 0.32cd/m^2 and 37.4± 0.3cd/m^2 respectively, with blue light less luminous than the other two wavelengths. This could be problematic if I compared the exact %BOLD changes of the different wavelengths. Rather, I compared the directions of signal changes, i.e. increase or decrease, along constant illumination of the same wavelength that would render this limitation less of a concern.

2.4.6.2 Effect of prior illumination on subsequent photic response

The sequence of presentation of various wavelengths in my study was not counterbalanced. The five scans with three different wavelengths in my study were performed in a sequence such that each scan was 1 to 2min apart from the previous one during which the filters were changed manually (except for the longer break between the fourth [blue] and fifth [green] scans in which subjects were allowed to rest their eyes while the structural scans were obtained). This order effect may confound the magnitudes of the signal changes as a source of bias. Indeed, studies have demonstrated how a pre-exposed flash of light would affect the subsequent photic response. For instance, one study showed that two 480nm light pulses 1min apart at the same intensity were able to evoke a smaller response in the ipRGCs by the second flash compared to the first one (Wong, Dunn, & Berson, 2005).

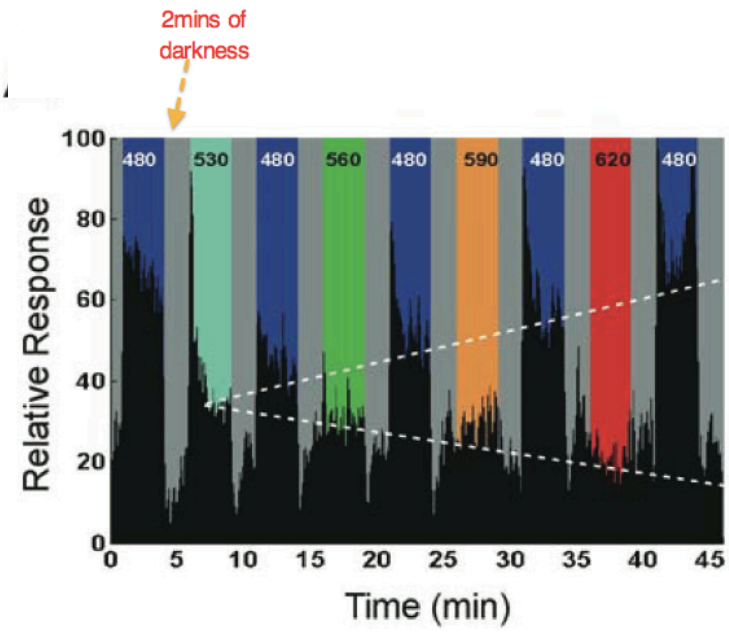

Figure 4.2. Pre-exposure to long wavelengths (above 560nm) aggravated the response of the SCN neurons to blue light (480nm) (Adapted from Mure et al. 2007)

Another study exposed mice to a sequence of 3-min 480nm light pulses separated by a spectrum of different wavelengths of light (flanked by 2-min darkness) ranging from 530nm to 620nm (Mure, et al., 2007) (figure 4.2). They found that the firing response to 480nm light in SCN declined after pre-stimulated with 530nm pulse and increased by prestimulating with 560nm illumination. They concluded that wavelengths above 560nm enhanced the response of SCN whereas those below 530nm reduced the subsequent SCN firing. They also found that melanopsin is responsible for this phenomenon by showing that $Opn4^{-/-}$ mice lacking melanopsin failed to show this enhancing effect. Furthermore, they confirmed this effect with the well-established functions of melanopsin by showing that 1) prior exposure to long wavelength (red) light enhanced the circadian phase shift caused by a short wavelength (blue) light 2) prestimultion with 620nm (red) light increased the amplitude of pupillary constriction induced by 480nm(blue) light.

In contrast, in vitro recording of mice retina (postnatal day 8 to 10) failed to replicate the results by showing no potentiation of ipRGCs firing in response to 480nm blue light after prior stimulation with 620nm red light(Mawad & Van Gelder, 2008). Presumably, the discrepancy of results may be due to the immaturity of the retina that the innervation between rods and the inner retina where the ipRGCs reside has not developed at this stage (P8-10). This suggests that the contribution of rods and cones to the potentiation phenomenon cannot be excluded. Also, the immaturity of the melanopsin system at this early stage as well as the different experimental methods used, in vitro versus in vivo, may lead to the inconsistent results among these studies(Wong, et al., 2005) (Mure, et al., 2007) (Mawad & Van Gelder, 2008).

Collectively, these studies generally indicate the presence of order effect on SCN signals elicited by the successive constant illumination – a long wavelength enhances whereas a short one attenuates the subsequent blue-light induced response. Since the main interest of my study was blue light, I arranged the color order in the majority of subjects so that the blue light was preceded by both yellow and green (figure 2.3A). As illustrated by Mure et al., the green light (515nm) in my stimulus order 1 which was shorter than the threshold of 530nm might have reduced the subsequent SCN+ response to blue light (460nm) whereas the yellow light (560nm) which was just at 560nm could have aggravated the subsequent blue light-evoked signal. Therefore, the stimulus order was changed for the final 4 subjects such that one of the blue lights was the first in the sequence and therefore not pre-stimulated by any other lights (figure 2.3 B). Figure 3.3 showed the %BOLD change at the SCN+ and V1 acquired using the new sequence of light presentation. Consistent with the results in the stimulus order 1, all wavelengths of light evoked higher signals in the initial “light onset” periods than the following “constant light” periods at V1, suggesting that

habituation or adaptation to steady light exposure may have occurred in the IF visual system. More importantly, the rearrangement of stimulus order did not seem to affect the striking response of the SCN+ towards melanopsin-specific blue-light illumination. Both blue-light scans triggered signals at the SCN+ that did not decline upon steady stimulation, but appeared to exhibit even higher responses in the "constant light" period. These findings were in accordance to my results in the stimulus order 1. Surprisingly, the responses to the two green lights appeared to be contradictory. The second green light at the SCN+ displayed a different response from the stimulus order 1, i.e. a response similar to one evoked by the blue light. Whether it was due to the pre-exposed effect of the preceding blue-light is yet to be determined. A bigger sample size might have been more convincing to address this issue. In summary, the stimulus order 2 provided additional evidence to support the findings in the stimulus order 1 that 1) light adaptation occurred in the IF visual system 2) this type of habituation did not exist in the melanopsin-specific blue-light, regardless of whether the blue light was pre-exposed to green-light, yellow-light or darkness. The inconsistency of the green-light induced response at the SCN+ warrants a future investigation in a larger sample size with fully counterbalanced stimulus presentation.

Taken together, the striking and unique absence of light adaptation of the SCN+ to blue-light illumination remained when the results of all 13 subjects in both orders of stimulation were analyzed together (figure 3.5), although the findings revealed no significant difference among the colors.

2.5 Conclusion

My findings provide the first neuroimaging evidence that the NIF visual system is more resistant to light adaptation than the IF visual system. All wavelength-induced responses at the IF visual system experienced light adaptation with only the blue-light induced signals at the SCN+ of the NIF visual system did not. This is consistent with previous electrophysiological and functional studies and highlights the distinct roles of the IF and NIF visual systems – the former generates robust visual information rapidly and the latter functions to photoentrain the circadian rhythms and maintain tonic pupillary restriction over a long period of light exposure. With the recent finding suggesting the implication of the NIF pathway in light-induced migraine, this study raises the question of whether this type of sustained photo-responsiveness might be impaired in these migraineurs. Further investigations of this distinct property of the NIF visual system in migraineurs is needed to address this question.

2.6 References

Baver, S. B., Pickard, G. E., & Sollars, P. J. (2008). Two types of melanopsin retinal ganglion cell differentially innervate the hypothalamic suprachiasmatic nucleus and the olivary pretectal nucleus. *The European journal of neuroscience, 27*(7), 1763-1770.

Berson, D. M. (2003). Strange vision: ganglion cells as circadian photoreceptors. *Trends in neurosciences, 26*(6), 314-320.

Berson, D. M., Castrucci, A. M., & Provencio, I. (2010). Morphology and mosaics of melanopsin-expressing retinal ganglion cell types in mice. *The Journal of comparative neurology, 518*(13), 2405-2422.

Berson, D. M., Dunn, F. A., & Takao, M. (2002). Phototransduction by retinal ganglion cells that set the circadian clock. *Science, 295*(5557), 1070-1073.

Carpenter, M. B. (1983) Human Neuroanatomy. Lippincott Williams & Wilkins, Baltimore, MD.

Cornsweet, T. N. (1970) Visual Perception. Academic Press, Inc. (London) Ltd.

Czeisler, C. A., Duffy, J. F., Shanahan, T. L., Brown, E. N., Mitchell, J. F., Rimmer, D. W., . . . Kronauer, R. E. (1999). Stability, precision, and near-24-hour period of the human circadian pacemaker. *Science, 284*(5423), 2177-2181.

Czeisler, C. A., Shanahan, T. L., Klerman, E. B., Martens, H., Brotman, D. J., Emens, J. S., . . . Rizzo, J. F., 3rd. (1995). Suppression of melatonin secretion in some blind patients by exposure to bright light. *The New England journal of medicine, 332*(1), 6-11.

Dacey, D. M., Liao, H. W., Peterson, B. B., Robinson, F. R., Smith, V. C., Pokorny, J., . . . Gamlin, P. D. (2005). Melanopsin-expressing ganglion cells in primate retina signal colour and irradiance and project to the LGN. *Nature, 433*(7027), 749-754.

Dowling, J. E. (1967). The site of visual adaptation. *Science, 155*(3760), 273-279.

Ebihara, S., & Tsuji, K. (1980). Entrainment of the circadian activity rhythm to the light cycle: effective light intensity for a Zeitgeber in the retinal degenerate C3H mouse and the normal C57BL mouse. *Physiology & behavior, 24*(3), 523-527.

Ecker, J. L., Dumitrescu, O. N., Wong, K. Y., Alam, N. M., Chen, S. K., LeGates, T., . . . Hattar, S. (2010). Melanopsin-expressing retinal ganglion-cell photoreceptors: cellular diversity and role in pattern vision. *Neuron, 67*(1), 49-60.

Fain, G. L., Matthews, H. R., Cornwall, M. C., & Koutalos, Y. (2001). Adaptation in vertebrate photoreceptors. *Physiological reviews, 81*(1), 117-151.

Falcon, J., Besseau, L., Fuentes, M., Sauzet, S., Magnanou, E., & Boeuf, G. (2009). Structural and functional evolution of the pineal melatonin system in vertebrates. *Annals of the New York Academy of Sciences, 1163*, 101-111.

Foster, R. G., Provencio, I., Hudson, D., Fiske, S., De Grip, W., & Menaker, M. (1991). Circadian photoreception in the retinally degenerate mouse (rd/rd). *Journal of comparative physiology. A, Sensory, neural, and behavioral physiology, 169*(1), 39-50.

Gamlin, P. D., McDougal, D. H., Pokorny, J., Smith, V. C., Yau, K. W., & Dacey, D. M. (2007). Human and macaque pupil responses driven by melanopsin-containing retinal ganglion cells. *Vision research, 47*(7), 946-954.

Gooley, J. J., Rajaratnam, S. M., Brainard, G. C., Kronauer, R. E., Czeisler, C. A., & Lockley, S. W. (2010). Spectral responses of the human circadian system depend on the irradiance and duration of exposure to light. *Science translational medicine, 2*(31), 31ra33.

Hankins, M. W., Peirson, S. N., & Foster, R. G. (2008). Melanopsin: an exciting photopigment. *Trends in neurosciences, 31*(1), 27-36.

Hardie, R. C., & Raghu, P. (2001). Visual transduction in Drosophila. [Review]. *Nature, 413*(6852), 186-193.

Hatori, M., & Panda, S. (2010). The emerging roles of melanopsin in behavioral adaptation to light. *Trends in molecular medicine, 16*(10), 435-446.

Hattar, S., Liao, H. W., Takao, M., Berson, D. M., & Yau, K. W. (2002). Melanopsin-containing retinal ganglion cells: architecture, projections, and intrinsic photosensitivity. *Science, 295*(5557), 1065-1070.

Hecht, S. (1920). The Dark Adaptation of the Human Eye. *The Journal of general physiology, 2*(5), 499-517.

Jenkinson, M., & Smith, S. (2001). A global optimisation method for robust affine registration of brain images. *Medical image analysis, 5*(2), 143-156.

Kankipati, L., Girkin, C. A., & Gamlin, P. D. (2010). Post-illumination pupil response in subjects without ocular disease. *Investigative ophthalmology & visual science, 51*(5), 2764-2769.

Keeler, C. E. Iris movements in blind mice. Am. J. Physiol. 81, 107–112 (1927).

Khalsa, S. B., Jewett, M. E., Cajochen, C., & Czeisler, C. A. (2003). A phase response curve to single bright light pulses in human subjects. *The Journal of physiology, 549*(Pt 3), 945-952.

Kovalevsky, G., DiLoreto, D., Jr., Wyatt, J., del Cerro, C., Cox, C., & del Cerro, M. (1995). The intensity of the pupillary light reflex does not correlate with the number of retinal photoreceptor cells. *Experimental neurology, 133*(1), 43-49.

Lockley, S. W., Brainard, G. C., & Czeisler, C. A. (2003). High sensitivity of the human circadian melatonin rhythm to resetting by short wavelength light. *The Journal of clinical endocrinology and metabolism, 88*(9), 4502-4505.

Lucas, R. J. (2006). Chromophore regeneration: melanopsin does its own thing. [Comment]. *Proceedings of the National Academy of Sciences of the United States of America, 103*(27), 10153-10154.

Lucas, R. J., Douglas, R. H., & Foster, R. G. (2001). Characterization of an ocular photopigment capable of driving pupillary constriction in mice. *Nature neuroscience, 4*(6), 621-626.

Lucas, R. J., Freedman, M. S., Munoz, M., Garcia-Fernandez, J. M., & Foster, R. G. (1999). Regulation of the mammalian pineal by non-rod, non-cone, ocular photoreceptors. *Science, 284*(5413), 505-507.

Lucas, R. J., Hattar, S., Takao, M., Berson, D. M., Foster, R. G., & Yau, K. W. (2003). Diminished pupillary light reflex at high irradiances in melanopsin-knockout mice. *Science, 299*(5604), 245-247.

Mai, J. K., Kedziora, O., Teckhaus, L., & Sofroniew, M. V. (1991). Evidence for subdivisions in the human suprachiasmatic nucleus. *The Journal of comparative neurology, 305*(3), 508-525.

Mawad, K., & Van Gelder, R. N. (2008). Absence of long-wavelength photic potentiation of murine intrinsically photosensitive retinal ganglion cell firing in vitro. *Journal of biological rhythms, 23*(5), 387-391.

Meijer, J. H., Watanabe, K., Detari, L., & Schaap, J. (1996). Circadian rhythm in light response in suprachiasmatic nucleus neurons of freely moving rats. *Brain research, 741*(1-2), 352-355.

Meijer, J. H., Watanabe, K., Schaap, J., Albus, H., & Detari, L. (1998). Light responsiveness of the suprachiasmatic nucleus: long-term multiunit and single-unit recordings in freely moving rats. *The Journal of neuroscience : the official journal of the Society for Neuroscience, 18*(21), 9078-9087.

Melyan, Z., Tarttelin, E. E., Bellingham, J., Lucas, R. J., & Hankins, M. W. (2005). Addition of human melanopsin renders mammalian cells photoresponsive. *Nature, 433*(7027), 741-745.

Mure, L. S., Cornut, P. L., Rieux, C., Drouyer, E., Denis, P., Gronfier, C., & Cooper, H. M. (2009). Melanopsin bistability: a fly's eye technology in the human retina. *PloS one, 4*(6), e5991.

Mure, L. S., Rieux, C., Hattar, S., & Cooper, H. M. (2007). Melanopsin-dependent nonvisual responses: evidence for photopigment bistability in vivo. *Journal of biological rhythms, 22*(5), 411-424.

Nayak, S. K., Jegla, T., & Panda, S. (2007). Role of a novel photopigment, melanopsin, in behavioral adaptation to light. [Review]. *Cellular and molecular life sciences : CMLS, 64*(2), 144-154.

Nelson, D. E., & Takahashi, J. S. (1991). Sensitivity and integration in a visual pathway for circadian entrainment in the hamster (Mesocricetus auratus). *The Journal of physiology, 439*, 115-145.

Newman, L. A., Walker, M. T., Brown, R. L., Cronin, T. W., & Robinson, P. R. (2003). Melanopsin forms a functional short-wavelength photopigment. *Biochemistry, 42*(44), 12734-12738.

Noseda, R., Kainz, V., Jakubowski, M., Gooley, J. J., Saper, C. B., Digre, K., & Burstein, R. (2010). A neural mechanism for exacerbation of headache by light. *Nature neuroscience, 13*(2), 239-245.

Ohba, N., & Alpern, M. (1972). Adaptation of the pupil light reflex. *Vision research, 12*(5), 953-967.

Panda, S., Nayak, S. K., Campo, B., Walker, J. R., Hogenesch, J. B., & Jegla, T. (2005). Illumination of the melanopsin signaling pathway. *Science, 307*(5709), 600-604.

Panda, S., Provencio, I., Tu, D. C., Pires, S. S., Rollag, M. D., Castrucci, A. M., . . . Hogenesch, J. B. (2003). Melanopsin is required for non-image-forming photic responses in blind mice. *Science, 301*(5632), 525-527.

Panda, S., Sato, T. K., Castrucci, A. M., Rollag, M. D., DeGrip, W. J., Hogenesch, J. B., . . . Kay, S. A. (2002). Melanopsin (Opn4) requirement for normal light-induced circadian phase shifting. *Science, 298*(5601), 2213-2216.

Pepe, I. M., & Cugnoli, C. (1992). Retinal photoisomerase: role in invertebrate visual cells. *Journal of photochemistry and photobiology. B, Biology, 13*(1), 5-17.

Pirenne MH. Dark adaptation and night vision. In: Davson H, editor. The eye. Vol 2. London: Academic Press; 1962

Provencio, I., Rodriguez, I. R., Jiang, G., Hayes, W. P., Moreira, E. F., & Rollag, M. D. (2000). A novel human opsin in the inner retina. *The Journal of neuroscience : the official journal of the Society for Neuroscience, 20*(2), 600-605.

Provencio, I., Wong, S., Lederman, A. B., Argamaso, S. M., & Foster, R. G. (1994). Visual and circadian responses to light in aged retinally degenerate mice. *Vision research, 34*(14), 1799-1806.

Qu, T., Dong, K., Sugioka, K., & Yamadori, T. (1996). Demonstration of direct input from the retina to the lateral habenular nucleus in the albino rat. *Brain research, 709*(2), 251-258.

Reppert, S. M., & Weaver, D. R. (2002). Coordination of circadian timing in mammals. *Nature, 418*(6901), 935-941.

Robinson, S. M., Fox, T. O., Dikkes, P., & Pearlstein, R. A. (1986). Sex differences in the shape of the sexually dimorphic nucleus of the preoptic area and suprachiasmatic nucleus of the rat: 3-D computer reconstructions and morphometrics. *Brain research, 371*(2), 380-384.

Rollag, M. D. (2008). Does melanopsin bistability have physiological consequences? [Comment]. *Journal of biological rhythms, 23*(5), 396-399.

Ruby, N. F., Brennan, T. J., Xie, X., Cao, V., Franken, P., Heller, H. C., & O'Hara, B. F. (2002). Role of melanopsin in circadian responses to light. *Science, 298*(5601), 2211-2213.

Rushton, W. A. (1958). Visual pigments in the colour blind. *Nature, 182*(4637), 690-692.

Rushton, W. A., & Henry, G. H. (1968). Bleaching and regeneration of cone pigments in man. *Vision research, 8*(6), 617-631.

Sexton, T., Buhr, E., & Van Gelder, R. N. (2012). Melanopsin and mechanisms of non-visual ocular photoreception. *The Journal of biological chemistry, 287*(3), 1649-1656.

Shibata, S., Oomura, Y., Kita, H., & Hattori, K. (1982). Circadian rhythmic changes of neuronal activity in the suprachiasmatic nucleus of the rat hypothalamic slice. *Brain research, 247*(1), 154-158.

Smith, S. M. (2002). Fast robust automated brain extraction. *Human brain mapping, 17*(3), 143-155.

Swaab, D. F., Chung, W. C., Kruijver, F. P., Hofman, M. A., & Hestiantoro, A. (2003). Sex differences in the hypothalamus in the different stages of human life. *Neurobiology of aging, 24 Suppl 1*, S1-16; discussion S17-19.

Swaab, D. F., Fliers, E., & Partiman, T. S. (1985). The suprachiasmatic nucleus of the human brain in relation to sex, age and senile dementia. *Brain research, 342*(1), 37-44.

Swaab, D. F., & Hofman, M. A. (1990). An enlarged suprachiasmatic nucleus in homosexual men. *Brain research, 537*(1-2), 141-148.

Takahashi, J. S., DeCoursey, P. J., Bauman, L., & Menaker, M. (1984). Spectral sensitivity of a novel photoreceptive system mediating entrainment of mammalian circadian rhythms. *Nature, 308*(5955), 186-188.

Thapan, K., Arendt, J., & Skene, D. J. (2001). An action spectrum for melatonin suppression: evidence for a novel non-rod, non-cone photoreceptor system in humans. *The Journal of physiology, 535*(Pt 1), 261-267.

Trejo, L. J., & Cicerone, C. M. (1982). Retinal sensitivity measured by the pupillary light reflex in RCS and albino rats. *Vision research, 22*(9), 1163-1171.

Tsujimura, S., Ukai, K., Ohama, D., Nuruki, A., & Yunokuchi, K. (2010). Contribution of human melanopsin retinal ganglion cells to steady-state pupil responses. *Proceedings. Biological sciences / The Royal Society, 277*(1693), 2485-2492.

Tu, D. C., Zhang, D., Demas, J., Slutsky, E. B., Provencio, I., Holy, T. E., & Van Gelder, R. N. (2005). Physiologic diversity and development of intrinsically photosensitive retinal ganglion cells. *Neuron, 48*(6), 987-999.

Vimal, R. L., Pandey-Vimal, M. U., Vimal, L. S., Frederick, B. B., Stopa, E. G., Renshaw, P. F., . . . Harper, D. G. (2009). Activation of suprachiasmatic nuclei and primary visual cortex depends upon time of day. *The European journal of neuroscience, 29*(2), 399-410.

Warren, E. J., Allen, C. N., Brown, R. L., & Robinson, D. W. (2003). Intrinsic light responses of retinal ganglion cells projecting to the circadian system. *The European journal of neuroscience, 17*(9), 1727-1735.

Wong, K. Y., Dunn, F. A., & Berson, D. M. (2005). Photoreceptor adaptation in intrinsically photosensitive retinal ganglion cells. *Neuron, 48*(6), 1001-1010.

Wright, K. P., Jr., Hughes, R. J., Kronauer, R. E., Dijk, D. J., & Czeisler, C. A. (2001). Intrinsic near-24-h pacemaker period determines limits of circadian entrainment to a weak synchronizer in humans. *Proceedings of the National Academy of Sciences of the United States of America, 98*(24), 14027-14032.

Wurtman, R. J., Axelrod, J., & Fischer, J. E. (1964). Melatonin Synthesis in the Pineal Gland: Effect of Light Mediated by the Sympathetic Nervous System. *Science, 143*(3612), 1328-1329.

Zhu, Y., Tu, D. C., Denner, D., Shane, T., Fitzgerald, C. M., & Van Gelder, R. N. (2007). Melanopsin-dependent persistence and photopotentiation of murine pupillary light responses. *Investigative ophthalmology & visual science, 48*(3), 1268-1275.

Chapter 3

Interictal Excitability in Migraine Visual Cortex

3.1 Introduction

3.1.1 Migraine and the visual system

The visual system appears to be implicated in various aspects of migraine. First, a widely acclaimed hypothesis suggests that the disease originates in the visual cortex via cortical spreading depression (CSD) that activates the trigeminovascular complex and causes headache (Welch, 2003). CSD is a wave of neuronal and glial depolarization followed by a period of inactivity that propagates slowly over the cortex (Lauritzen, 1994). Experimental studies supported its role in visual aura (Dalkara, Zervas, & Moskowitz, 2006). Second, photophobia is present in the majority of migraine sufferers, both during and between attacks, and is one of the key diagnostic symptoms of migraine(Vanagaite et al., 1997) (Drummond, 1986) ("The International Classification of Headache Disorders: 2nd edition," 2004) (Boulloche et al., 2010).

Photophobia, an abnormal tolerance of light, is a common symptom that can be due to a variety of neurological or ophthalmological diseases. It is considered as a

discomfort feeling of the eye innervated by the ophthalmic division of the trigeminal nerve which also involves peripheral and central components of visual and pain systems such as the optic nerve, brainstem, thalamus, limbic system and the visual cortices (Lebensohn, 1951) (Jan, Groenveld, & Anderson, 1993). Numerous hypotheses have been proposed for the mechanism underlying photophobia in migraine. These speculations include 1) activations of the trigeminal nerve nociceptors innervating the eye lead to the activations of spinal trigeminal nucleus, diencephalic structures and the thalamus(Lebensohn, 1951), 2) sympathetic overdrive (Chronicle & Mulleners, 1996) (Noseda & Burstein, 2011), 3) hyperexcitability of the visual cortex (Aurora, Cao, Bowyer, & Welch, 1999) 4) abnormal habituation of the brainstem (Sand & Vingen, 2000). A recent study showed that the photic signals from the melanopsin(OPN4)-containing ipRGCs converge with the dura-sensitive neurons at thalamus(Noseda et al., 2010). This suggests the implication of the NIF visual system in the pathophysiology of photophobia. Lastly, although migraine sufferers often report their headache to be initiated by light, the mechanism underlying this phenomenon remains elusive. For example, can altered cortical sensitivity to light initiate classic migraine attack? Moreover, a clear distinction between the mechanism of migraine "induced" by and "worsened" by light has not yet been examined.

3.1.2 Cortical Excitability

Several lines of evidence exist in the literature regarding the abnormal cerebral responsiveness of migraine to environmental stimuli (Siniatchkin et al., 2011). These

studies, however, revealed inconsistent results with one line of research supporting the notion of hyperexcitability in migraine while the other stated that the brains of migraineurs are hypoexicitable(Coppola, Pierelli, et al., 2007). One of the reasons is that migraine is an episodic, dynamic and relatively unpredictable disease. The various stages in migraine cycle including pre-ictal, aura, ictal, postictal and interictal stages render the consistency of study methodology difficult. The complexity in research methodology is further magnified by the multigenic (Montagna, 2008)and polyphenotypic, i.e. migraine with (MA) or without aura (MwoA), characteristics of the disease.

3.1.2.1 Transcranial magnetic stimulation studies

Transcranial magnetic stimulation (TMS) is an non-invasive method of inducing temporary cortical changes of the human brain(Hallett, 2000). Above a certain threshold of intensity, applying TMS to the visual cortex produces visual phosphenes that can be observed by the receiver. This TMS-induced phosphene threshold can be used as a measure of visual cortical excitability. A series of studies performed by Aurora and other colleagues using TMS showed increased excitability of the visual cortex in MA compared to controls(Aurora, Ahmad, Welch, Bhardhwaj, & Ramadan, 1998) (Aurora, al-Sayeed, & Welch, 1999) (Aurora, Welch, & Al-Sayed, 2003) (Aurora, Barrodale, Chronicle, & Mulleners, 2005) (Aurora, Barrodale, Tipton, & Khodavirdi, 2007). Contrary to these findings, other studies showed decreased excitability of the visual cortex elicited by TMS in MA (Afra, Mascia, Gerard, Maertens de Noordhout, & Schoenen, 1998) (Bohotin et al., 2002). While the reason

behind these controversies remains elusive, it is suggested that the discordancy of results may be due to the different methods, patients and the low reliability of subjective phosphene reporting(Fumal, Bohotin, Vandenheede, & Schoenen, 2003).

3.1.2.2 Neuroimaging studies

Functional magnetic resonance imaging (fMRI)

A number of fMRI studies, using various experimental paradigms, have also attempted to explore the cortical responsiveness of migraineurs during ictal or interictal stages – thermal(Maleki et al., 2012) (Russo et al., 2012) (Aderjan, Stankewitz, & May, 2010) (Moulton et al., 2011) (Moulton et al., 2008), photic (Cao, Welch, Aurora, & Vikingstad, 1999) (Shepherd, 2000) (Cao, Aurora, Nagesh, Patel, & Welch, 2002) (Vincent et al., 2003) (J. Huang, Cooper, Satana, Kaufman, & Cao, 2003) (Bramanti et al., 2005) (Antal et al., 2011) (Denuelle et al., 2011) (Martin et al., 2011) (Coutts, Cooper, Elwell, & Wilkins, 2012) and olfactory stimuli (Demarquay, Royet, Mick, & Ryvlin, 2008) (Denuelle, et al., 2011). Nevertheless, only very limited studies have focused on the cerebral responses to visual stimuli and their different experimental methodology revealed controversial results, with some supporting the presence of cortical hyperexcitability and others reporting the opposite results. For example, using parallel alternating white and black bars oriented at a specific angle, Vincent al et. showed that the occipital cortex of MA was more active than controls(Vincent, et al., 2003). The visual stimuli they used contained incongruent lines presented at specific angulations, presumably mimicking the fortification pattern of visual aura. In addition to V1, their analysis also involved the peristrate cortex (V2/V3/V4) that was associated with early visual processing. Using

square-wave gratings, another study also provoked higher interictal responses at the visual cortex of MA compared to controls and the responses were strongly dependent to the stimulus spatial frequency (J. Huang, et al., 2003). Likewise, a recent study using white flickering light as stimuli showed higher activation of the occipital cortex in the migraine group in terms of the number of activated voxels but not intensity (Martin, et al., 2011). These three studies support the hypothesis of cortical hyperexcitability in MA between attacks and suggest that the increased excitability at visual cortex may underlie the pathophysiology of migraine. In contrast, one study used flickering checkerboards as visual stimuli and revealed significantly lower occipital response in migraineurs (Bramanti, et al., 2005). By presenting alternating red-green checkerboards in 8 rest/stimulus periods, they found that the occipital cortex of migraineurs was significantly less activated than controls. Furthermore, the size of the area activated was inversely proportional to the frequency of migraine attacks.

3.1.3 Potassium channel (TRESK) and migraine

TWIK-related spinal cord potassium channel(TRESK) is a two-pore domain K+ channel that is encoded by the KCNK18 gene (D. Y. Huang, Yu, & Fan, 2008). Its role in pain and volatile anesthesia led to the recent discovery of its mutation in a family with typical migraine with visual aura (MA), suggesting the malfunction of TRESK that results in altered neuronal excitability may underlie the mechanism of migraine with aura (Lafreniere et al., 2010). This genetically homogeneous group of migraine subjects provides a unique insight into the pathophysiology of migraine.

3.1.4 Purpose of the current study

The aim of the current study was to explore the interictal cortical excitability of migraineurs with aura who had visually-triggered migraine. The first part of the study includes analyzing the MRI data of non-TRESK migraineurs and healthy controls that were collected by our research group. The second part consistes of an fMRI study performed independently by myself on subjects with the TRESK mutation. Using two stimulus paradigms, i.e. diffuse constant illumination and flickering checkerboards, the functional and metabolic characteristics of the three groups were investigated with fMRI. Metabolite in the visual cortex including glutamate, γ-aminobutyric acid (GABA) and N-acetylaspartate (NAA) were also studied by MRS and will be discussed in the next chapter.

I hypothesized that migraineurs with aura would exhibit higher cortical response compared to healthy controls. Since TRESK migraineurs are considered as a genetically homogeneous cohort in which abnormal neuronal excitability is strongly evidenced, I hypothesized that these unique subjects would manifest an extreme of the findings observed in the non-TRESK migraine group.

3.2 Methods

3.2.1. Subjects, ethic approval and informed consent

3.2.1.1 TRESK migraineurs

Four affected subjects (3female and 1male), age (mean 57 ± 7), of the family with TRESK-associated migraine with aura participated in the study. Another affected subject who agreed to participate in the study failed to receive the scan because of claustrophobia was excluded.

As shown in table 2.1, the frequency of migraine attack was about 1 to 2 times per month with three of the subjects under regular prophylactic medication (Verapamil 240mg per day, a calcium channel blocker). All subjects described the headache as severe and required additional medication such as Rizatriptan10mg during acute attack. The duration of a typical attack varied about 2hr to 3 days and most of them interfered with their work and quality of life.

All subjects reported the presence of visual aura, described as scotoma, flashing lights or enlarging and migrating white spots, that accompanied 25 to 100% of each attack. All were sensitive to light during the attacks and theirs headache can be triggered by visual stimuli such as bright light, flashing checkerboards, flashing florescent light, computer screens, light through trees etc. In addition, they also reported various degrees of heightened sensation towards auditory, olfactory or thermal stimuli during the attacks.

All subjects gave written informed consent and the study was approved by the Lawson Health Research Institute, Health Sciences REB#:17793. Before the scans, all subjects were informed of the potential adverse effects of the scans. Two hours after the scan, subject 1 experienced headache preceded by visual aura. Within 24 hours, subject 2 reported to have photophobia and subject 3 experienced visual aura without headache. Subject 4, however, did not experience any headache or visual discomfort within the 24 hours after the scan. The next attack was reported to be 5 days after the scan. With regard to migraine prophylaxis, one of the subjects stopped taking the prophylactic medication two weeks prior to the scan and the other two kept their use of Verapamil. Subject 4 did not take any prophylactic medication.

Subject ID	1	2	3	4
gender	Female	female	female	male
age	62	66	64	36
No. of years with migraine	48	40	46	16
Frequency of migraine/month	2(under prophylactic medication)	1 (under prophylactic medication)	1(under prophylactic medication)	1
Duration of a typical episode of attack	12hr to24hr	2 to 3days	4hr to 2days	4 to 12 hours
Severity	severe	severe	severe	severe
Pattern of visual aura	Scotoma Flashing light	White circle becoming Zigzag pattern moving from lower to upper visual field	Enlarging spot that forms a line and moves to the left side	Starts with a spot which grows to a inverted "C" shape
% of attacks accompanied by visual aura	75%	25%	25%	100%
Visual triggers	Bright light, checkerboard, Light through trees, flashing on vibrating florescent light	Bright light, light through trees	Bright light, light through trees, light from reflecting surfaces such as glass or metal	Computer screen, flashing lights
Other triggers	Coffee, alcohol, stress	stress	Loud noises, extreme heat, stress	
No. of attack-free days leading to the scan	2weeks	17days	2 weeks	2 weeks
No. of days after the scan before the next attack	Visual aura followed by headache started 2hr after scan	Photophobia	Photophobia after the scan Visual aura without headache in 24hr	5 days after the scan
Acute or prophylactic medications	Verapamil SR 120mg, stopped for 2 weeks before scan	Verapamil 240mg daily	Verapamil 240mg daily; Rizatriptan10mg during attacks	nil

Table 2.1 Clinical characteristics of TRESK migraineurs.

3.2.1.2 Non-TRESK migraineurs and healthy controls

The fMRI data of 12 non-TRESK migraineurs (all female, age 23 to 38, mean 28.18 ± 2, one subject was excluded because of a large occipital cyst) who experienced light-triggered migraine as well as 11 normal healthy controls (all female, age 24 to 49, mean 33.09 ± 2.3) that were collected by our research group were also analyzed in the present study. One migraine subject who fell asleep was excluded from the analysis in the Light Adaptation Task and Visual Sensitivity Task. A control subject was excluded from the Visual Sensitivity Task because we forgot to place the mirror on the head coil. Accordingly, 11 migraineurs and 11 controls were analyzed in the Light Adaptation study, whereas 11migraineurs and 10 controls were analyzed in the Visual Sensitivity study. The patients were recruited from Dr. Zameel Cader's clinic and via an advertisement posted on the Migraine Trust's website.

All 23 subjects gave their written consent and were scanned at the Oxford Centre for Functional MRI of the Brain (FMRIB) according to the ethics approved by the Oxfordshire Research Ethics Committee (Staffordshire REC number 11/WM/0088). All scans were performed between 8am to 12pm under the same protocol as in the TRESK study described in the following section except that only one MRS scan was done in each subject.

Migraine subject	Age	Migraine duration (years)	Frequency of attack (month)	Migraine-free (days)	Medication
1	23	14	8-10	<5	Topiramate
2 (excluded)	46	3	-	4	None
3	35	22	4-6	<7	Sumatriptan
4	32	17	4-6	>7	Pizotifen
5	41	N/A	4-6	N/A	N/A
6	49	40	8	7	Almotriptan/Lamotrigine)
7	30	21	2	1	Sumatriptan
8	32	7	4	8	Almotriptan
9	28	2.5	4.5	1	Botox
10	41	35	5	14	Nurofen express
11	27	10	2	8	Pizotifen/Naratriptan
12	26	13	2.5	>14	Amitriptyline

Table 2.1 Clinical characteristics of non-TRESK migraine patients. Subject no.2 was excluded because she fell asleep in the experiment.

3.2.2 Experimental design, pre-study requirements and preparations

We followed the same protocol for scanning the three groups of subjects – TRESK migraineurs, non-TRESK migraineurs and healthy controls. Each study lasted about 50min and was performed at approximately the same time of day, i.e. 8am to 12pm. This minimized the potential fluctuations in cerebral metabolites due to circadian rhythm. As illustrated in figure 2.1, subjects were allowed to adapt to complete darkness for more than 20min during which the structural scan, the first MRS and the resting state fMRI (data was acquired but not analyzed in the present study) data were acquired. This was followed by the two fMRI tasks, namely the Light Adaptation Study and the Visual Sensitivity Study, during which the subjects were exposed to various visual stimuli. Finally, only TRESK subjects were in complete darkness again and received the second MRS acquisition that lasted about 10min.

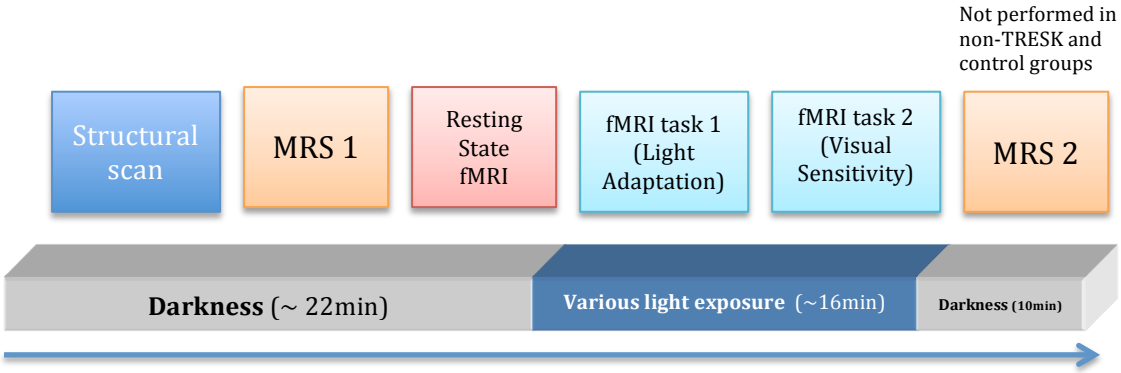

Figure 2.1. Experimental design. The entire experiment lasted about 50min and was performed in the following order: structural scan, the first MRS, resting state fMRI, fMRI task 1(Light Adaptation Task), fMRI task 2 (Visual Sensitivity Task). An additional MRS that followed the entire study was performed only in the TRESK group.

3.2.2.1 fMRI Task 1: Light Adaptation Study

The same ON/OFF visual stimuli in my first experiment, the Wavelength Study, were employed except that only black and white backgrounds were presented. The black and white backgrounds, 1 and 2 min respectively, were presented for 3 blocks with a total of 9min (figure 2.2). During the entire period of the fMRI task, subjects were instructed to explicitly open their eyes and wear semiopaque goggles covering the entire visual field as to avoid the forming of shape or moving images. As such, subjects were only able to detect white diffuse light during the presentation of white background.

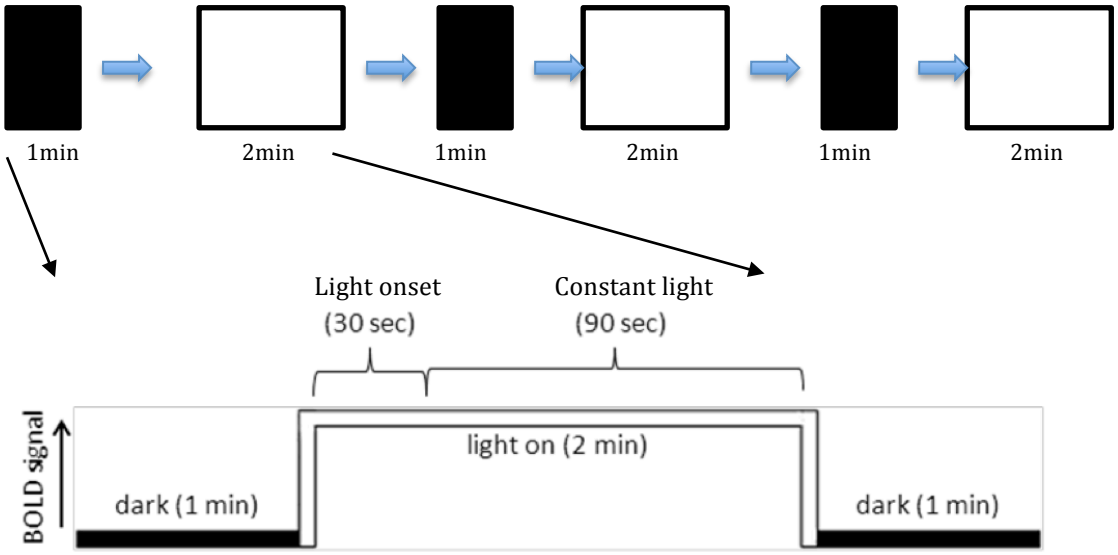

Figure 2.2 1-min black screen was alternated with 2-min white background. The magnitude of light adaptation was defined as the % BOLD change of the initial 30s (light onset) minus that of the remaining 90s (constant light).

fMRI Task 2: Visual Sensitivity Study

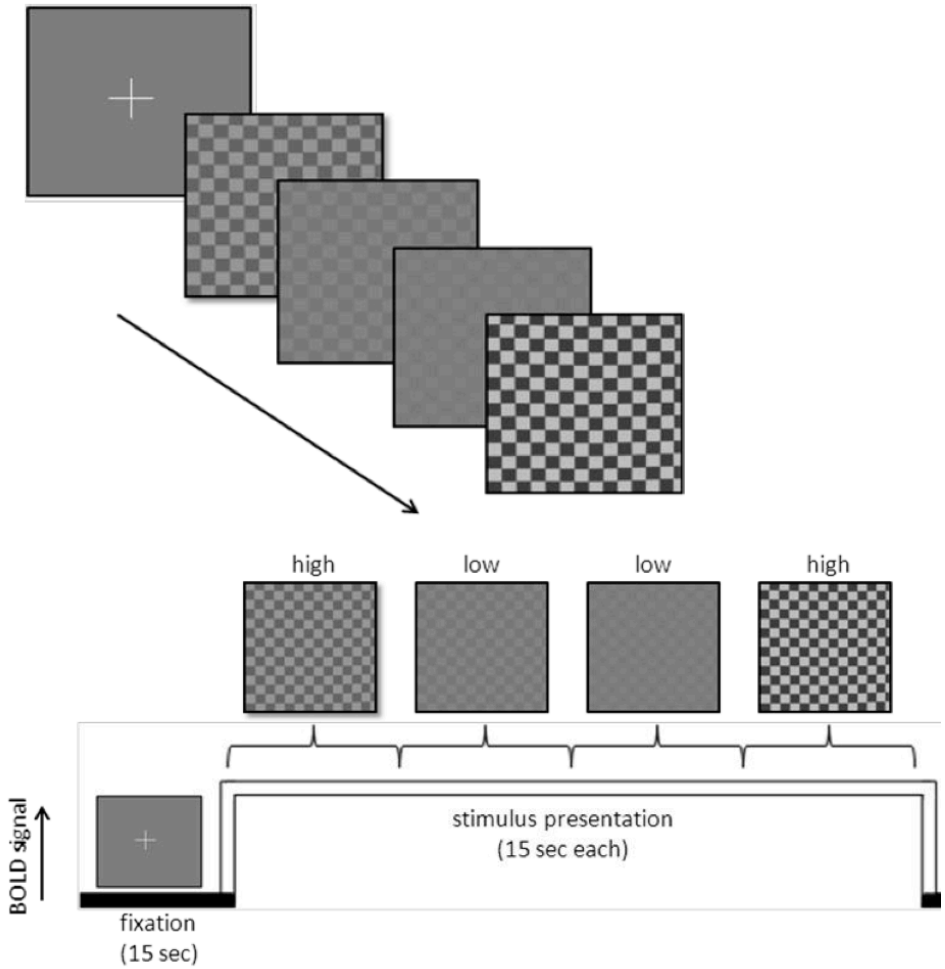

Figure 2.3. Model for one block with 15s of fixation followed by 1-min of low (2%, 5%) and high (20%, 50%) contrast phase-reversing black-and-white checkerboards alternating at 8Hz (5blocks).

The goggles were removed from the subjects before the start of the *Visual Sensitivity Study*. Using an ON/OFF block design, five blocks of phase-reversing black and white checkerboards were presented to the subjects. The checkerboards consist of 16 x 12 checks that were displayed on a 1024 x 768 screen resolution. One block of the stimuli consisted of checkerboards alternating at 8 Hz at 2, 5, 20 and 50% contrasts. The contrasts lasted 15s each and were presented in a pseudo-random and fully counterbalanced order (figure 2.3). A 50% contrast mid-grey screen with a central fixation cross were also presented for 15s before each block. Again, the subjects were instructed to keep their eyes open and fixate on the cross or center of the checkerboards.

3.2.3 Protocol Programming and Presentation of Stimuli

The same visual stimuli programmed in my first experiment, the Wavelength Study, were used by the Light Adaptation Study. The presentation in the Visual Sensitivity Study was also programmed and run by the software *Presentation 2.0* (Neurobehavioral Systems, Inc). All stimuli presentation followed the same experimental settings in the Wavelength Study. The visual stimuli were presented from a computer connected to a LCD screen in the scanner room. The subjects then viewed the visual stimuli on the screen via a mirror that was fit onto the head coil of the scanner.

3.2.4 MR imaging acquisition

The non-TRESK subjects and healthy controls were scanned at the FMIRB in Oxford, whereas the TRESK scans were performed at the Centre for Functional and Metabolic Mapping (CFMM) at Robarts Research Institute of Western's University in London, Ontario, Canada. Siemens Verio 3T scanner and Siemens MAGNETOM Tim Trio 3T scanner were used for image acquisition for the Oxford and Canada studies respectively. All scans followed the same protocols and parameters. First, we determined the position of head in the scanner by a 3-D localizer scan. Anatomical images were acquired using a T1-weighted sequence (MPRAGE) with isotropic voxels (voxel size 1 x 1 x 1mm^3, repetition time[TR] = 2040ms, echo time[TE] = 4.68ms, field of view[FOV] = 200mm, a slice thickness of 1mm, matrix 192 x 192, 192 slices).

Details of MR spectroscopic acquisition will be described in the next chapter.

Next, the light adaptation (9min) followed by the visual sensitivity (6min) fMRI tasks were performed while data of T2-weighted functional MR images were acquired: voxel size = 3.0 x 3.0 x 2.5 mm^3, TR = 3000ms, TE = 30ms, 44 slices, a thickness of 2.5mm, a flip angle of 90°, 180 volumes for the Light Adaptation Study and 125 volumes for the Visual Sensitivity Study.

Finally, a second MRS was acquired with the same protocol as the first one for the TRESK subjects. During the entire study, with the exception of the structural scan and

the functional resting state scan, subjects were instructed to remain alert, keep their eyes opened and fixated onto the screen. Each subject's head was immobilized in a head brace by using small cushions to reduce head motion.

3.2.5 Data Analysis

3.2.5.1 Pre-processing steps

FMRI data were analyzed using FSL version 6.00. The pre-processing steps followed all the steps in the Wavelength Study including skull extraction by BET, motion correction by MCFLIRT, spatially smoothing and prewhitening by FILM.

3.2.5.2 First-level fMRI analysis for the Light Adaptation Study

First-level fMRI analysis of individual subject data were performed using FEAT and followed the steps as described in the Wavelength Study. The initial EPI images were registered to the standard MNI152 via two steps by first registering to each subject's own T1-weighted structural images using FLIRT. We also employed the same experimental model and contrasts used in the Wavelength Study, i.e. light onset, constant light, light onset – constant light and constant light – light onset. Images

were threshold using clusters determined by $Z > 2.3$ with a corrected cluster significance threshold of $p = 0.05$.

3.2.5.3 First-level fMRI analysis for the Visual Sensitivity Study

The same analysis method in the Light Adaptation Study was used for analyzing the Visual Sensitivity Study. I defined the 2 and 5% contrasts as "low contrast" and the 20 and 50% contrasts as "high contrast". Our model then analyzed the activations in the low contrast, the high contrast and the difference contrasts "low minus high" and "high minus low". Images were thresholded using clusters determined by $Z > 2.3$ with a corrected cluster significance threshold of $p = 0.05$.

3.2.5.4 Group-level fMRI analysis for both fMRI experiments

Comparisons of brain activations for the light adaptation and visual sensitivity experiments were performed using the higher-level analysis function of FEAT with mixed effect FLAME1 modelling. I demeaned age within group and used the following 4 contrasts for the higher-level analysis – control group mean, migraineurs group mean, activation greater in control than migraineurs and activation greater in migraineurs than control. For the TRESK study, 4 additional contrasts for the higher-level analysis were defined – TRESK group mean, activation greater in TRESK than

controls, activation greater in TRESK than migraineurs, activation in migraineurs greater than TRESK and activation in activation in controls greater than TRESK. Clusters were thresholded at Z>2.3 with a corrected cluster significance threshold of p =0.05.

3.2.5.5 Calculation of %BOLD change within the visual cortices in both fMRI studies

Featquery was used to extract the mean percentage BOLD change associated with our modeled experimental paradigm within the visual cortices in both fMRI studies. The standard space masks “GM visual cortex V1 BA17” in the Juelich Histological Atlas for the left and right visual cortices (figure 2.6) were used to determine the mean %BOLD change in these brain regions. Mean percentage BOLD change in both V1 were then averaged.

3.3 Results

3.3.1 Light adaptation study – non-TRESK migraineurs and controls

In both groups, signals in light onset period were higher than constant light period (figure 3.1). T-test analysis revealed that there was a significant difference in signal between light onset and constant light in the control group (*$p < 0.05$) but not in the non-TRESK migraineurs group ($p = 0.09$). The figure also illustrated the difference of signal between "light onset" and "Constant light" ("light onset – constant light") in which both groups demonstrated positive "light onset – constant light", suggesting the presence of light adaptation.

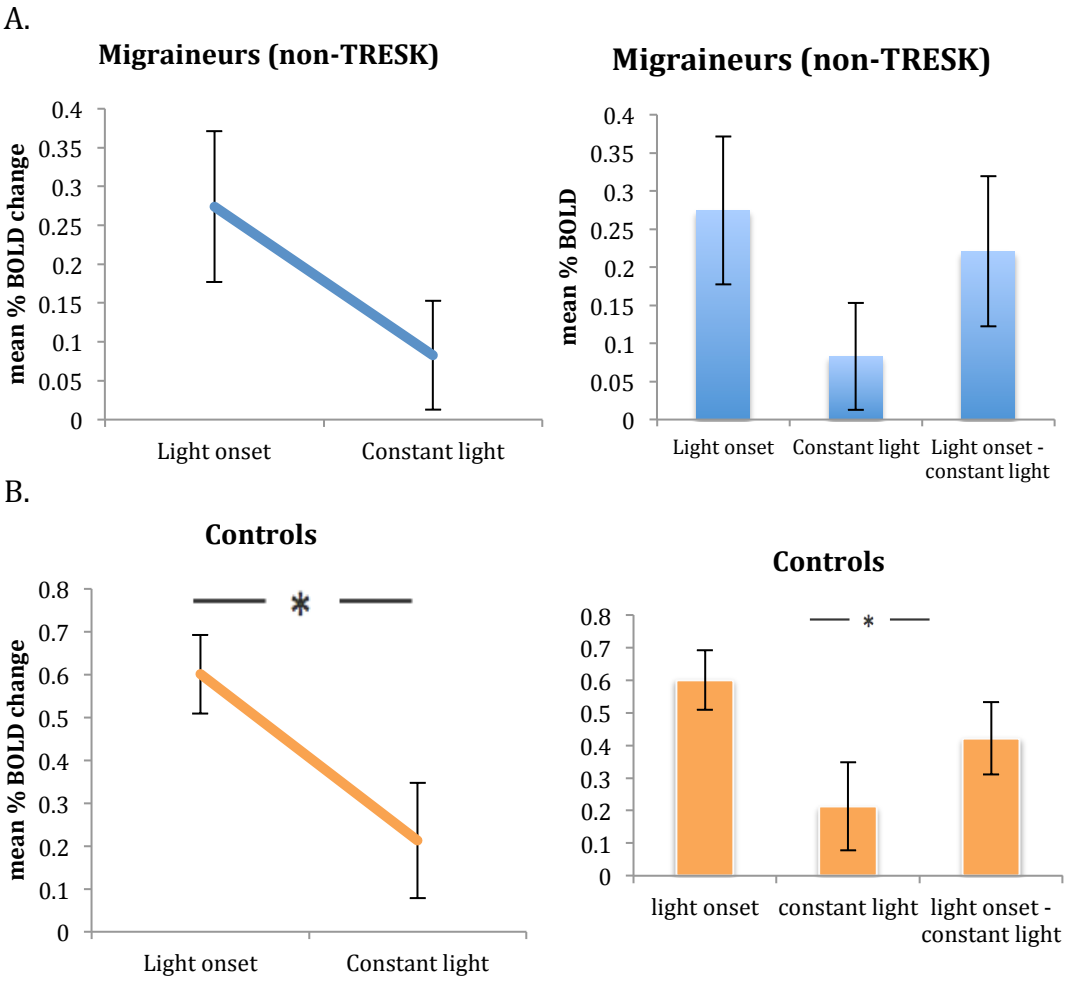

Figure 3.1 Within group signal comparison between light onset and constant light periods recorded at V1. A. Non-TRESK migraineurs B. controls. Signals were higher in light onset than constant light in both groups. The decline of signal along continuous illumination was defined as (light onset – contant light). Signals are presented as mean ± s.e.m. percentage of BOLD change. * $p < 0.05$ (2-tailed).

As shown in figure 3.2, mean percentage BOLD change at both light onset and constant light were lower in the non-TRESK migraineurs than controls. At light onset, activation of non-TRESK migraineurs was significantly lower than that of controls (t = -2.45; d.f. = 20; *p =0.024) but not in constant light (t = -0.86; d.f. = 20; p =0.40). In addition, the "light onset – constant light" magnitude was relatively lower in the non-TRESK migraineurs than controls, although the difference did not reach statistical significance (t = -1.35; d.f. = 20; p =0.19).

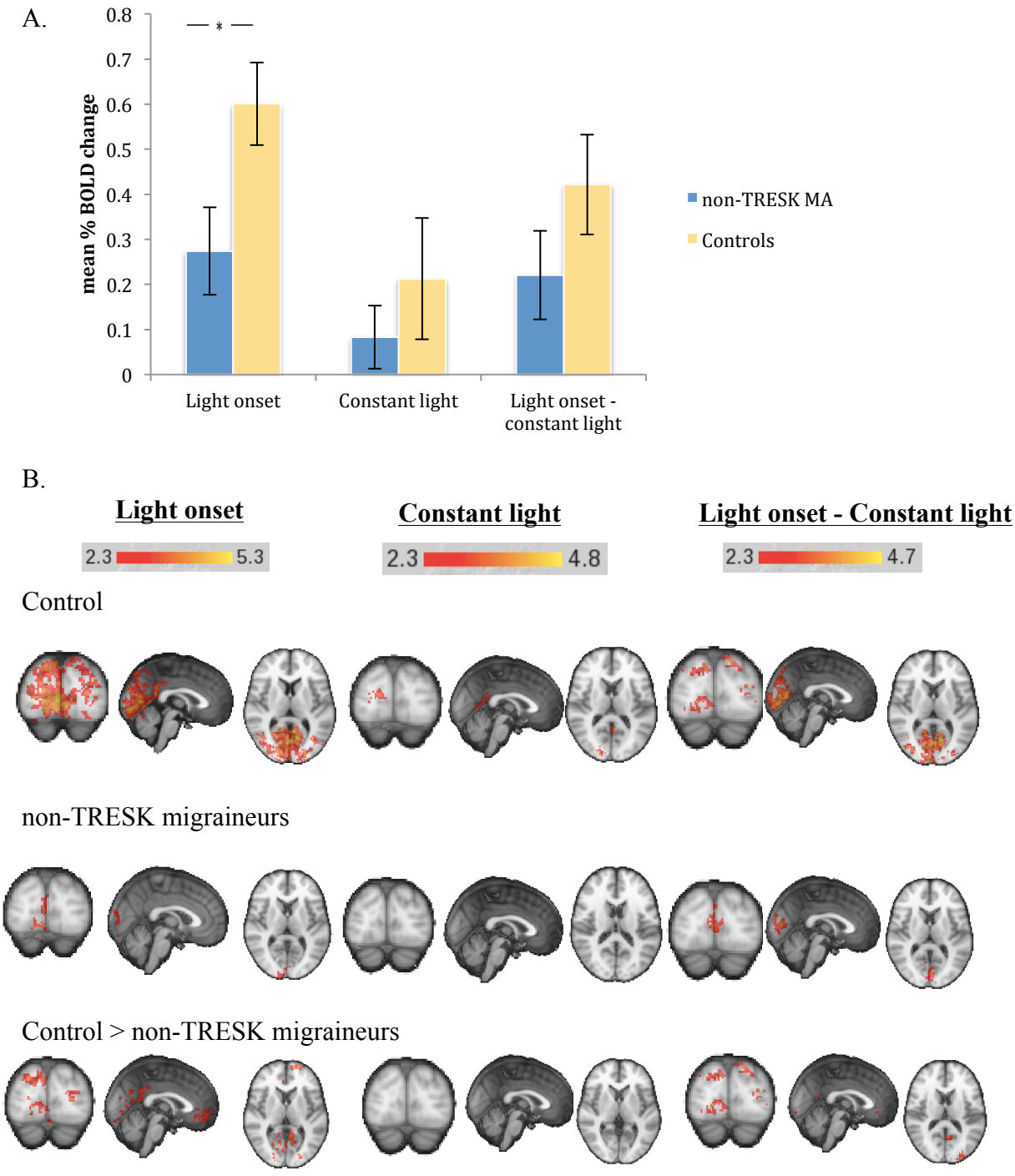

Figure 3.2 Between group signal comparison of the light onset, constant light and "light onset – constant light" at V1. **A.** Mean percentage BOLD change in light onset, constant light and their difference. Both responses evoked by light onset and constant light were lower in non-TRESK migraineurs than controls, in particular the signal at light onset. * $p < 0.05$ (2-tailed). Signals are presented as mean ± s.e.m. percentage of BOLD change. **B.** Brain images of group % BOLD change. Activations at V1 were lower in non-TRESK migraineurs compared to controls, both in light onset and constant light. Within group signal comparison showed higher responses elicited at light onset than constant light in both migraineurs and controls. Images were threshold using clusters determined by Z>2.3 with a corrected significance threshold of $p = 0.05$.

3.3.2 Visual sensitivity study – non-TRESK migraineurs and controls

Within group comparisons between low and high contrasts are shown in figure 3.3. As expected, a glance of the figures 3.3A and 3.3B revealed higher signals in high contrasts than low contrasts. Independent t-test comparisons between low and high contrasts revealed significant differences in the non-TRESK migraine group (t = -2.08; d.f. = 20; *p =0.05)) but not in normal controls (t = -1.71; d.f. = 18; p =0.08). However, this would not survive Bonferroni correction.

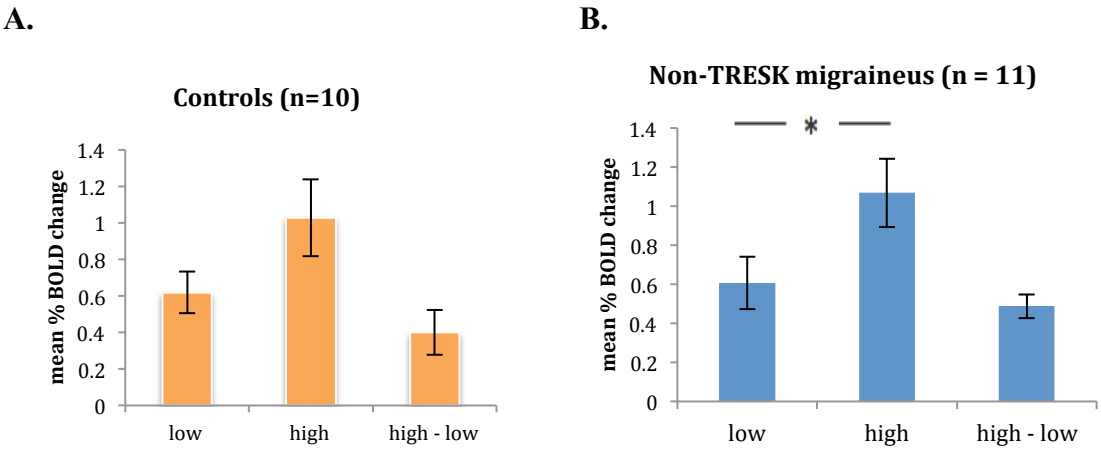

Figure 3.3 Cortical signals at V1 evoked by low and high contrast checkerboards. A. control group, B. non-TRESK migraineurs. In both groups, high contrast checkerboards elicited higher cortical signals than low contrast checkerboards. The difference between high and low contrast-induced signals are presented as (high – low). Signals are presented as mean ± s.e.m. percentage of BOLD change. * p < 0.05 (2-tailed).

Figure 3.4 showed the mean percentage BOLD change of the two groups (non-TRESK migraineurs [n=11] and normal controls [n=10]). There was no signal difference between the two groups in both low (t = -0.60; d.f. = 19; p =0.95) and high contrasts (t = 0.15; d.f. = 19; p =0.891). Neither was there any difference between the "high – low" contrasts (t = 0.654; d.f. = 19; p =0.10).

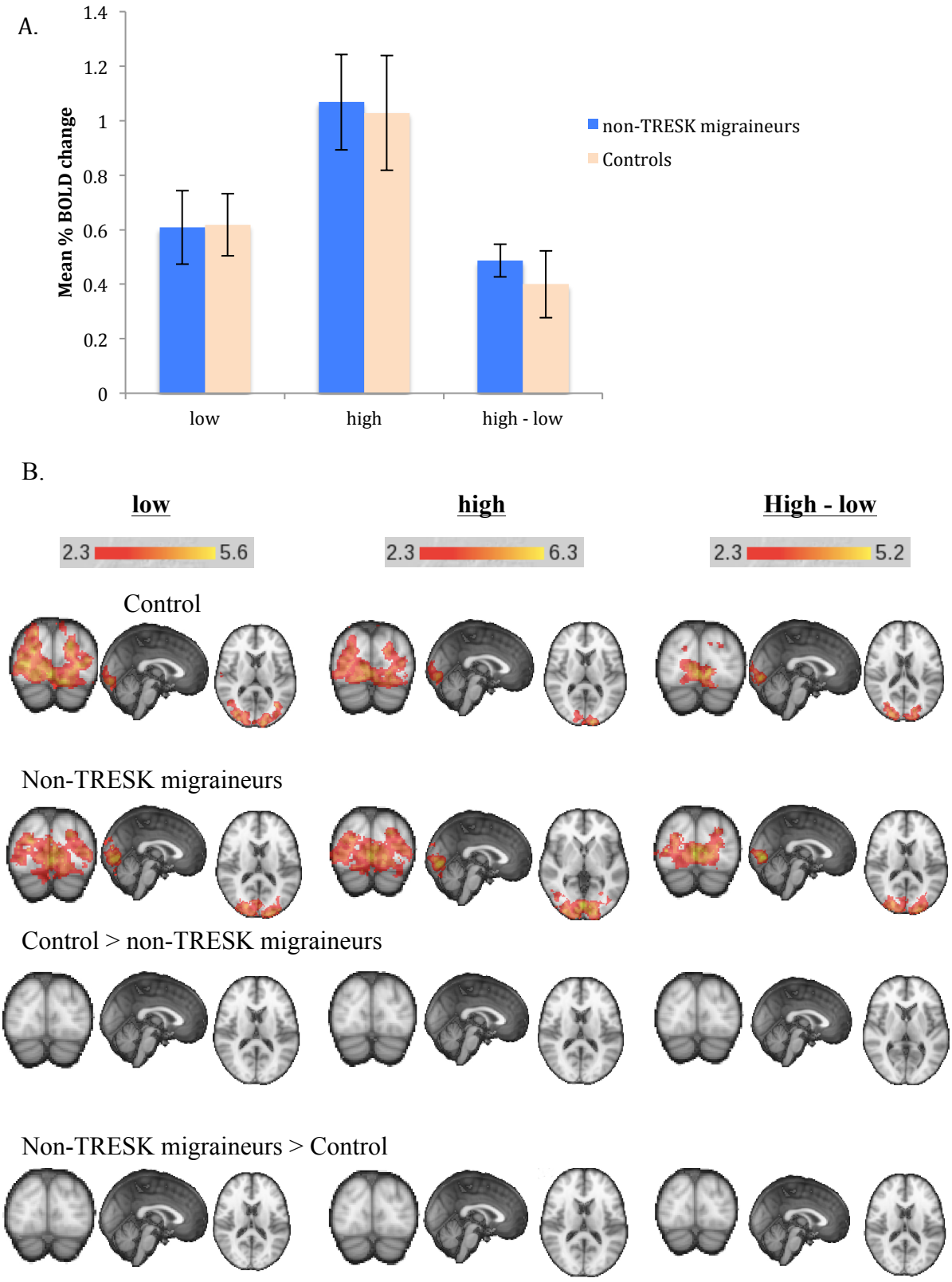

Figure 3.4. Between group signal comparison of low contrast, high contrast and their difference "high – low" at V1. **A**. Mean percentage BOLD change at V1 evoked by low and high contrasts, and their difference. No difference of cortical responses elicited by both low and high contrasts was found between groups. The differences between signals evoked by high and low contrasts were also comparable between groups. Signals are presented as mean ± s.e.m. percentage of BOLD change. **B.** Brain images of group % BOLD change. Activations at V1 induced by high contrasts were higher than low contrasts in both migraineurs and controls. A comparison of V1 signals between non-TRESK migraineurs and controls showed no significant difference. Images were threshold using clusters determined by Z>2.3 with a corrected significance threshold of $p = 0.05$.

3.3.3 Light adaptation study – TRESK migraineurs

Figure 3.5 and 3.6 illustrated the results of the light adaptation study. Subject 4 reported having fallen asleep during this part of the experiment and the result was thus excluded from the analysis. Individual analysis of the results showed that both subject 2 and 3 exhibited a diminished signal along the constant illumination (signals presented in figure 3.5 are means of percentage BOLD change ± standard deviations). Subject 1 showed a trend of relatively sustained activations in both the initial light onset and the remaining constant light periods. Figure 3.5B showed the individual light adaptation performance of the three subjects.

A.

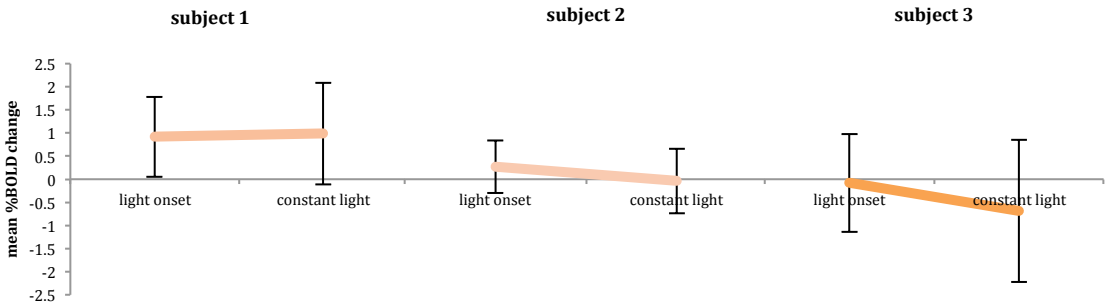

B.

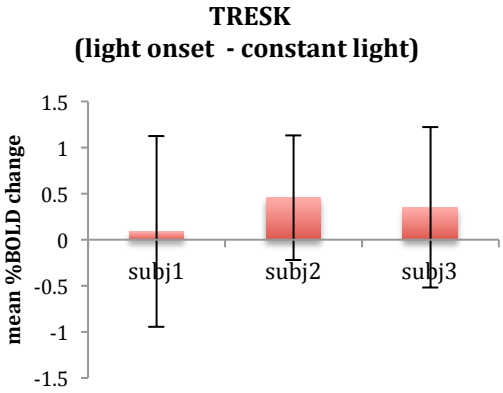

Figure 3.5 Individual results of Light Adaptation Study of TRESK subjects. **A**. BOLD signals of light onset and constant light periods at V1 **B.** Light adaptation magnitude (light onset – constant light) at V1. Signals are presented as percentage BOLD change ± standard deviation.

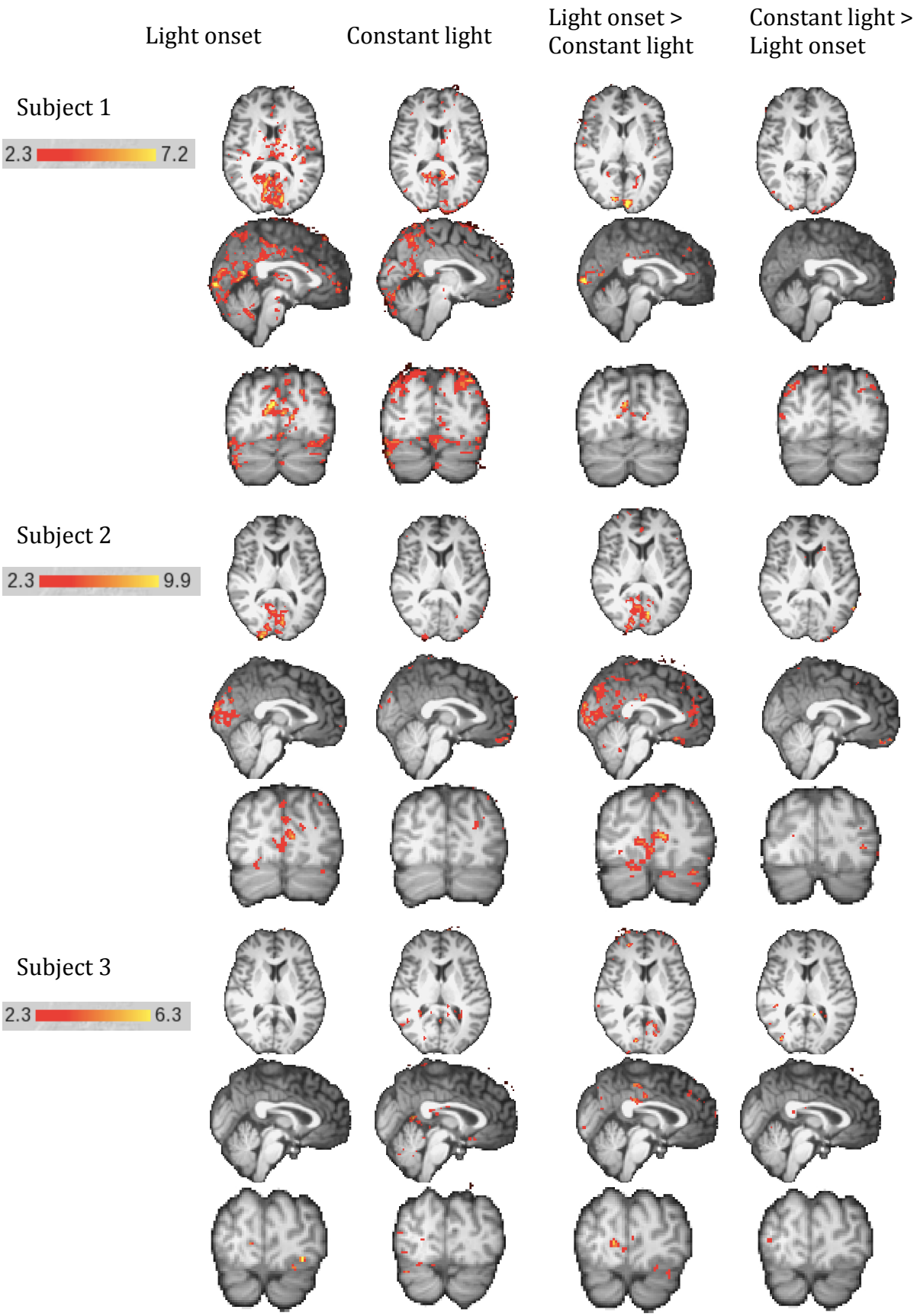

Figure 3.6 Individual results of TRESK migraneurs in the Light Adaptation Study. There is a trend showing higher signals at V1 elicited by light onset than constant light. Images were threshold using clusters determined by $Z > 2.3$ with a corrected cluster significance threshold of $p = 0.05$.

Due to the small sample size among the TRESK group, I attempted to compare the TRESK individual results with the group results of the other two groups (figure 3.7). Both light onset and constant light activations of TRESK subject 2 and 3 were lower than controls. Comparing with non-TRESK migraineurs, TRESK subject 2 exhibited an even lower response to both periods of light. TRESK subject 1, however, displayed the opposite trend by showing greater activations in both light onset and constant light. TRESK subject 2 and 3 had comparable degree of light adaptation with controls but subject 1 had negligible light adaptation.

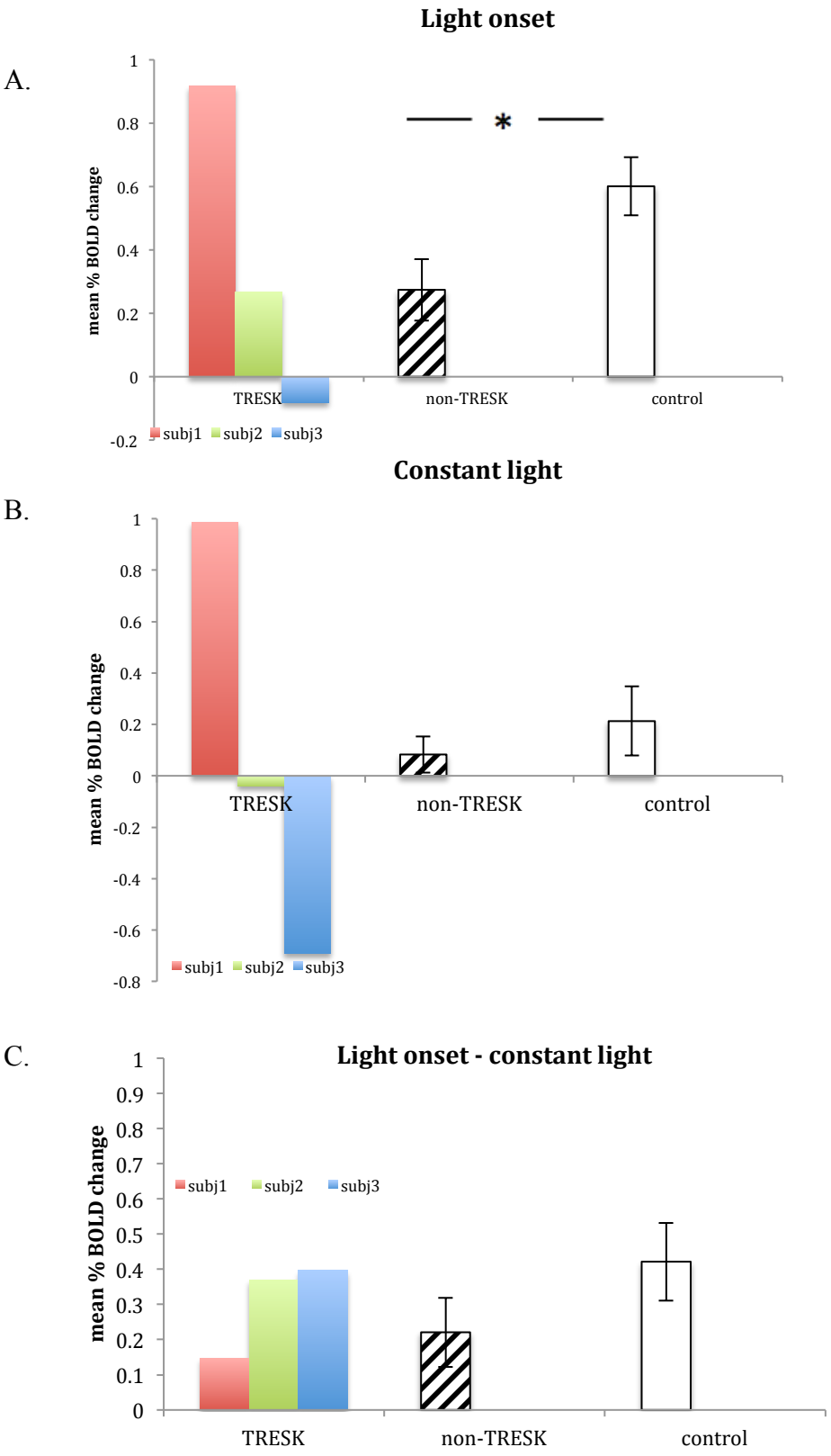

Figure 3.7 Between group comparison of light-induced signals at V1. **A.** light onset. Except TRESK subject 1 who exhibited higher response than controls and non-TRESK migraineurs, TRESK subject 2 and 3 showed relatively lower responses than controls **B.** constant light. TRESK subject 2 and 3 showed markedly reduced responses compared to other groups, whereas TRESK subject 1 showed a distinct response which was much higher than all the other subjects. **C**. "light onset – constant light". All subjects in the TRESK group showed higher responses evoked by light onset than constant light. Signals are presented either as mean ± s.e.m. for the non-TRESK migraineurs (shaded bars) and healthy controls(open bars), or as individual values (subject 1, 2, and 3 in red, green and blue bars respectively) in the TRESK subjects. *$p < 0.05$.

3.3.4 Visual sensitivity study – TRESK migraineurs and overall results

Group analysis showed significantly lower signal activations to low-contrast than high-contrast flickering checkerboards in the TRESK group(figure 3.8). Figure 3.9 showed the mean percentage BOLD change of the three groups of subjects (TRESK-associated migraineurs [n = 4], migraineurs with visual aura [n = 11] and healthy controls [n = 10]). In low contrasts, ANOVA showed a significant difference between the responses of the three groups [$F(2, 22) = 6.63$, $^{**}p < 0.01$]. Post-hoc t-tests showed significant difference between the TRESK group and the non-TRESK migraine group ($^{**}p < 0.01$) and between the TRESK group and controls ($^{**}p < 0.01$). In high contrasts, however, the three groups did not differ from each other [$F(2, 22) = 0.50$, $p = 0.62$], although it appeared that the response of the TRESK group may be lower than that of the non-TRESK migraine group. When comparing the signal difference of high and low contrasts, i.e. high – low, among the three groups, ANOVA showed significant difference [$F(2, 22) = 4.74$, $^{*}p < 0.05$]. Post-hoc t-tests revealed significant difference between the TRESK and the non-TRESK migraineurs ($^{*}p < 0.05$) and between the TRESK group and the controls ($^{*}p < 0.05$).

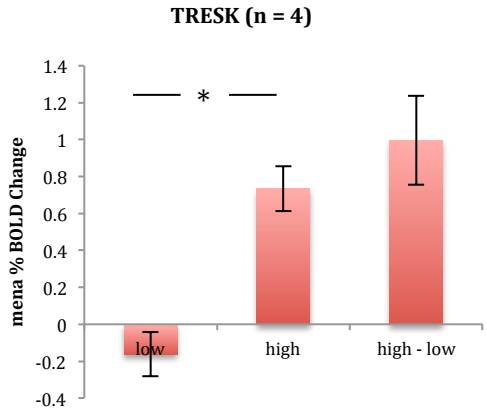

Figure 3.8 Group results for Visual Sensitivity Study of TRESK subjects. There was a significant difference between responses evoked by low and high contrasts recorded at V1. Signals are presented as mean ± s.e.m. % BOLD change. $^{*}p < 0.05$.

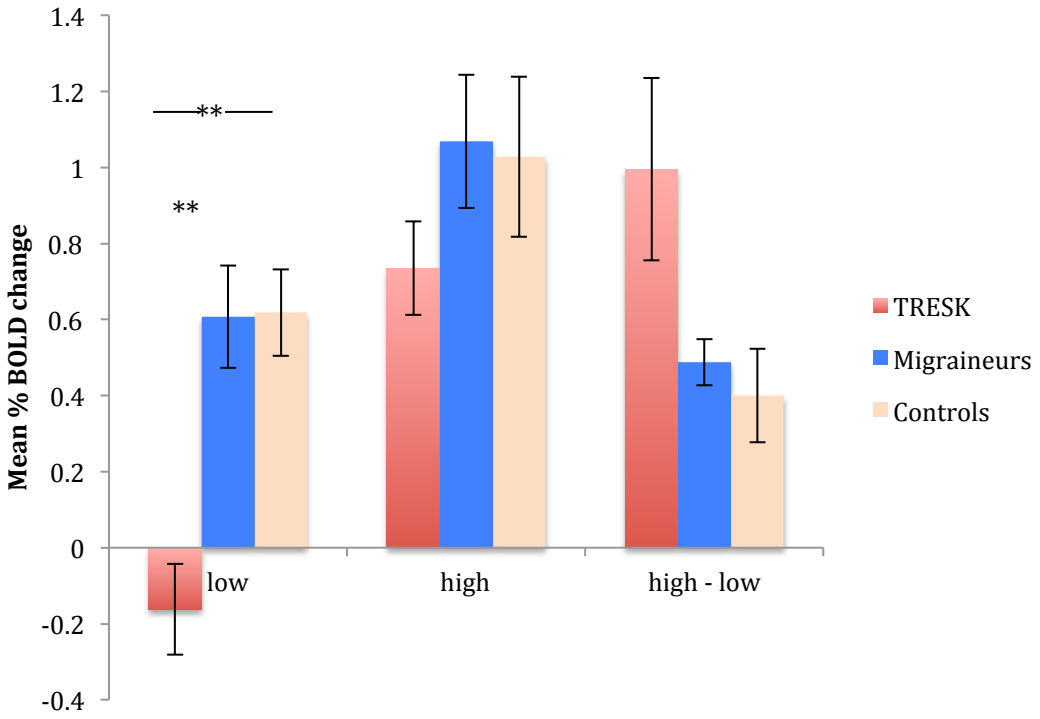

Figure 3.9. Between group signal comparison of signals evoked by low contrast, high contrast checkerboards and their difference "high – low" recorded at V1. When presented to low contrast checkerboards, TRESK subjects responded significantly lower than non-TRESK migraineurs and controls. However, there was no significant difference of signals evoked by high contrast checkerboards between groups. Signals are presented as mean ± s.e.m. % BOLD change. $^{**}p < 0.01$.

3.3.5 Correlation between frequency of attack and cortical activation evoked by diffuse constant illumination in non-TRESK migraine subjects

As shown in figure 3.10B and table 3.1, there was inverse correlation between the frequency of attack and the cortical activations at constant light period: $r(10) = -0.52$, $^*p < 0.05$, although this correlation did not survive a Bonferroni correction. However, there was no significant correlation between attack frequency and percentage BOLD change at onset of light, $r(10) = -0.32$, $p = 0.17$, figure 3.8A.

Migraine Subject no	Frequency of attack (month)	%BOLD change (light onset)	%BOLD change (constant light)
1	9	0.02	-0.22
3	5	0.17	-0.04
4	5	0.24	-0.15
5	4	0.94	0.25
6	8	-0.16	0.07
7	2	-0.09	-0.05
8	4	0.52	0.07
9	4.5	0.30	0.02
10	5	0.46	0.02
11	2	0.52	0.37
12	2.5	0.10	0.58

Table 3.1 Frequency of attack and cortical activations at V1 of non-TRESK migraineurs in response to diffuse constant illumination in the Light Adaptation experiment

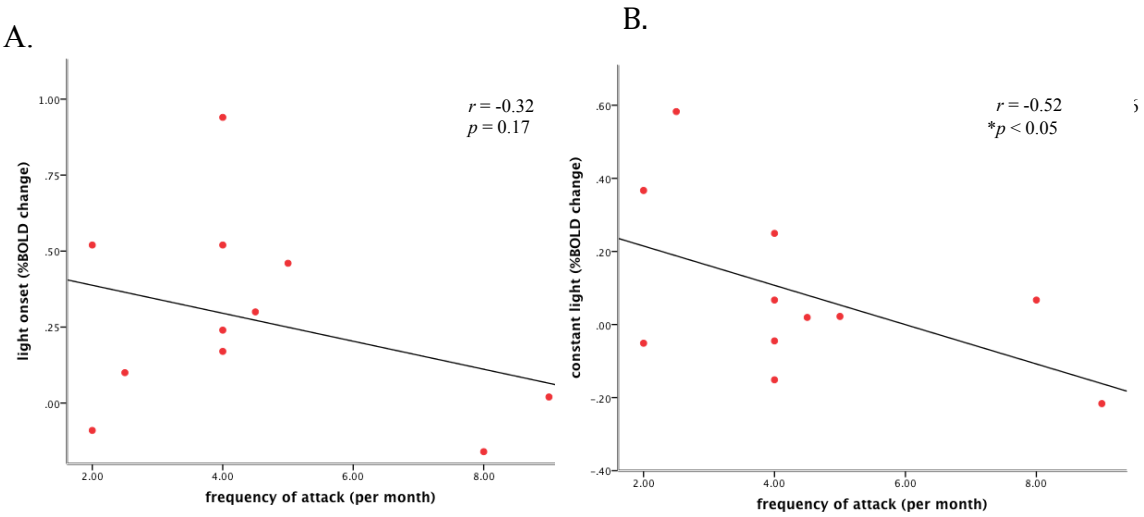

Figure 3.10. Light Adaptation experiment. Negative correlation between frequency of attack (per month) and **A.** %BOLD change evoked by diffuse constant illumination at light onset, $r(10) = -0.32$, $p = 0.17$, one-tailed. **B.** %BOLD change at constant light, $r(10) = -0.52$, $^*p < 0.05$, one-tailed.

3.3.6 Correlation between frequency of attack and cortical activation evoked by checkerboard stimuli in non-TRESK migraine subjects

As shown in figure 3.11 and table 3.2, there was no correlation between frequency of attack and the cortical activations evoked by either low or high contrast checkerboards: $r(10) = -0.12$, $p = 0.37$ and $r(10) = -0.32$, $p = 0.19$ respectively.

Migraine Subject no	Frequency of attack (month)	%BOLD change (low contrast)	%BOLD change (high contrast)
1	9	0.85	1.22
3	5	0.34	0.79
4	5	0.06	0.48
5	4	1.15	1.98
6	8	0.36	0.50
7	2	1.12	1.87
8	4	0.74	1.26
9	4.5	0.40	0.70
10	5	0.09	0.73
11	2	1.31	1.77
12	2.5	0.25	0.47

Table 3.2 Frequency of attack and cortical activations at V1 of non-TRESK migraineurs in response to flickering checkerboards in the Visual Sensitivity experiment.

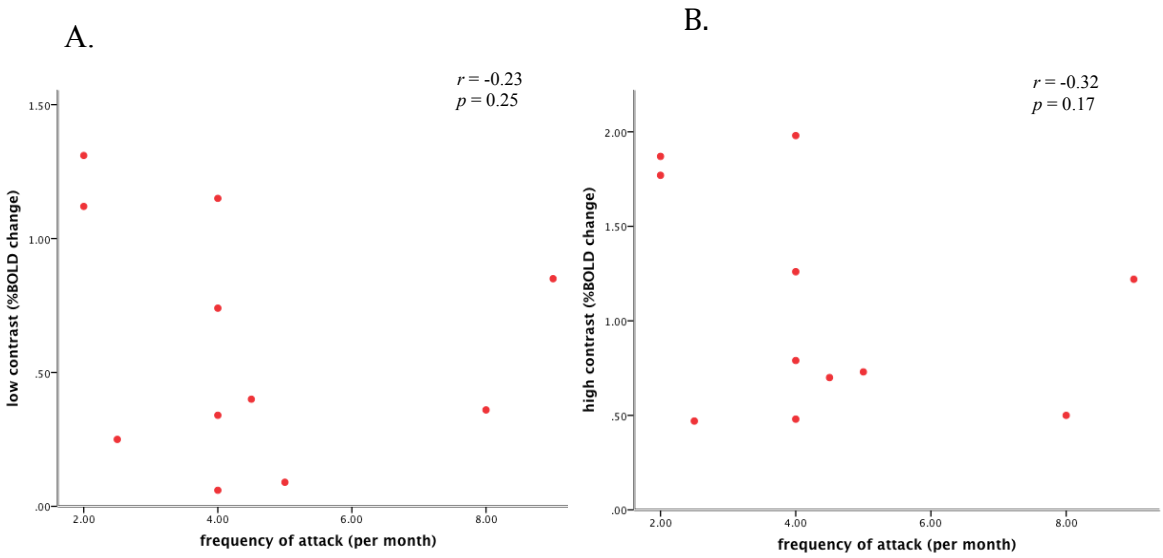

Figure 3.11. Visual Sensitivity Experiment. No correlation between frequency of attack (per month) and **A.** %BOLD change evoked by low contrast checkerboard, $r(10) = -0.23$, $p = 0.25$, one-tailed. **B.** %BOLD change to high contrast checkerboard, $r(10) = -0.32$, $p = 0.17$, one-tailed.

3.3.7 Comparison of cortical signal between prophylactic drug users and non-users in non-TRESK migraineurs

No difference of signal recorded during the light onset period of the diffuse continuous illumination was found between prophylactic drug users and non-users in migraineurs ($t = -0.81$, $df = 8$, $p = 0.441$).

Migraine subject	BOLD (light onset)	Prophylactic Medication
1	0.02	Topiramate
4	0.24	Pizotifen
6	-0.16	Almotriptan/Lamotrigine)
11	0.52	Pizotifen/Naratriptan
12	0.10	Amitriptyline

Table 3.3 % BOLD change evoked by initial light onset period of diffuse constant illumination in migraine subjects under prophylactic migraine medication.

Migraine subject	BOLD (light onset)	Abortive/other Medication
3	0.17	Sumatriptan
7	-0.09	Sumatriptan
8	0.52	Almotriptan
9	0.30	Botox
10	0.46	Nurofen express

Table 3.4 % BOLD change evoked by initial light onset period of diffuse constant illumination in migraine subjects without prophylactic migraine medication.

3.4. Discussion

3.4.1 Summary of findings

Under diffuse constant illumination, migraineurs exhibited a significantly lower visual cortical response compared to controls, especially during the initial "light onset" period. Along the continuous diffuse illumination, both groups showed decline of cortical activations, suggesting the presence of light adaptation. However, the non-TRESK migraine group revealed a relatively smaller magnitude of light adaptation compared to controls, although the difference did not reach statistical significance. Nevertheless, this reduced cortical activation in the non-TRESK migraineurs was not found in the Visual Sensitivity task, neither in response to low nor high contrasts. Inverse correlation between attack frequency and BOLD signal was only found in the latter constant light period, suggesting a trend that frequent attackers might exhibit a lower occipital response.

These findings were compared to the results in the TRESK study. Consistent with the results in non-TRESK migraineurs, 2 out of the 3 TRESK subjects showed lower occipital activations compared to controls, both in the light onset and constant light periods of the Light Adaptation experiment (figure 3.6). The remaining subject showed somewhat opposite results, with higher signals recorded at both periods of continuous illumination. More strikingly, the TRESK group exhibited a markedly reduced response to low contrast checkerboards in comparison to both non-TRESK

migraineurs and normal subjects (figure 3.8). At high contrasts, however, the groups were indistinguishable, suggesting it is specific to the lower contrasts.

Taken together, the experiments suggest that with diffuse light, migraineurs exhibited cortical hypo-excitability compared to controls. This finding was also observed in 2 of the 3 genetically homogeneous TRESK migraineurs, suggesting the presence of a reduced baseline level of cortical response towards continuous illumination, presumably a protective mechanism. There also seems to be a tendency that non-TRESK migraineurs displayed a reduced degree of light adaptation compared to controls, although it could be a floor effect due to the lower responses of the former at both onset of light and constant illumination. Nevertheless, the hypo-excitability appeared to normalize when exposed to the more aversive checkerboard stimuli. This pattern was also seen in the TRESK group who showed significantly reduced responses to low but not high contrast checkerboards. Finally, this notion of pre-activation cortical hypo-excitability as a protective mechanism in attack-free migraineurs appears to be supported by the inverse correlation between frequency of attacks and cortical activations that existed only in the milder form of diffuse continuous stimulation. Although the correlation was not significant in my study, a larger study population in the future might be warranted to support this trend.

3.4.2 Hypothesis of reduced cortical pre-activation

Our findings are supported by electrophysiology studies showing a deficit of habituation upon repetitive stimulation (Afra, et al., 1998) (Antal, et al., 2011) (Schoenen, Ambrosini, Sandor, & Maertens de Noordhout, 2003) (Valeriani, Fierro, & Brighina, 2007). This phenomenon was found in studies using repetitive visual (VEP) (Afra, et al., 1998) (Bohotin, et al., 2002) (Coppola et al., 2007) and auditory stimuli (Sand, Zhitniy, White, & Stovner, 2008) (Judit, Sandor, & Schoenen, 2000). Several hypotheses for this lack of cortical habituation in migraineurs have been proposed including the impairment of inhibitory processes (Welch, 2003), floor effect due to the low baseline excitability (Schoenen, et al., 2003) and hyper-responsiveness due to increased metabolic demand (Antal, et al., 2011). Yet, a more plausible interpretation of the lack of habituation between attacks has been suggested by a number of VEP studies – decreased pre-activation level of the visual cortex (Afra, et al., 1998) (Coppola, et al., 2009) (Judit, et al., 2000) (Bohotin, et al., 2002). For example, the N1-P1 and P1-N2 amplitudes of the first block of VEP during a 15min of repetitive stimulation were found to be lower in attack-free migraineurs than controls(Afra, et al., 1998). The low initial VEP amplitude was also found to be inversely proportional to the amplitude change in consecutive stimulation, suggesting that the lack of habituation of attack-free migraineurs may be dependent on the low level of cortical pre-activation (Afra, Proietti Cecchini, Sandor, & Schoenen, 2000) (Coppola et al., 2007). Taken together, this line of evidence generally indicates that the initial VEP amplitudes in migraineurs are lower than in healthy subjects, suggesting that a reduced level of cortical pre-activation, i.e. hypo-excitability, may exist in migraineurs between attacks.

The findings in the current study are in accordance with the reduced cortical pre-activation hypothesis in VEP studies. First, the two fMRI tasks in the current study revealed somewhat distinct results, with the continuous diffuse light exposure generally eliciting lower activations in TRESK and non-TRESK migraineurs than controls and the checkerboard task tended to evoke no difference of response between groups. Indeed, the two tasks can be viewed as two levels of visual stimuli. Since flickering checkerboards are established visual triggers for migraine and are frequently reported as causing visual discomfort (Wilkins et al., 1984), continuous diffuse light exposure is presumably a milder level of stimulation compared to the former. Accordingly, it can be hypothesized that in response to a milder form of visual stimuli between attacks such as the diffuse constant light exposure in the present study, the visual cortices of migraineurs exhibit hypo-excitability or reduced cortical pre-activation, presumably serving as a protective mechanism against the development of attacks(Coppola, et al., 2009). However, in response to stronger and more aversive photic stimuli such as the flickering checkerboards, this interictal protective mechanism is overwhelmed and a normal cortical response is displayed– no difference in BOLD change between migraineurs and controls when presented to both low and high contrast checkerboards. Since TRESK migraineurs can be seen as an extreme of the spectrum of MA based on their genetic homogeneity and physiological property of altered neuronal excitability (details will be discussed in chapter 4), this hypothesis of pre-activation cortical hypo-excitability was supported by the findings in 2 of our 3 TRESK subjects showing attenuated cortical responses compared to controls. More strikingly, the protective hypo-excitable state of TRESK MA to continuous illumination further extended towards the more aversive level of stimulation, i.e. low contrast checkerboard. Beyond this level of visual stimulation,

the cortical hypo-excitability normalized again in response to high contrast checkerboards.

Our correlation analysis also provides additional insights and evidence into the hypothesis of pre-activation cortical hypo-excitability. Assuming that hypo-excitability serves as a role of protection against future attacks, the inverse correlation between attack frequency and cortical activations may explain how the visual cortices of migraineurs with more frequent attacks responded less towards mild visual stimuli in order to avoid the onset of a triggered attack. This protective mechanism, however, may not exist in the more aversive form of stimuli, the checkerboards, as demonstrated by the absence of correlation between attack frequency and the former. Our interpretation that visual cortex is hypo-excitable to diffuse light exposure between attacks also parallels to the clinical observation that migraineurs often find ordinary luminous light intolerable during attacks but not between attacks.

3.4.3 Controversies and plausible explanations

A possible explanation for the discordancy of results in neuroimaging studies could be that cortical responsiveness and the degree of habituation may depend on the stimulus paradigm. Notably, I used different methods of visual stimuli, i.e. flickering checkerboards and diffuse continuous illumination, as compared to the square-wave gratings (J. Huang, et al., 2003) and angulated incongruent lines (Vincent, et al., 2003) in two other imaging studies that supported cortical hyperexcitability in migraine. Indeed, a study showed that the BOLD signal at visual cortex remained constant during the entire 6min of flashing light stimulation at 10Hz, whereas signal

declined rapidly to baseline after 1min of non-flashing constant illumination(Bandettini et al., 1997). This suggests that the type as well as temporal and spatial frequencies of the stimuli (Coppola, et al., 2009) may affect the ability of the stimuli to differentiate the cortical excitability between migraineurs and healthy controls.

Second, migraine is a fluctuating disease that is closely related to ongoing biological status such as circadian rhythm(Alstadhaug, Salvesen, & Bekkelund, 2008), sex hormone (MacGregor, Frith, Ellis, Aspinall, & Hackshaw, 2006), food intake (Finocchi & Sivori, 2012) and stress level (Sauro & Becker, 2009). While all these factors should be taken into account, controlling all of them may not be feasible. In the current study, we limited our study population to female subjects and performed the scans between 8am and 12pm in order to minimize the confounding factors due to sex dimorphism and circadian cycle. A more sophisticated experimental design would have been performed based on the same phase of menstrual cycle. Nevertheless, the findings of the present study consisting of mainly female subjects (only one male TRESK subject in the checkerboard task) may not be generalized to both sexes.

Another important consideration is the phase of migraine cycle being investigated. An fMRI BOLD study explored the dynamic trend of cortical signal change of visually-triggered migraine attacks and showed that the onset of headache was preceded by suppression of initial activation(Cao, et al., 1999). Recently, by recording the TMS-induced phosphene threshold in migraineurs during peri-ictal period, Siniatchkin et al. showed that occipital excitability was attenuated 1 to 2 days before migraine attack(Siniatchkin et al., 2009). Consistent with these results, a longitudinal

EEG study showed increased EEG slowing within 36 hours before migraine attacks, suggesting that hypoexcitability may be associated with attack initiation(Bjork, Stovner, Hagen, & Sand, 2011). These studies indicate that there is a tendency of attenuation of cortical excitability towards the onset of migraine attack. Intriguingly, all our migraine subjects were attack-free within 24hours prior to the scans and most experienced either headache or visual discomfort 24hours after the study. An important question remains to be answered is whether the cortical hypoexcitability I observed simply reflects the interictal cortical state of migraineurs or is the early stage of a natural onset of migraine attack.

Subject 1 of TRESK group is the only exception to our hypothesis. Diffuse constant illumination elicited higher cortical responses compared to all migraineurs and controls. Further investigation revealed that this particular subject intentionally stopped her prophylactic medication, verapamil, for 2 weeks prior to the scan. Conversely, two other TRESK subjects and 5 out the 12non-TRESK migraineurs reported to have taken migraine prophylaxis. These medications included calcium channel blockers, Pizotifen, Amitriptyline, Topiramate and Lamotrigine (table 2.1 and 2.2). Arguably, although the compliance of prophylaxis in these migraineurs cannot be traced due to the lack of information, the hypo-excitability found in our study could be due to the effect of prophylaxis rather than the disease per se. In fact, studies have shown that the cortical excitability, as measured by TMS-induced phosphene threshold, of migraineurs treated with several types of migraine prophylaxis such as propranolol, levetiracetam, valproate and Topiramate was reduced compared to medication-free patients (Mulleners, Chronicle, Vredeveld, & Koehler, 2002) (Young,

Shaw, Bloom, & Gebeline-Myers, 2008) (Aurora, Barrodale, Vermaas, & Rudra, 2010) (Gerwig, Niehaus, Stude, Katsarava, & Diener, 2012). However, comparison of signals in subjects with and without prophylactic migraine treatment showed no significant difference. A plausible explanation for the relatively higher cortical responses in TRESK subject 1 would, therefore, be a rebound phenomenon after medication withdrawal. Nevertheless, another more plausible explanation could be that this particular subject was experiencing a developing migraine attack that either occurred naturally or induced by the prior diffuse continuous illumination, albeit there was a two hour gap between the scan and the actual onset of visual aura.

3.5 Conclusion

The aim of the current study was to explore the interictal cortical excitability non-TRESK and TRESK migraineurs using two photic stimulation tasks – the diffuse constant white light stimulation and the flickering checkerboards. Consistent with the hypothesis of reduced pre-activation cortical hypo-excitability, our findings indicate that migraineurs were hyporeactive to diffuse constant illumination, suggesting the presence of interictal cortical hypo-excitability as a protective mechanism. Any visual stimuli exceeding this level, such as the flickering checkerboards, would possibly normalize the cortical response and potentially trigger a migraine attack.

3.6 Reference

Aderjan, D., Stankewitz, A., & May, A. (2010). Neuronal mechanisms during repetitive trigemino-nociceptive stimulation in migraine patients. *Pain, 151*(1), 97-103.

Afra, J., Mascia, A., Gerard, P., Maertens de Noordhout, A., & Schoenen, J. (1998). **Visual evoked potentials** during long periods of pattern-reversal stimulation in migraine. *Brain,* 121, 233-241.

Afra, J., Proietti Cecchini, A., Sandor, P. S., & Schoenen, J. (2000). Comparison of visual and auditory evoked cortical potentials in migraine patients between attacks. *Clinical neurophysiology : official journal of the International Federation of Clinical Neurophysiology, 111*(6), 1124-1129.

Alstadhaug, K., Salvesen, R., & Bekkelund, S. (2008). 24-hour distribution of migraine attacks. *Headache, 48*(1), 95-100.

Antal, A., Polania, R., Saller, K., Morawetz, C., Schmidt-Samoa, C., Baudewig, J., . . . Dechent, P. (2011). Differential activation of the middle-temporal complex to visual stimulation in migraineurs. *Cephalalgia : an international journal of headache, 31*(3), 338-345.

Aurora, S. K., Ahmad, B. K., Welch, K. M., Bhardhwaj, P., & Ramadan, N. M. (1998). Transcranial magnetic stimulation confirms hyperexcitability of occipital cortex in migraine. *Neurology, 50*(4), 1111-1114.

Aurora, S. K., al-Sayeed, F., & Welch, K. M. (1999). The cortical silent period is shortened in migraine with aura. *Cephalalgia : an international journal of headache, 19*(8), 708-712.

Aurora, S. K., Barrodale, P., Chronicle, E. P., & Mulleners, W. M. (2005). Cortical inhibition is reduced in chronic and episodic migraine and demonstrates a spectrum of illness. *Headache, 45*(5), 546-552.

Aurora, S. K., Barrodale, P. M., Tipton, R. L., & Khodavirdi, A. (2007). Brainstem dysfunction in chronic migraine as evidenced by neurophysiological and positron emission tomography studies. *Headache, 47*(7), 996-1003; discussion 1004-1007.

Aurora, S. K., Barrodale, P. M., Vermaas, A. R., & Rudra, C. B. (2010). Topiramate modulates excitability of the occipital cortex when measured by transcranial magnetic stimulation. *Cephalalgia : an international journal of headache, 30*(6), 648-654.

Aurora, S. K., Cao, Y., Bowyer, S. M., & Welch, K. M. (1999). The occipital cortex is hyperexcitable in migraine: experimental evidence. *Headache, 39*(7), 469-476.

Aurora, S. K., Welch, K. M., & Al-Sayed, F. (2003). The threshold for phosphenes is lower in migraine. *Cephalalgia : an international journal of headache, 23*(4), 258-263.

Bandettini, P. A., Kwong, K. K., Davis, T. L., Tootell, R. B., Wong, E. C., Fox, P. T., . . . Rosen, B. R. (1997). Characterization of cerebral blood oxygenation and flow changes during prolonged brain activation. *Human brain mapping, 5*(2), 93-109.

Bjork, M., Stovner, L. J., Hagen, K., & Sand, T. (2011). What initiates a migraine attack? Conclusions from four longitudinal studies of quantitative EEG and steady-state visual-evoked potentials in migraineurs. *Acta neurologica Scandinavica. Supplementum*(191), 56-63.

Bohotin, V., Fumal, A., Vandenheede, M., Gerard, P., Bohotin, C., Maertens de Noordhout, A., & Schoenen, J. (2002). Effects of repetitive transcranial magnetic stimulation on visual evoked potentials in migraine. [Research Support, Non-U.S. Gov't]. *Brain : a journal of neurology, 125*(Pt 4), 912-922.

Boulloche, N., Denuelle, M., Payoux, P., Fabre, N., Trotter, Y., & Geraud, G. (2010). Photophobia in migraine: an interictal PET study of cortical hyperexcitability and its modulation by pain. *Journal of neurology, neurosurgery, and psychiatry, 81*(9), 978-984.

Bramanti, P., Grugno, R., Vitetta, A., Di Bella, P., Muscara, N., & Nappi, G. (2005). Migraine with and without aura: electrophysiological and functional neuroimaging evidence. *Functional neurology, 20*(1), 29-32.

Cao, Y., Aurora, S. K., Nagesh, V., Patel, S. C., & Welch, K. M. (2002). Functional MRI-BOLD of brainstem structures during visually triggered migraine. *Neurology, 59*(1), 72-78.

Cao, Y., Welch, K. M., Aurora, S., & Vikingstad, E. M. (1999). Functional MRI-BOLD of visually triggered headache in patients with migraine. *Archives of neurology, 56*(5), 548-554.

Chronicle, E. P., & Mulleners, W. M. (1996). Visual system dysfunction in migraine: a review of clinical and psychophysical findings. *Cephalalgia : an international journal of headache, 16*(8), 525-535; discussion 523.

Coppola, G., Ambrosini, A., Di Clemente, L., Magis, D., Fumal, A., Gerard, P., . . . Schoenen, J. (2007). Interictal abnormalities of gamma band activity in visual evoked responses in migraine: an indication of thalamocortical dysrhythmia? *Cephalalgia : an international journal of headache, 27*(12), 1360-1367.

Coppola, G., Pierelli, F., & Schoenen, J. (2007). Is the cerebral cortex hyperexcitable or hyperresponsive in migraine? *Cephalalgia : an international journal of headache, 27*(12), 1427-1439.

Coppola, G., Pierelli, F., & Schoenen, J. (2009). Habituation and migraine. *Neurobiology of learning and memory, 92*(2), 249-259.

Coutts, L. V., Cooper, C. E., Elwell, C. E., & Wilkins, A. J. (2012). Time course of the haemodynamic response to visual stimulation in migraine, measured using near-infrared spectroscopy. *Cephalalgia : an international journal of headache*.

Dalkara, T., Zervas, N. T., & Moskowitz, M. A. (2006). From spreading depression to the trigeminovascular system. [Review]. *Neurological sciences : official journal of the Italian Neurological Society and of the Italian Society of Clinical Neurophysiology, 27 Suppl 2*, S86-90. doi: 10.1007/s10072-006-0577-z

Demarquay, G., Royet, J. P., Mick, G., & Ryvlin, P. (2008). Olfactory hypersensitivity in migraineurs: a H(2)(15)O-PET study. *Cephalalgia : an international journal of headache, 28*(10), 1069-1080.

Denuelle, M., Boulloche, N., Payoux, P., Fabre, N., Trotter, Y., & Geraud, G. (2011). A PET study of photophobia during spontaneous migraine attacks. *Neurology, 76*(3), 213-218.

Drummond, P. D. (1986). A quantitative assessment of photophobia in migraine and tension headache. *Headache, 26*(9), 465-469.

Finocchi, C., & Sivori, G. (2012). Food as trigger and aggravating factor of migraine. *Neurological sciences : official journal of the Italian Neurological Society and of the Italian Society of Clinical Neurophysiology, 33 Suppl 1*, S77-80.

Fumal, A., Bohotin, V., Vandenheede, M., & Schoenen, J. (2003). Transcranial magnetic stimulation in migraine: a review of facts and controversies. *Acta neurologica Belgica, 103*(3), 144-154.

Gerwig, M., Niehaus, L., Stude, P., Katsarava, Z., & Diener, H. C. (2012). Beta-blocker migraine prophylaxis affects the excitability of the visual cortex as revealed by transcranial magnetic stimulation. *The journal of headache and pain, 13*(1), 83-89.

Hallett, M. (2000). Transcranial magnetic stimulation and the human brain. *Nature, 406*(6792), 147-150.

Huang, D. Y., Yu, B. W., & Fan, Q. W. (2008). Roles of TRESK, a novel two-pore domain K+ channel, in pain pathway and general anesthesia. *Neuroscience bulletin, 24*(3), 166-172.

Huang, J., Cooper, T. G., Satana, B., Kaufman, D. I., & Cao, Y. (2003). Visual distortion provoked by a stimulus in migraine associated with hyperneuronal activity. *Headache, 43*(6), 664-671.

The International Classification of Headache Disorders: 2nd edition. (2004). *Cephalalgia : an international journal of headache, 24 Suppl 1*, 9-160.

Jan, J. E., Groenveld, M., & Anderson, D. P. (1993). Photophobia and cortical visual impairment. *Developmental medicine and child neurology, 35*(6), 473-477.

Judit, A., Sandor, P. S., & Schoenen, J. (2000). Habituation of visual and intensity dependence of auditory evoked cortical potentials tends to normalize just before and during the migraine attack. *Cephalalgia : an international journal of headache, 20*(8), 714-719.

Lafreniere, R. G., Cader, M. Z., Poulin, J. F., Andres-Enguix, I., Simoneau, M., Gupta, N., . . . Rouleau, G. A. (2010). A dominant-negative mutation in the TRESK potassium channel is linked to familial migraine with aura. *Nature medicine, 16*(10), 1157-1160.

Lauritzen, M. (1994). Pathophysiology of the migraine aura. The spreading depression theory. *Brain : a journal of neurology, 117 (Pt 1)*, 199-210.

Lebensohn, J. E. (1951). Photophobia: mechanism and implications. *American journal of ophthalmology, 34*(9), 1294-1300.

MacGregor, E. A., Frith, A., Ellis, J., Aspinall, L., & Hackshaw, A. (2006). Incidence of migraine relative to menstrual cycle phases of rising and falling estrogen. *Neurology, 67*(12), 2154-2158.

Maleki, N., Becerra, L., Brawn, J., Bigal, M., Burstein, R., & Borsook, D. (2012). Concurrent functional and structural cortical alterations in migraine. *Cephalalgia : an international journal of headache*.

Martin, H., del Rio, M. S., de Silanes, C. L., Alvarez-Linera, J., Hernandez, J. A., & Pareja, J. A. (2011). Photoreactivity of the occipital cortex measured by functional magnetic resonance imaging-blood oxygenation level dependent in migraine patients and healthy volunteers: pathophysiological implications. [Research Support, Non-U.S. Gov't]. *Headache, 51*(10), 1520-1528.

Mekle, R., Mlynarik, V., Gambarota, G., Hergt, M., Krueger, G., & Gruetter, R. (2009). MR spectroscopy of the human brain with enhanced signal intensity at ultrashort echo times on a clinical platform at 3T and 7T. *Magnetic resonance in medicine : official journal of the Society of Magnetic Resonance in Medicine / Society of Magnetic Resonance in Medicine, 61*(6), 1279-1285.

Montagna, P. (2008). Migraine: a genetic disease? *Neurological sciences : official journal of the Italian Neurological Society and of the Italian Society of Clinical Neurophysiology, 29 Suppl 1*, S47-51.

Moulton, E. A., Becerra, L., Maleki, N., Pendse, G., Tully, S., Hargreaves, R., . . . Borsook, D. (2011). Painful heat reveals hyperexcitability of the temporal pole in interictal and ictal migraine States. *Cerebral cortex, 21*(2), 435-448.

Moulton, E. A., Burstein, R., Tully, S., Hargreaves, R., Becerra, L., & Borsook, D. (2008). Interictal dysfunction of a brainstem descending modulatory center in migraine patients. *PloS one, 3*(11), e3799.

Mulleners, W. M., Chronicle, E. P., Vredeveld, J. W., & Koehler, P. J. (2002). Visual cortex excitability in migraine before and after valproate prophylaxis: a pilot study using TMS. *European journal of neurology : the official journal of the European Federation of Neurological Societies, 9*(1), 35-40.

Noseda, R., & Burstein, R. (2011). Advances in understanding the mechanisms of migraine-type photophobia. *Current opinion in neurology, 24*(3), 197-202.

Noseda, R., Kainz, V., Jakubowski, M., Gooley, J. J., Saper, C. B., Digre, K., & Burstein, R. (2010). A neural mechanism for exacerbation of headache by light. *Nature neuroscience, 13*(2), 239-245.

Russell, M. B., & Olesen, J. (1996). Migrainous disorder and its relation to migraine without aura and migraine with aura. A genetic epidemiological study. *Cephalalgia : an international journal of headache, 16*(6), 431-435.

Russo, A., Tessitore, A., Esposito, F., Marcuccio, L., Giordano, A., Conforti, R., . . . Tedeschi, G. (2012). Pain processing in patients with migraine: an event-related fMRI study during trigeminal nociceptive stimulation. *Journal of neurology*.

Sand, T., & Vingen, J. V. (2000). Visual, long-latency auditory and brainstem auditory evoked potentials in migraine: relation to pattern size, stimulus intensity, sound and light discomfort thresholds and pre-attack state. *Cephalalgia : an international journal of headache, 20*(9), 804-820.

Sand, T., Zhitniy, N., White, L. R., & Stovner, L. J. (2008). Brainstem auditory-evoked potential habituation and intensity-dependence related to serotonin metabolism in migraine: a longitudinal study. *Clinical neurophysiology : official journal of the International Federation of Clinical Neurophysiology, 119*(5), 1190-1200.

Sauro, K. M., & Becker, W. J. (2009). The stress and migraine interaction. *Headache, 49*(9), 1378-1386.

Schoenen, J., Ambrosini, A., Sandor, P. S., & Maertens de Noordhout, A. (2003). Evoked potentials and transcranial magnetic stimulation in migraine: published data and viewpoint on their pathophysiologic significance. *Clinical neurophysiology : official journal of the International Federation of Clinical Neurophysiology, 114*(6), 955-972.

Shepherd, A. J. (2000). Visual contrast processing in migraine. *Cephalalgia : an international journal of headache, 20*(10), 865-880.

Siniatchkin, M., Reich, A. L., Shepherd, A. J., van Baalen, A., Siebner, H. R., & Stephani, U. (2009). Peri-ictal changes of cortical excitability in children suffering from migraine without aura. *Pain, 147*(1-3), 132-140.

Siniatchkin, M., Sendacki, M., Moeller, F., Wolff, S., Jansen, O., Siebner, H., & Stephani, U. (2011). Abnormal Changes of Synaptic Excitability in Migraine with Aura. *Cerebral cortex*.

Stewart, W. F., Shechter, A., & Rasmussen, B. K. (1994). Migraine prevalence. A review of population-based studies. *Neurology, 44*(6 Suppl 4), S17-23.

Valeriani, M., Fierro, B., & Brighina, F. (2007). Brain excitability in migraine: hyperexcitability or inhibited inhibition? *Pain, 132*(1-2), 219-220; author reply 220-212. doi: 10.1016/j.pain.2007.08.016

Vanagaite, J., Pareja, J. A., Storen, O., White, L. R., Sand, T., & Stovner, L. J. (1997). Light-induced discomfort and pain in migraine. *Cephalalgia : an international journal of headache, 17*(7), 733-741.

Vincent, M., Pedra, E., Mourao-Miranda, J., Bramati, I. E., Henrique, A. R., & Moll, J. (2003). Enhanced interictal responsiveness of the migraineous visual cortex to incongruent bar stimulation: a functional MRI visual activation study. *Cephalalgia : an international journal of headache, 23*(9), 860-868.

Welch, K. M. (2003). Concepts of migraine headache pathogenesis: insights into mechanisms of chronicity and new drug targets. *Neurological sciences : official journal of the Italian Neurological Society and of the Italian Society of Clinical Neurophysiology, 24 Suppl 2*, S149-153.

Wilkins, A., Nimmo-Smith, I., Tait, A., McManus, C., Della Sala, S., Tilley, A., . . . Scott, S. (1984). A neurological basis for visual discomfort. *Brain : a journal of neurology, 107 (Pt 4)*, 989-1017.

Young, W., Shaw, J., Bloom, M., & Gebeline-Myers, C. (2008). Correlation of increase in phosphene threshold with reduction of migraine frequency: observation of levetiracetam-treated subjects. *Headache, 48*(10), 1490-1498.

Chapter 4

Glutamate, GABA and NAA Levels at Interictal Migraine Visual Cortex

4.1 Introduction

Magnetic resonance spectroscopy is a non-invasive technique that is employed for the study of cerebral metabolic changes(Gujar, Maheshwari, Bjorkman-Burtscher, & Sundgren, 2005). It has been widely used for research and clinical purposes and its application has been mainly focused on brain and muscle. Theoretically, it can detect any nuclei in the body but only two types of nuclei, namely phosphorus (^{31}P) and hydrogen (^{1}H), are currently feasible for clinical evaluation. ^{31}P MRS can be used to study energy metabolites such as adenosine triphosphate (ATP), adenosine diphosphate (ADP), phosphocreatine (PCr), inorganic phosphate, phosphorylation potential (PP), magnesium and intracellular pH. These phosphorylated compounds are involved directly in cell energy metabolism(Montagna, Cortelli, & Barbiroli, 1994). ^{1}H MRS, on the other hand, estimates the concentration of N-acetyl aspartate (NAA), choline, creatine, phosphocreatine as well as excitatory (glutamate, glutamine) and inhibitory (GABA) neurotransmitters. It is thus possible that use of MRS could help the understanding of migraine.

4.1.1 ^{31}P MRS

The results from ^{31}P MRS studies generally indicate an abnormal mitochondrial function in migraine. These studies investigated the occipital cortex in various subtypes of migraine during and between attacks. For instance, the only study performed during ictal phase showed that PCr concentration decreased and Pi concentration increased in migraine with aura (MwA) but not migraine without aura (MwoA), suggesting the low availability of free energy in the cell (Welch, Levine, D'Andrea, Schultz, & Helpern, 1989). These changes were also observed in the interictal period of various migraine subtypes (Barbiroli et al., 1990) (Uncini et al., 1995) (Lodi et al., 1997) (Schulz et al., 2007). Second, with the exception of one study which showed no difference of calculated ADP between MwoA and control(Reyngoudt, Paemeleire, Descamps, De Deene, & Achten, 2011), all subsequent studies showed increased ADP in the occipital lobe, suggesting that the brain tissue is in a higher metabolic rate (Barbiroli et al., 1992) (Montagna et al., 1994) (Uncini, et al., 1995) (Lodi, et al., 1997). Third, phosphorylation potential (PP), an index of mitochondrial functionality, was consistently lower than controls across studies, indicating a low intracellular energy status (Sacquegna et al., 1992) (Barbiroli, et al., 1992) (Uncini, et al., 1995) (Lodi, et al., 1997) (Reyngoudt, Paemeleire, Descamps, et al., 2011). Taken together, these results suggest that there is an altered energy state in the occipital lobes of migraineurs, regardless of the migraine subtypes and phases of disease. Intriguingly, the authors suggested that these findings are in accordance with the results in mitochondrial encephalomyopathies, implying that mitochondrial dysfunction may also be implicated in the pathophysiology of migraine(Sparaco, Feleppa, Lipton, Rapoport, & Bigal, 2006). However, whether the

phenomenon reflects a primary mitochondrial disorder or merely a consequence of altered cortical excitability is yet to be determined(Sparaco, et al., 2006).

4.1.2 ^{1}H MRS

The limited number of ^{1}H-MRS studies in migraine revealed inconsistent results across various subtypes including migraine with aura (MwA), migraine without aura (MwoA), migraine with aura associated with paraesthesia, paresis or dysphasia (MAplus), familial hemiplegic migraine type 2(FHM2), basilar migraine and migrainous infarction. These studies focused on the evaluation of lactate and NAA at the occipital area during the interictal phase. Among them, only three studies investigated the changes in metabolites after photic stimulation.

4.1.2.1 Lactate

Lactate is an anaerobic metabolite that accumulates in mitochondrial dysfunction or when mitochondrial enzymes are near saturation(Montagna, Cortelli, & Barbiroli, 1994). MwA patients who experienced attack within 2 months prior to the scans showed higher occipital lactate level interictally whereas the patient who had been attack-free in the prior 4 years did not show the surge in lactate (Watanabe, Kuwabara, Ohkubo, Tsuji, & Yuasa, 1996). The researchers proposed that anaerobic glycolysis in migraine leads to lactate accumulation and attack-free periods may

reverse the abnormality. Similarly, Sandor et al. showed that the interictal lactate at visual cortex was higher in MwA. They further explored the effect of photic stimulation but failed to reveal any change in lactate level (Sandor et al., 2005). The increased resting lactate in MwA is in accordance with the low mitochondrial PP found in ^{31}P MRS studies, suggesting the presence of mitochondrial dysfunction. No further rise of lactate after photic stimulation was observed because the lactate transport system may have been saturated.

Arguably, the increased lactate level at rest was not observed in other migraine subtypes. For instance, in the same ^{1}H-MRS study performed by Sandor et al., they demonstrated that the lactate level was normal at baseline but increased during photic stimulation in migraineurs with visual as well as somatosensory, dysphasic and/or paretic aura (MAplus). Similarly, in a patient with FHM2, lactate was mildly increased at the lateral ventricles but not the visual cortex (Grimaldi et al., 2010). In MwoA, there was no difference in the absolute lactate concentrations in the visual cortex compared to controls (Reyngoudt, De Deene, Descamps, Paemeleire, & Achten, 2010). Likewise, a recent study observed comparable lactate between MwoA and controls. Lactate remained constant before, during and after photic stimulation(Reyngoudt et al., 2011).

Taken together, the limited data in ^{1}H-MRS studies indicate that occipital lactate increases only in MwA at rest, but not in MwoA, MAplus or FHM2, and is related to the presence of recent attack, suggesting that anaerobic glucose metabolism may be associated exclusively with MwA. This finding can be explained by and is consistent with the notion that extracellular lactate, which is an inhibitor of cortical spreading

depression(CSD), is implicated in the pathophysiology of aura(Scheller, Kolb, & Tegtmeier, 1992) (Tong & Chesler, 2000). The change in cortical lactate, reflecting mitochondrial dysfunction, may lead to migraine attacks via CSD.

4.1.2.2 NAA

Another cerebral metabolite NAA was shown to be low in migraine. NAA is an indicator of axonal integrity and believed to be a marker of mitochondrial function because it is synthesized and mainly located at neural mitochondria(Clark, 1998). Sarchielli et al. found that the interictal NAA in visual cortex is low at baseline and decreased more significantly after photic stimulation in MwA compared to MwoA and controls (Sarchielli et al., 2005). Other studies also support the decrease in NAA signal in migraine, albeit in different cerebral regions and migraine subtypes (Dichgans, Herzog, Freilinger, Wilke, & Auer, 2005) (Jacob et al., 2006) (Gu, Ma, Xu, Xiu, & Li, 2008).

4.1.2.3 Glutamate

Neuronal hyperexcitability has been widely hypothesized as the proposed mechanism underlying aura in migraine. Glutamate is of particular interest in this respect because it is the main excitatory neurotransmitter in the central nervous system. Furthermore, the propagation of CSD requires glutamate and N-methyl-D-aspartate (NMDA) receptors play an important role in this process(Obrenovitch & Zilkha, 1996). Several

lines of evidence indicate the role of glutamatergic abnormality in the pathogenesis of migraine.

First, since glutamate level is difficult to measure directly in the brain, platelets that metabolize glutamate in a similar way to neurons have been studied in migraine in the past two decades. For example, D'Andrea et al. showed that glutamate levels in platelets were higher in patients with MwA relative to controls(D'Andrea et al., 1991). The levels further increased during headache. Moreover, the same research group showed that higher glutamate levels in plasma but not in platelets exist in MwoA patients. The opposite was true for MwA(Cananzi, D'Andrea, Perini, Zamberlan, & Welch, 1995). Another study showed that platelet glutamate uptake was increased in MwA but reduced in MwoA relative to healthy controls, indicating that glutamate might be implicated in the aura symptom of migraine (Vaccaro et al., 2007).

Second, the disturbance of this neurotransmitter in migraine was supported by CSF studies showing that CSF glutamic acid concentration was higher in migraineurs relative to controls(Martinez, Castillo, Rodriguez, Leira, & Noya, 1993) (Peres et al., 2004). Third, migraine prophylaxis such as topiramate, amitriptyline, flunarizine and propranolol were found to reduce the plasma glutamate level of migraineurs compared to their own baseline levels (A. Ferrari, Spaccapelo, Pinetti, Tacchi, & Bertolini, 2009).

At present, only 4 ^{1}H-MRS studies in the literature examined the role of glutamate in migraine and generally showed no evidence of elevated glutamate, albeit the different migraine subtypes and research methodologies. One study showed no difference of the metabolite at anterior cingulate cortex and insula in MwA and MwoA compared

to controls(Prescot et al., 2009). Another study found no difference of glutamate at occipital cortex between MwoA and controls (Reyngoudt, et al., 2010). Furthermore, although there is established evidence that mutations in Cav2.1 channels of familial hemiplegic migraine subtype 1(FHM1) enhance glutamate release from presynaptic terminals(Tottene et al., 2002), the only ^{1}H-MRS study in FHM1 revealed a reduction of glutamate level in the cerebellum (Dichgans, et al., 2005). Lastly, in healthy subjects, excitatory (anodal) and inhibitory (cathodal) transcranial direct current stimulation (tDCS) were able to increase and decrease the glutamate/creatine ratios at visual cortex respectively, which were reversed to baseline by subsequent photic stimulation(Siniatchkin et al., 2011). By contrast, in patients suffering from migraine with visual aura, both anodal and cathodal tDCS decreased the glutamate/creatine ratios which were not reversed by photic stimulation. In addition, the modifiability of visual evoked potentials (VEPs) amplitudes by tDCS was reduced in migraineurs relative to normal subjects. These findings indicate a deficient regulatory mechanism for cortical excitability in migraine(Siniatchkin, et al., 2011).

Taken together, the MRS studies of glutamate migraineurs revealed discordant results, with different migraine subtypes and methodologies being adopted.

4. 1.2.4 GABA

Being the main inhibitory neurotransmitter in the brain, Gamma-aminobutyric acid (GABA) is another neurotransmitter that plays an important role in the hypothesis of altered excitability in migraine(McCormick, 1989). Although the mechanism remains elusive, GABA agonists and analogs such as gabapentin, topiramate and baclofen have been proven to be effective prophylaxis for reducing the frequency of attacks(McCormick, 1989) (Puppe & Limmroth, 2007) (Rothrock, 2012). Nevertheless, in vitro and in vivo studies of GABA in migraine are exceedingly rare. An early study showed that GABA was only detected in CSF during migraine attack (Welch, Chabi, Bartosh, Achar, & Meyer, 1975). Another study showed no difference in CSF GABA levels between chronic migraineurs and controls(Vieira et al., 2006). There have also been investigations into the relationship between GABA A receptor genes and migraine susceptibility, providing evidence for suggestive linkage(Russo et al., 2005) (Fernandez et al., 2008) (Netzer et al., 2008). The only in vivo study to use MRS to measure the interictal GABA level at the occipital cortex of migraineurs showed no significant difference compared to controls(Bigal et al., 2008). However, there was a significant correlation between GABA level and the severity of headache attacks, suggesting that GABA plays a role in suppressing headache attacks.

4.1.3 Aim

In the present study, I investigated the glutamate, GABA and NAA levels at visual cortices of interictal migraineurs. Based on the background that these metabolites may modulate the cortical excitability and energy metabolism, I speculated that migraineurs would exhibit changes of these metabolites between attacks. In addition, I attempted to examine the effect of photic stimulation on the levels of glutamate and NAA in the TRESK group.

4.2. Methods

4.2.1 Subjects and MR spectroscopic acquisition

The MRS data of the 11 non-TRESK migraineurs and 11 controls were analyzed. One of the migraine subjects (subject no. 5) who took Lithium was excluded from the analysis. The MR spectroscopic acquisition(10min) was performed before the two fMRI tasks (please refer to Chapter 3, figure 2.1 for the entire experimental protocol). The SPECIAL (spin-echo full-intensity acquired localized) sequence (Mekle et al., 2009) was applied with the following parameters: TE = 6 ms, TR = 4000 ms, average number = 128, vector size =2048, delta. The volume of interest (VOI) with a size of 20 x 20 x 20mm^3 was placed in the primary visual cortex (Brodmann area 17), centered on the calcarine sulcus (Figure 2.1). All subjects were instructed to keep their eyes opened during the MRS acquisition.

For the TRESK study performed in Canada, in addition to the four MwA with documented TRESK variant, another two unaffected (without MwA or TRESK variant) members of the TRESK family were also scanned. Additionally, all of them received a second MRS acquisition in complete darkness after the two fMRI scans. A longer echo time (TE=135ms) was used due to the difference in standard MRS protocol at Robarts Research Institute in Canada.

A. B.

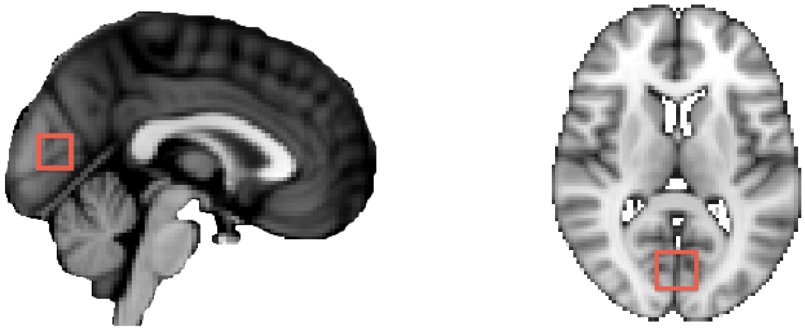

Figure 2.1 T_1-weighted image with a 20 x 20 x 20mm^3 cubic volume of interest (VOI) localized in the occipital visual cortex A. Sagittal section B. Axial section.

4.2.2 MRS data analysis

MRS data was analyzed using LCModel (Provencher 6.3-0C). The LCModel method analyzes the spectra by a linear combination of a set of model spectra(Provencher, 1993). For the non-TRESK migraineurs, TRESK migraineurs and control subjects, raw spectrum averages were drift corrected. Peak values for metabolites such as creatine, glutamate, GABA, NAA and lactate were then calculated and expressed in concentration as well as values normalized by creatine. Since the sample box that we located at V1 contained voxels across grey matter, white matter and the surrounding CSF, I determined the percentage of grey matter within the sample box in each subject by using FAST (FMRIB's Automated Segmentation Tool) in FSL. GABA and glutamate were assumed to be only in grey matter and their values were therefore normalized by the percentage of gray matter.

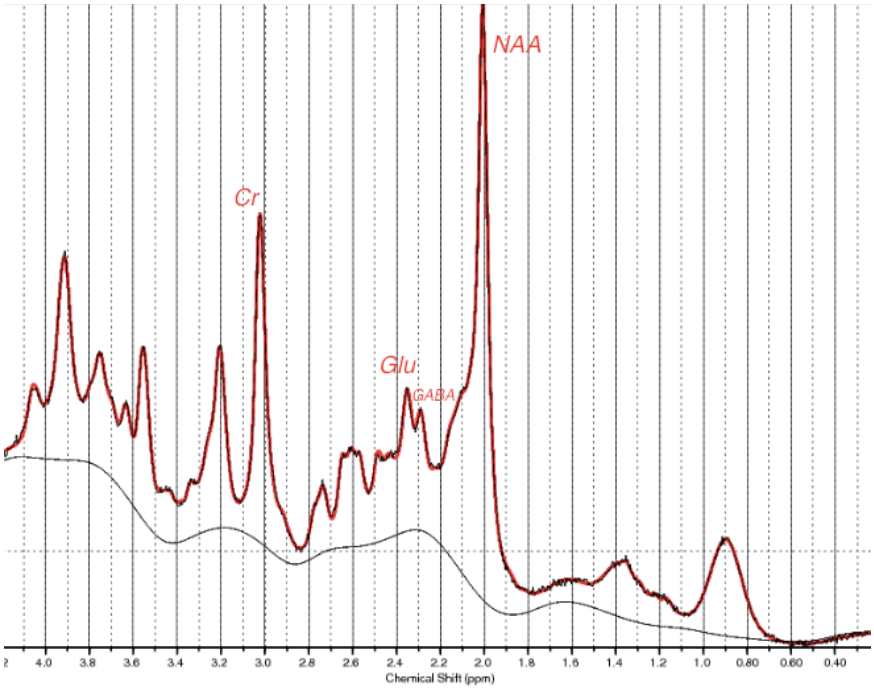

Figure 2.2. Example spectrum of a subject (subject no. 1). Peaks for N-acetylaspartate (NAA), glutamate (Glu), creatine (Cr) and GABA are labelled.

4.3. Results

4.3.1 Non-TRESK migraineurs and controls

As shown in figure 3.1, the corrected GABA level in the occipital cortex showed no difference between the non-TRESK migraineurs and healthy controls (t = -0.21, df = 20, p = 0.83). Similarly, there was no difference in either occipital glutamate (t = 0.09, df = 20, p = 0.93) or NAA level (t = 0.12, df = 20, p = 0.91) between the two groups

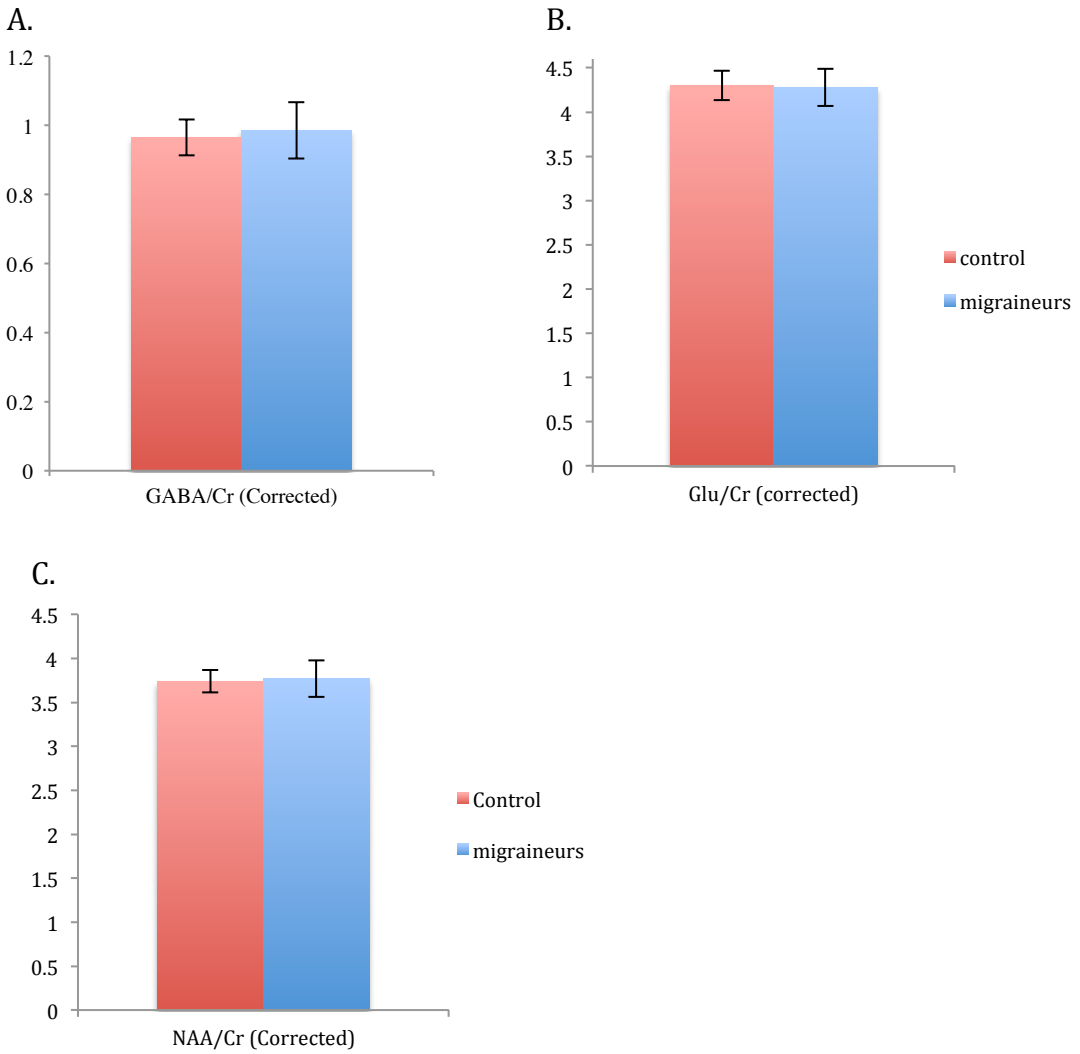

Figure 3.1 Comparison of levels of metabolites relative to creatine in occipital cortex of non-TRESK migraineurs and controls. A. GABA B. Glutamate C. NAA. There was no difference in any of the metabolites measured at the occipital cortex between non-TRESK migraineurs and controls. Red and blue bars depict controls and migraineurs respectively. Levels of metabolites are presented as ratios relative to creatine in means ± s.e.m.

4.3.2 Correlation of Glutamate level in non-TRESK migraine subjects between frequency of attack and BOLD signal in diffuse constant illumination

Although the glutamate levels showed no difference between groups, it is possible that the levels could be linked to the migraine characteristics for individual migraineurs. I therefore explored the correlation of glutamate level with attack frequency and the BOLD signal of the same individual extracted from V1 during diffuse constant illumination. As shown in figure 3.2, corrected glutamate level showed no relationship with frequency of attack. However, there is a non-significant trend for glutamate level to be correlated with V1 activation to light onset.

Migraine subject	Frequency of attack (month)	%BOLD change (light onset)	Glu:Cr ratio
1	9	0.02	4.70
3	5	0.17	4.01
4	5	0.24	3.97
6	8	-0.16	3.90
7	2	-0.09	2.63
8	4	0.52	4.18
9	4.5	0.30	4.07
10	5	0.46	4.95
11	2	0.52	4.88
12	2.5	0.10	4.45

Table 3.1 Frequency of attack, cortical activations elicited by diffuse light illumination and glutamate level at rest of non-TRESK migraineurs

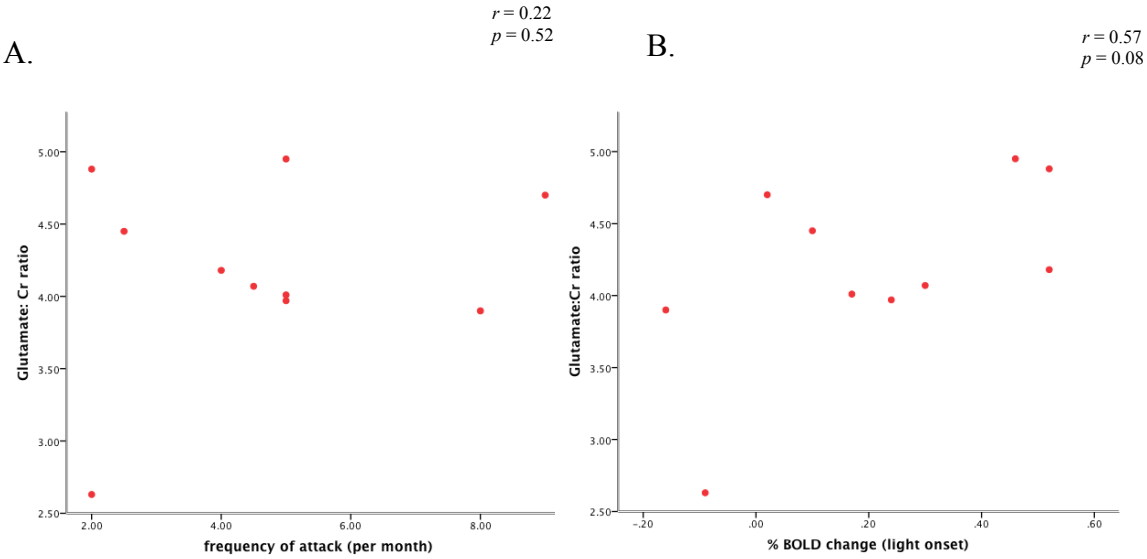

Figure 3.2. Correlation of occipital glutamate at rest between A. frequency of attack per month: no significant correlation was found (r = 0.22, p = 0.52) B. %BOLD change at visual cortex with diffuse constant illumination: a trend showing a positive correlation (r = 0.57, p = 0.08).

Since there was a trend of positive correlation between occipital glutamate and BOLD signal in the non-TRESK migraine group, I also investigated the correlation in healthy controls. In contrast to the migraine subjects, there was no trend of correlation between glutamate and BOLD change in the control group (r = 0.04, p = 0.90).

Healthy controls	%BOLD change (light onset)	Glu:Cr ratio
1	1.12	3.73
2	0.62	4.76
3	0.28	4.20
4	0.95	4.22
5	0.31	4.47
6	0.45	4.65
7	0.42	3.15
8	0.92	4.81
9	0.53	3.85
10	0.21	4.49
11	0.79	4.99

Table 3.2 Cortical activations elicited by diffuse light illumination and glutamate level at rest of healthy controls.

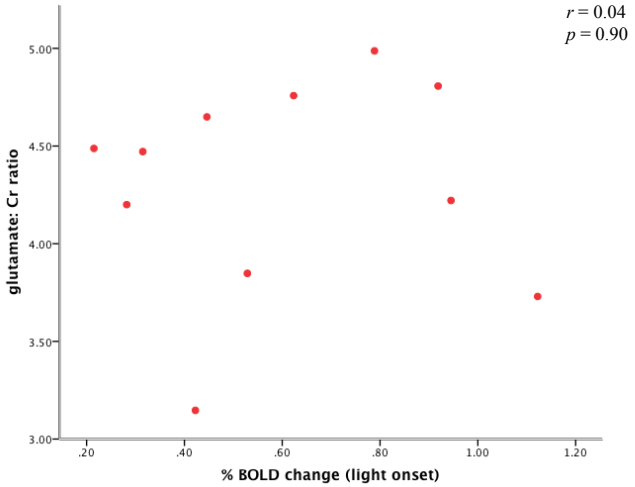

Figure 3.3. No correlation between occipital glutamate at rest and %BOLD change with diffuse constant illumination in healthy subjects (r = 0.04, p = 0.90).

4.3.3 Correlation of GABA level in non-TRESK migraine subjects between frequency of attack and BOLD signal in diffuse constant illumination

I hypothesized that if occipital GABA level between attack were related to migraine, there would be a correlation of the level between attack frequency or BOLD signal elicited by diffuse constant illumination. Similar to the result in glutamate, corrected GABA level was neither correlated with BOLD signal nor the frequency of attack (figure 3.4).

Migraine subject	Frequency of attack (month)	%BOLD change (light onset)	GABA:Cr ratio
1	9	0.02	1.14
3	5	0.17	1.00
4	5	0.24	0.86
6	8	-0.16	1.00
7	2	-0.09	0.56
8	4	0.52	0.96
9	4.5	0.30	0.72
10	5	0.46	1.03
11	2	0.52	0.76
12	2.5	0.1	1.27

Table 3.3 Frequency of attack, cortical activations elicited by diffuse light illumination and GABA level at rest of non-TRESK migraineurs

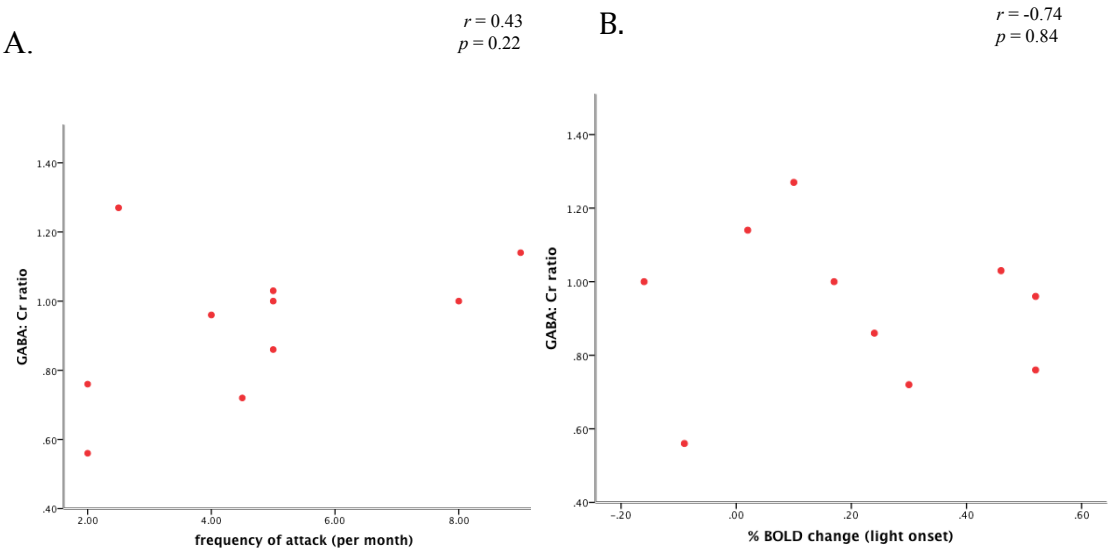

Figure 3.4. No correlation of occipital GABA at rest between A. frequency of attack per month (r = 0.43, p = 0.22). B. %BOLD change at visual cortex elicited by diffuse constant illumination (r = -0.74, 0.84).

4.3.4 Correlation of NAA level in non-TRESK migraine subjects between frequency of attack and BOLD signal in diffuse constant illumination

I also analyzed the correlation of NAA level between attack frequency and BOLD signal elicited by diffuse constant illumination. Similar to the results in GABA, a correlation was also not found (figure 3.5).

Migraine subject	Frequency of attack (month)	%BOLD change (light onset)	NAA:Cr ratio
1	9	0.02	3.96
3	5	0.17	3.86
4	5	0.24	3.41
6	8	-0.16	3.77
7	2	-0.09	2.54
8	4	0.52	3.43
9	4.5	0.30	3.66
10	5	0.46	4.32
11	2	0.52	3.36
12	2.5	0.10	3.84

Table 3.4 Frequency of attack, cortical activations elicited by diffuse light illumination and NAA level at rest of non-TRESK migraineurs

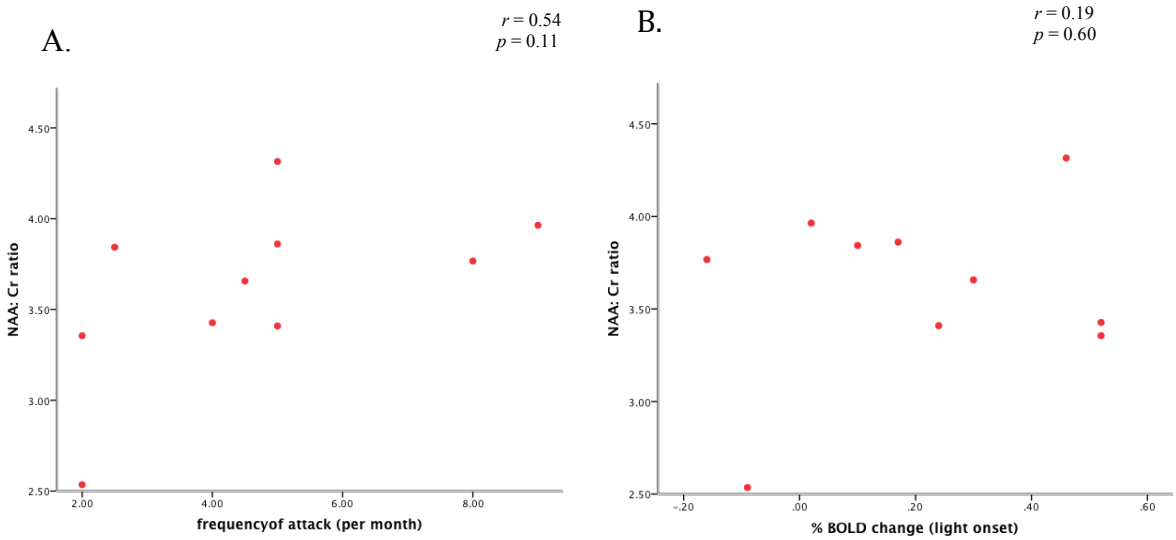

Figure 3.5. No correlation of occipital NAA at rest between A. frequency of attack per month (r = 0.54, p = 0.11). B. %BOLD change at visual cortex elicited by the initial onset of diffuse constant illumination (r = 0.19, p = 0.60).

4.3.5 TRESK migraineurs (affected and unaffected members) – pre and post illumination

4.3.5.1 Glutamate

Figure 3.6 shows the pre- and post-stimulus glutamate levels of four affected and two un-affected members of the TRESK family. Unfortunately, due to the long echo time (TE = 135ms) we used for acquiring these data, GABA was not detectable and the results were omitted. In addition, we were not able to compare these results with those of the non-TRESK migraineurs and healthy controls that we acquired previously using a much shorter echo time (TE = 6ms).

Despite these limitations, within group comparison showed no significant difference in glutamate level before and after photic stimulation in the affected subjects (pre-stimulus: 7.78 ± 0.73; post-stimulus: 6.28 ± 0.48, t = 1.73, df = 6, $p = 0.14$). For the unaffected TRESK subjects (pre-stimulus: 8.37 ± 1.82; post-stimulus: 6.45 ± 0.37, t = 1.04, df = 2, $p = 0.41$), however, a solid conclusion could not be drawn because the two subjects showed different trend of change. Therefore, visual stimuli appeared to reduce the occipital glutamate levels in the affected group. A comparison of the glutamate change (pre- minus post-stimulus glutamate levels) between groups showed a relatively smaller reduction of glutamate in the affected group than the unaffected group (affected: 1.51 ± 0.97, unaffected: 1.93 ± 2.19, t = -0.213, df = 4, $p = 0.84$), but this is clearly driven by a single unaffected subject.

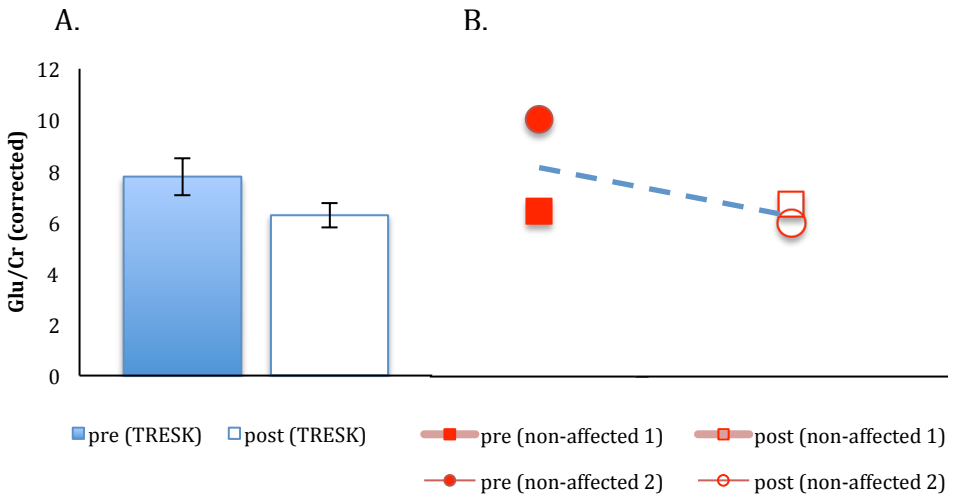

Figure 3.6 Glutamate levels in TRESK family of A. affected migraineurs (n=4) B. unaffected subject 1 and 2. There was a trend showing higher occipital glutamate level in pre-stimulation than post-stimulation in both affected and unaffected subjects. Levels of glutamate are presented as ratios relative to creatine in means ± s.e.m. Pre- and post-stimulus data in the affected group are presented in blue shaded bar and blue open bar respectively. Subject 1 and 2 are presented as red square and red circle respectively (pre-stimulus data as shaded circle and square, post-stimulus data as open circle and square). Dotted line depicts the trend of change between the means of the pre- and post stimulus glutamate levels in the non-affected subjects.

4.3.5.2 NAA

Similar to the results in non-TRESK MwA, comparing the cortical NAA levels between affected and unaffected TRESK subjects showed no significant difference both before (TRESK: 6.28 ± 0.63; controls: 6.69 ± 0.68, t = -0.40, df = 4, p = 0.71) and after stimulation (TRESK: 5.39 ± 0.38; controls: 5.70 ± 1.03, t = -0.36, df = 4, p = 0.74).

Within group comparison showed no significant difference of NAA level before and after stimulation in the affected subjects (pre-stimulus: 6.28 ± 0.63; post-stimulus: 5.39 ± 0.38, t = 1.21, df = 6, p = 0.27). For the unaffected TRESK subjects (pre-stimulus: 6.70 ± 0.68; post-stimulus: 5.70 ± 1.03, t = 1.04, df = 2, p = 0.41), however, the two subjects again demonstrated opposite trends of change and thus a general trend cannot be concluded. A comparison of the NAA change (pre- minus post-stimulus NAA levels) between groups showed no significant difference between the affected and unaffected group (affected: 0.89 ± 0.58, unaffected: 1.00 ± 1.71, t = -0.079, df = 4, p = 0.94).

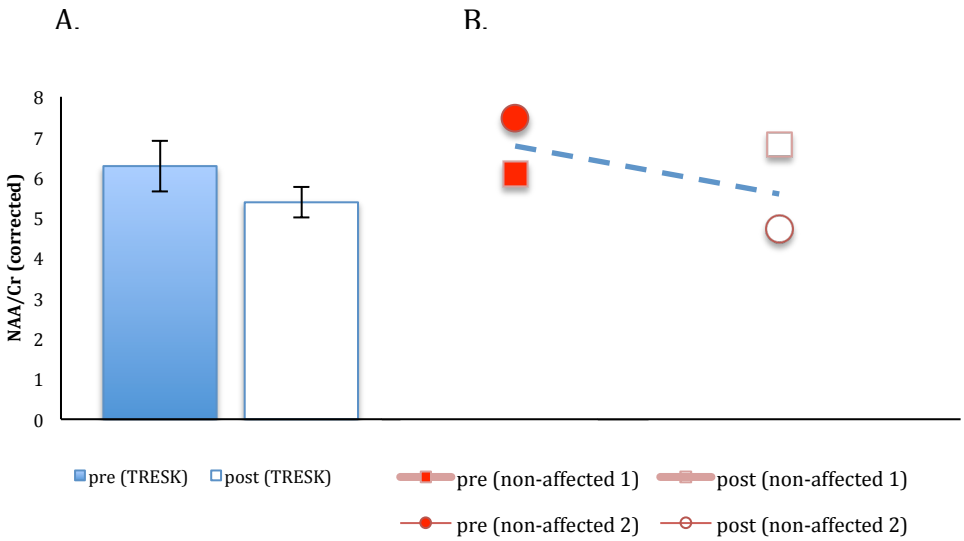

Figure 3.7 NAA levels in TRESK family showing A. affected migraineurs (n=4) B. unaffected subject 1 and 2. There was a trend showing higher NAA level in pre-stimulation visual cortex than post-stimulation in the affected subjects. Levels of NAA are presented as ratios relative to creatine in means ± s.e.m. Pre- and post-stimulus data in the affected group are presented in blue shaded bar and blue open bar respectively. Subject 1 and 2 are presented as red square and red circle respectively (pre-stimulus data as shaded circle and square, post-stimulus data as open circle and square). Dotted line depicts the trend of change between the means of the pre- and post stimulus NAA levels in the non-affected subjects.

4.4 Discussion

4.4.1 Summary of findings

My findings showed no significant difference in occipital GABA, Glutamate or NAA levels between attack-free non-TRESK migraineurs and healthy controls. In addition, GABA and NAA levels were not significantly correlated either with the frequency of attack nor the BOLD signals evoked by constant light, suggesting that there is no direct evidence of altered interictal glutaminergic, gabaergic or mitochondrial dysfunction in the visual cortex that would serve as the predisposing environment for initiating migraine attacks. However, although glutamate level was normal in non-TRESK migraineurs, there was a trend showing a positive correlation between glutamate and BOLD signal, which was absent from control subjects.

In the TRESK study, no significant difference in glutamate and NAA were found either at rest or post-stimulation between affected and unaffected TRESK family members. Stimulus paradigms reduced the occipital glutamate and NAA levels in the affected group, a conclusion of stimulation effect on these metabolites in the unaffected group can not be made due to the small sample size and opposite trends of results.

4.4.2 Justifications for results

Glutamate has been proposed as implicated in cortical spreading depression (CSD) which is regarded as the electrophysiological correlate of migraine aura(Van

Harreveld & Fifkova, 1973). This idea is based on the finding that glutamate is released in the initiation and propagation of CSD and N-methyl-D-aspartate (NMDA) receptor antagonists suppressed the development of CSD (Marrannes, Willems, De Prins, & Wauquier, 1988) (McLachlan, 1992). In addition, blocking NMDA receptor with antagonists suppressed the propagation of CSD(Lauritzen & Hansen, 1992) (McLachlan, 1992; Obrenovitch & Zilkha, 1996). Furthermore, altered plasma, platelet and CSF glutamate levels have been reported in migraine patients and intake of food containing monosodium glutamate is a well known trigger of migraine. On the other hand, although direct evidence is exceedingly rare, GABA, being the main inhibitory neurotransmitter in the CNS, was only detectable in CSF after migraine attacks(Welch, et al., 1975).

Based on this background, I speculated the presence of altered occipital glutamate and GABA levels in migraineurs with visual aura. Nevertheless, in contrary to my speculation, the results showed no significant difference between the disease and control groups. Furthermore, only the level of glutamate, but not GABA, seemed to be correlated with the cortical BOLD response elicited by constant illumination. I attempt to justify these results as follow.

4.4.2.1 Glutamate

First, the two CSF studies that supported higher glutamate level in migraineurs were performed either during attacks (Martinez, et al., 1993) or with another subtype of migraine subjects, i.e. chronic migraineurs with and without fibromyalgia(Peres, et al., 2004). Since glutamate is related to CSD, the lack of difference in occipital

glutamate between MA and controls in my study might suggest the return of the level to baseline after attacks.

Second, the findings in altered plasma glutamate level in migraine are contradictory. Whilst two studies showed elevated levels in MA between attacks (Alam, Coombes, Waring, Williams, & Steventon, 1998) (M. D. Ferrari, Odink, Bos, Malessy, & Bruyn, 1990), other studies showed normal (Cananzi, et al., 1995) or lower plasma glutamate level than controls (Martinez, et al., 1993). Again, the inconsistency may be due to the dynamicity of the disease, but even when these levels are altered in plasma, the changes are not good indicators for glutaminergic abnormalities in the brain.

Third, only 4 ^{1}H-MRS studies in the literature examined the role of glutamate in migraine and showed no evidence of elevated glutamate. Whilst one study examined the metabolite at the occipital cortex in MwoA(Reyngoudt, et al., 2010), other two studies focused on the cerebellum in FHM1(Dichgans, et al., 2005) and the anterior cingulate cortex and insula in MwA and MwoA (Prescot, et al., 2009). The fourth study, however, did not measure the glutamate peak directly but showed a relatively higher Glx peak (unresolved glutamine, glutamate and GABA peaks between 2.2-2.4ppm) in MwA compared to controls, thus the results cannot be compared to other studies that measured glutamate (Siniatchkin, et al., 2011). As such, the role of glutamate at visual cortex of MwA between attacks has not yet been investigated. My study, therefore, provides the first MRS evidence showing no difference of occipital glutamate between interictal MwA and controls. This finding is critical because if CSD is of greater importance in the pathogenesis of MwA than MwoA, glutamate that relates closely to CSD would be more implicated in this specific migraine subtype. In

addition, all my subjects had visually-triggered migraine, suggesting that the visual cortex may be of particular interest in this cohort.

Taken together, my findings revealed no altered glutaminergic level at the visual cortex of interictal MwA that would directly predispose them to migraine attacks. However, there seems to be a trend showing positive correlation between glutamate level and BOLD response evoked by continuous light, suggesting that there may still be a role for glutamate to mediate baseline excitability in migraine, further studies are needed to clarify this finding.

4.4.2.2 GABA

With regard to GABA, only one ^{1}H-MRS study examined the occipital GABA level of migraineurs(Bigal, et al., 2008). My finding is consistent with their result by showing no difference in occipital GABA level between MwA and controls. However, the inverse correlation between GABA and frequency of severe migraine attacks in the previous study was not found in my study. This may be due to the different methodologies adopted. First, Bigal et al. pooled MwA and MwoA data for analysis, whereas I recruited only MwA who also experienced visually-triggered migraine. Second, they found the correlation only existing in severe headache but this piece of information is lacking in my study, suggesting that the stratification of headache severity may be a factor to be considered in future studies of examining the correlation between GABA and migraine frequency.

4.4.2.3 NAA

NAA is a axonal marker that has been proposed as a marker of mitochondrial function(Clark, 1998). This notion was further supported by the reversible decrease of NAA signal in neurological diseases after clinical improvement(De Stefano, Matthews, & Arnold, 1995). In contrast to the only ^{1}H-MRS study that examined the visual cortex of MwA and showed significantly lower NAA in MwA between attacks, my finding revealed no difference of NAA levels between MwA and controls(Sarchielli, et al., 2005). The authors of the study hypothesized the presence of mitochondrial dysfunction in MwA compared to MwoA and controls(Sarchielli, et al., 2005). The discordance in results might be due to the heterogeneity of subjects. Whilst both studies examined subjects with visual aura, the majority of subjects recruited in the previous study were concomitant with other aura subtypes such as sensory (10 out of 11) and dysphasic aura (1 out of 11), as opposed to my migraine with visual aura subjects who also experienced visually-triggered migraine. In conclusion, my findings suggest that there was no NAA disturbance in the interictal visual cortex of MwA. This does not provide evidence to support the previous suggestion of mitochondrial dysfunction in migraine. Further studies of NAA in other brain regions or other mitochondria-related metabolites such as lactate (which cannot be measured easily at 3 Tesla) or ATP.

4.4.2.4 TRESK subjects

Consistent with my previous findings in the non-TRESK MwA group, there was no significant difference in glutamate levels either at rest or post-stimulation between affected TRESK MwA and unaffected family members. While there were some small differences, the subject numbers mean that no conclusions can be made at this point, although there is sufficient data to encourage further investigation.

The early changes of occipital glutamate after photic stimulation have not yet been explored in migraine. My protocol of MRS acquisition in the TRESK study allowed a direct comparison of occipital glutamate levels before and after the photic stimulus paradigm. The finding showed a trend of glutamate reduction after stimulation in the affected subjects, suggesting that the stimulus paradigms might have reduced the occipital glutamate levels. Intriguingly, the magnitude of glutamate reduction in the TRESK MwA group was relatively smaller than the unaffected controls. Three out of four of the TRESK MwA experienced various degrees of headache, aura or photophobia after the scans. It is, therefore, very tempting to suggest that the smaller reduction of occipital glutamate, or indeed a relative rise in occipital glutamate, might be related to the very early ongoing process of migraine attacks. However, a very cautious interpretation of my TRESK data must be undertaken because of the small sample size. A larger sample size would have been able to clarify this aspect but was not feasible due to the limited availability of the TRESK family. In addition, it might be worthwhile to consider how reproducible the MRS data are. A question remains to

be answered is whether the levels of the metabolites remain constant or fluctuate even at rest without light stimulation.

Photic stimulation relatively reduced the occipital NAA level in the TRESK MwA subjects. This finding is in accordance with the only study of light-induced change of NAA in the literature(Sarchielli, et al., 2005). They found a significantly larger decline of NAA in MwA and hypothesized a less efficient mitochondrial function in MwA than MwoA and controls. Again, due to the small size of subjects in my study and the opposite trends of change in the two control subjects, it is difficult to have a clear comparison between the TRESK MwA and control groups. Larger studies in the future could provide more definitive evidence.

4.4.3 Limitations and future studies

Notably, although my study revealed no significant difference of metabolites between groups, there is a trend of positive correlation between glutamate level and BOLD response, suggesting that there might still be a role for glutamate in the modulation of cortical responsiveness in migraine. It would be possible that my study cohort was not large enough to show significance in this correlation, further investigations with larger sample sizes could help to provide more evidence. Second, as commented by (Siniatchkin, et al., 2011), there is a potential spectral overlap of glutamine, glutamate and GABA between 2.2 and 2.4ppm, even when the magnetic field was at 3T. Future studies, therefore, would be benefited by using higher field strength such as 7T to clarify these results. Third, since the essence of the glutamate hypothesis is its

relationship with CSD, the metabolite levels at occipital cortex might have returned to baseline level when examined during interictal phase. Further studies with assessment of occipital metabolites both at rest and during migraine attacks may be needed to address this issue.

Fourth, migraine is believed to develop as a cascade of reactions, with networks between the cortex, brainstem and peripheral nociceptors. The hypotheses of interictal reduced pre-activation or glutaminergic disturbance may be an interaction and net consequences of these networks and therefore take part in multiple areas of the brain. Indeed, animal studies have identified glutamate and its receptors in the trigeminal nucleus caudalis which is thought to be one of the major components in the pathophysiology of migraine (Clements, Magnusson, Hautman, & Beitz, 1991) (Tallaksen-Greene, Young, Penney, & Beitz, 1992) (Storer & Goadsby, 1999). In addition, glutamate receptors have been found in other brainstem nuclei such as the locus coeruleus, the dorsal raphe nucleus and the periaqueductal grey matter (Akerman, Williamson, Kaube, & Goadsby, 2002) (Fejes, Pardutz, Toldi, & Vecsei, 2011). Therefore, even the lack of change of these metabolites in the visual cortex between attacks does not essentially refute these hypotheses. Furthermore, the mechanism underlying the susceptibility of the brain of MwA to visually-triggered attacks may not be mediated solely by the altered GABA or glutamate levels. Other metabolites such as nitric oxide (Akerman, et al., 2002) and those related to energy metabolism, PCr, PP and lactate, might also contribute to the complex mechanism of visually-triggered migraine in this specific subject cohort.

4.5. Conclusion

Although some previous studies have implicated glutamate, GABA and NAA in migraine aura, my findings showed no altered levels of these metabolites at the visual cortex of MwA and TRESK MwA between attacks. This may suggest that there is no role for alteration of glutaminergic, gabaergic or mitochondrial metabolism in the visual cortex at rest as a predisposing factor for the initiation of migraine attacks. Other brain locations or metabolites may contribute to the trigger of headache by light at the visual cortex (or through the non-image forming system). However, the trend of correlation between glutamate and BOLD signal induced by light is of interest and needs to be repeated in a larger study.

Finally, my stimulus paradigms reduced occipital glutamate and NAA in the TRESK subjects. A trend of smaller reduction in glutamate in the TRESK group might suggest the early onset of migraine cascade. However, it is necessary to recruit a larger group of control subjects to get some normalized metabolite levels, perhaps at higher field strength to determine whether there are any differences in the TRESK group..

4.6. References

Akerman, S., Williamson, D. J., Kaube, H., & Goadsby, P. J. (2002). Nitric oxide synthase inhibitors can antagonize neurogenic and calcitonin gene-related peptide induced dilation of dural meningeal vessels. *British journal of pharmacology, 137*(1), 62-68.

Alam, Z., Coombes, N., Waring, R. H., Williams, A. C., & Steventon, G. B. (1998). Plasma levels of neuroexcitatory amino acids in patients with migraine or tension headache. *Journal of the neurological sciences, 156*(1), 102-106.

Barbiroli, B., Montagna, P., Cortelli, P., Funicello, R., Iotti, S., Monari, L., . . . Lugaresi, E. (1992). Abnormal brain and muscle energy metabolism shown by 31P magnetic resonance spectroscopy in patients affected by migraine with aura. *Neurology, 42*(6), 1209-1214.

Barbiroli, B., Montagna, P., Cortelli, P., Martinelli, P., Sacquegna, T., Zaniol, P., & Lugaresi, E. (1990). Complicated migraine studied by phosphorus magnetic resonance spectroscopy. *Cephalalgia : an international journal of headache, 10*(5), 263-272.

Bigal, M. E., Hetherington, H., Pan, J., Tsang, A., Grosberg, B., Avdievich, N., . . . Lipton, R. B. (2008). Occipital levels of GABA are related to severe headaches in migraine. *Neurology, 70*(22), 2078-2080.

Cananzi, A. R., D'Andrea, G., Perini, F., Zamberlan, F., & Welch, K. M. (1995). Platelet and plasma levels of glutamate and glutamine in migraine with and without aura. *Cephalalgia : an international journal of headache, 15*(2), 132-135.

Clark, J. B. (1998). N-acetyl aspartate: a marker for neuronal loss or mitochondrial dysfunction. *Developmental neuroscience, 20*(4-5), 271-276.

Clements, J. R., Magnusson, K. R., Hautman, J., & Beitz, A. J. (1991). Rat tooth pulp projections to spinal trigeminal subnucleus caudalis are glutamate-like immunoreactive. *The Journal of comparative neurology, 309*(2), 281-288.

D'Andrea, G., Cananzi, A. R., Joseph, R., Morra, M., Zamberlan, F., Ferro Milone, F., . . . Welch, K. M. (1991). Platelet glycine, glutamate and aspartate in primary headache. *Cephalalgia : an international journal of headache, 11*(4), 197-200.

De Stefano, N., Matthews, P. M., & Arnold, D. L. (1995). Reversible decreases in N-acetylaspartate after acute brain injury. *Magnetic resonance in medicine : official journal of the Society of Magnetic Resonance in Medicine / Society of Magnetic Resonance in Medicine, 34*(5), 721-727.

Dichgans, M., Herzog, J., Freilinger, T., Wilke, M., & Auer, D. P. (2005). 1H-MRS alterations in the cerebellum of patients with familial hemiplegic migraine type 1. *Neurology, 64*(4), 608-613.

Fejes, A., Pardutz, A., Toldi, J., & Vecsei, L. (2011). Kynurenine metabolites and migraine: experimental studies and therapeutic perspectives. *Current neuropharmacology, 9*(2), 376-387.

Fernandez, F., Esposito, T., Lea, R. A., Colson, N. J., Ciccodicola, A., Gianfrancesco, F., & Griffiths, L. R. (2008). Investigation of gamma-aminobutyric acid (GABA) A receptors genes and migraine susceptibility. *BMC medical genetics, 9*, 109.

Ferrari, A., Spaccapelo, L., Pinetti, D., Tacchi, R., & Bertolini, A. (2009). Effective prophylactic treatments of migraine lower plasma glutamate levels. *Cephalalgia : an international journal of headache, 29*(4), 423-429.

Ferrari, M. D., Odink, J., Bos, K. D., Malessy, M. J., & Bruyn, G. W. (1990). Neuroexcitatory plasma amino acids are elevated in migraine. *Neurology, 40*(10), 1582-1586.

Grimaldi, D., Tonon, C., Cevoli, S., Pierangeli, G., Malucelli, E., Rizzo, G., . . . Cortelli, P. (2010). Clinical and neuroimaging evidence of interictal cerebellar dysfunction in FHM2. *Cephalalgia : an international journal of headache, 30*(5), 552-559.

Gu, T., Ma, X. X., Xu, Y. H., Xiu, J. J., & Li, C. F. (2008). Metabolite concentration ratios in thalami of patients with migraine and trigeminal neuralgia measured with 1H-MRS. *Neurological research, 30*(3), 229-233.

Gujar, S. K., Maheshwari, S., Bjorkman-Burtscher, I., & Sundgren, P. C. (2005). Magnetic resonance spectroscopy. *Journal of neuro-ophthalmology : the official journal of the North American Neuro-Ophthalmology Society, 25*(3), 217-226.

Jacob, A., Mahavish, K., Bowden, A., Smith, E. T., Enevoldson, P., & White, R. P. (2006). Imaging abnormalities in sporadic hemiplegic migraine on conventional MRI, diffusion and perfusion MRI and MRS. *Cephalalgia : an international journal of headache, 26*(8), 1004-1009.

Lauritzen, M., & Hansen, A. J. (1992). The effect of glutamate receptor blockade on anoxic depolarization and cortical spreading depression. *Journal of cerebral blood flow and metabolism : official journal of the International Society of Cerebral Blood Flow and Metabolism, 12*(2), 223-229.

Lodi, R., Montagna, P., Soriani, S., Iotti, S., Arnaldi, C., Cortelli, P., . . . Barbiroli, B. (1997). Deficit of brain and skeletal muscle bioenergetics and low brain magnesium in juvenile migraine: an in vivo 31P magnetic resonance spectroscopy interictal study. *Pediatric research, 42*(6), 866-871.

Marrannes, R., Willems, R., De Prins, E., & Wauquier, A. (1988). Evidence for a role of the N-methyl-D-aspartate (NMDA) receptor in cortical spreading depression in the rat. *Brain research, 457*(2), 226-240.

Martinez, F., Castillo, J., Rodriguez, J. R., Leira, R., & Noya, M. (1993). Neuroexcitatory amino acid levels in plasma and cerebrospinal fluid during migraine attacks. *Cephalalgia : an international journal of headache, 13*(2), 89-93.

McCormick, D. A. (1989). GABA as an inhibitory neurotransmitter in human cerebral cortex. *Journal of neurophysiology, 62*(5), 1018-1027.

McLachlan, R. S. (1992). Suppression of spreading depression of Leao in neocortex by an N-methyl-D-aspartate receptor antagonist. *The Canadian journal of neurological sciences. Le journal canadien des sciences neurologiques, 19*(4), 487-491.

Mekle, R., Mlynarik, V., Gambarota, G., Hergt, M., Krueger, G., & Gruetter, R. (2009). MR spectroscopy of the human brain with enhanced signal intensity at ultrashort echo times on a clinical platform at 3T and 7T. *Magnetic resonance in medicine : official journal of the Society of Magnetic Resonance in Medicine / Society of Magnetic Resonance in Medicine, 61*(6), 1279-1285.

Montagna, P., Cortelli, P., & Barbiroli, B. (1994). Magnetic resonance spectroscopy studies in migraine. *Cephalalgia : an international journal of headache, 14*(3), 184-193.

Montagna, P., Cortelli, P., Monari, L., Pierangeli, G., Parchi, P., Lodi, R., . . . et al. (1994). 31P-magnetic resonance spectroscopy in migraine without aura. *Neurology, 44*(4), 666-669.

Netzer, C., Freudenberg, J., Toliat, M. R., Heinze, A., Heinze-Kuhn, K., Thiele, H., . . . Kubisch, C. (2008). Genetic association studies of the chromosome 15 GABA-A receptor cluster in migraine with aura. *American journal of medical genetics. Part B, Neuropsychiatric genetics : the official publication of the International Society of Psychiatric Genetics, 147B*(1), 37-41.

Obrenovitch, T. P., & Zilkha, E. (1996). Inhibition of cortical spreading depression by L-701,324, a novel antagonist at the glycine site of the N-methyl-D-aspartate receptor complex. *British journal of pharmacology, 117*(5), 931-937.

Peres, M. F., Zukerman, E., Senne Soares, C. A., Alonso, E. O., Santos, B. F., & Faulhaber, M. H. (2004). Cerebrospinal fluid glutamate levels in chronic migraine. *Cephalalgia : an international journal of headache, 24*(9), 735-739.

Prescot, A., Becerra, L., Pendse, G., Tully, S., Jensen, E., Hargreaves, R., . . . Borsook, D. (2009). Excitatory neurotransmitters in brain regions in interictal migraine patients. *Molecular pain, 5*, 34.

Provencher, S. W. (1993). Estimation of metabolite concentrations from localized in vivo proton NMR spectra. *Magnetic resonance in medicine : official journal of the Society of Magnetic Resonance in Medicine / Society of Magnetic Resonance in Medicine, 30*(6), 672-679.

Puppe, A., & Limmroth, V. (2007). GABAergic drugs for the treatment of migraine. *CNS & neurological disorders drug targets, 6*(4), 247-250.

Reyngoudt, H., De Deene, Y., Descamps, B., Paemeleire, K., & Achten, E. (2010). (1)H-MRS of brain metabolites in migraine without aura: absolute quantification using the phantom replacement technique. *Magma, 23*(4), 227-241.

Reyngoudt, H., Paemeleire, K., Descamps, B., De Deene, Y., & Achten, E. (2011). 31P-MRS demonstrates a reduction in high-energy phosphates in the occipital lobe of migraine without aura patients. *Cephalalgia : an international journal of headache, 31*(12), 1243-1253.

Reyngoudt, H., Paemeleire, K., Dierickx, A., Descamps, B., Vandemaele, P., De Deene, Y., & Achten, E. (2011). Does visual cortex lactate increase following photic stimulation in migraine without aura patients? A functional (1)H-MRS study. *The journal of headache and pain, 12*(3), 295-302.

Rothrock, J. F. (2012). Topiramate for migraine prevention: an update. *Headache, 52*(5), 859-860.

Russo, L., Mariotti, P., Sangiorgi, E., Giordano, T., Ricci, I., Lupi, F., . . . Gurrieri, F. (2005). A new susceptibility locus for migraine with aura in the 15q11-q13 genomic region containing three GABA-A receptor genes. *American journal of human genetics, 76*(2), 327-333.

Sacquegna, T., Lodi, R., De Carolis, P., Tinuper, P., Cortelli, P., Zaniol, P., . . . Barbiroli, B. (1992). Brain energy metabolism studied by 31P-MR spectroscopy in a case of migraine with prolonged aura. *Acta neurologica Scandinavica, 86*(4), 376-380.

Sandor, P. S., Dydak, U., Schoenen, J., Kollias, S. S., Hess, K., Boesiger, P., & Agosti, R. M. (2005). MR-spectroscopic imaging during visual stimulation in subgroups of migraine with aura. *Cephalalgia : an international journal of headache, 25*(7), 507-518.

Sarchielli, P., Tarducci, R., Presciutti, O., Gobbi, G., Pelliccioli, G. P., Stipa, G., . . . Capocchi, G. (2005). Functional 1H-MRS findings in migraine patients with and without aura assessed interictally. *NeuroImage, 24*(4), 1025-1031.

Scheller, D., Kolb, J., & Tegtmeier, F. (1992). Lactate and pH change in close correlation in the extracellular space of the rat brain during cortical spreading depression. *Neuroscience letters, 135*(1), 83-86.

Schulz, U. G., Blamire, A. M., Corkill, R. G., Davies, P., Styles, P., & Rothwell, P. M. (2007). Association between cortical metabolite levels and clinical manifestations of migrainous aura: an MR-spectroscopy study. *Brain : a journal of neurology, 130*(Pt 12), 3102-3110.

Siniatchkin, M., Sendacki, M., Moeller, F., Wolff, S., Jansen, O., Siebner, H., & Stephani, U. (2011). Abnormal Changes of Synaptic Excitability in Migraine with Aura. *Cerebral cortex*, 22(10), 2207-2216.

Sparaco, M., Feleppa, M., Lipton, R. B., Rapoport, A. M., & Bigal, M. E. (2006). Mitochondrial dysfunction and migraine: evidence and hypotheses.. *Cephalalgia : an international journal of headache, 26*(4), 361-372.

Storer, R. J., & Goadsby, P. J. (1999). Trigeminovascular nociceptive transmission involves N-methyl-D-aspartate and non-N-methyl-D-aspartate glutamate receptors.. *Neuroscience, 90*(4), 1371-1376.

Tallaksen-Greene, S. J., Young, A. B., Penney, J. B., & Beitz, A. J. (1992). Excitatory amino acid binding sites in the trigeminal principal sensory and spinal trigeminal nuclei of the rat. *Neuroscience letters, 141*(1), 79-83.

Tong, C. K., & Chesler, M. (2000). Modulation of spreading depression by changes in extracellular pH. *Journal of neurophysiology, 84*(5), 2449-2457.

Tottene, A., Fellin, T., Pagnutti, S., Luvisetto, S., Striessnig, J., Fletcher, C., & Pietrobon, D. (2002). Familial hemiplegic migraine mutations increase Ca(2+) influx through single human CaV2.1 channels and decrease maximal CaV2.1 current density in neurons. *Proceedings of the National Academy of Sciences of the United States of America, 99*(20), 13284-13289. doi: 10.1073/pnas.192242399

Uncini, A., Lodi, R., Di Muzio, A., Silvestri, G., Servidei, S., Lugaresi, A., . . . Barbiroli, B. (1995). Abnormal brain and muscle energy metabolism shown by 31P-MRS in familial hemiplegic migraine. *Journal of the neurological sciences, 129*(2), 214-222.

Vaccaro, M., Riva, C., Tremolizzo, L., Longoni, M., Aliprandi, A., Agostoni, E., . . . Ferrarese, C. (2007). Platelet glutamate uptake and release in migraine with and without aura. *Cephalalgia : an international journal of headache, 27*(1), 35-40.

Van Harreveld, A., & Fifkova, E. (1973). Mechanisms involved in spreading depression. *Journal of neurobiology, 4*(4), 375-387.

Vieira, D. S., Naffah-Mazacoratti, M. G., Zukerman, E., Senne Soares, C. A., Alonso, E. O., Faulhaber, M. H., . . . Peres, M. F. (2006). Cerebrospinal fluid GABA levels in chronic migraine with and without depression. *Brain research, 1090*(1), 197-201.

Watanabe, H., Kuwabara, T., Ohkubo, M., Tsuji, S., & Yuasa, T. (1996). Elevation of cerebral lactate detected by localized 1H-magnetic resonance spectroscopy in migraine during the interictal period. *Neurology, 47*(4), 1093-1095.

Welch, K. M., Chabi, E., Bartosh, K., Achar, V. S., & Meyer, J. S. (1975). Cerebrospinal fluid gamma aminobutyric acid levels in migraine. *British medical journal, 3*(5982), 516-517.

Welch, K. M., Levine, S. R., D'Andrea, G., Schultz, L. R., & Helpern, J. A. (1989). Preliminary observations on brain energy metabolism in migraine studied by in vivo phosphorus 31 NMR spectroscopy. *Neurology, 39*(4), 538-541.

Chapter 5

Insights into the Molecular Mechanisms of Migraine

5.1 Introduction

5.1.1 Ion channels and migraine

Migraine is a disease with a substantial heritability. First-degree relatives of migraine with aura (MA) have a fourfold increase of risk for MA(Russell & Olesen, 1995). Complex segregation analysis shows that both migraine without aura (MO) and MA have multifactorial inheritance, suggesting the multigenic nature of migraine(Russell, Iselius, & Olesen, 1995). However until recently, the common variants underlying typical forms of migraine have been unknown. Significant insights into the genetic basis of common disease can also come from the study of monogenic subtypes such as familial hemiplegic migraine (FHM) - a rare autosomal dominant form of MA (Joutel et al., 1993), wherein the associated headache is considered comparable to typical forms of migraine.

To date, mutations in three genes have been identified to cause FHM. The CACNA1A (FHM1) encodes the CaV2.1 (P/Q-type) voltage-gated calcium channel and its defect is believed to cause a "gain-of-function, with a proposed increase in excitatory neurotransmission (Ophoff et al., 1996) (van de Ven et al., 2007). ATP1A2 (FHM2) encodes the α2 subunit of Na^+/K^+ ATPase pumps (De Fusco et al., 2003) and SCNA1

(FHM3) encodes the pore-forming α1 subunit of neuronal $Na_v1.1$ Na^+ channels (Dichgans et al., 2005). These gene mutations may increase glutamate and K^+ level in the synaptic cleft, providing an environment that renders the cortex more susceptible to cortical spreading depression (CSD) and thereby aura (de Vries, Frants, Ferrari, & van den Maagdenberg, 2009). Indeed, it appears that these FHM subtypes of migraine are related to ionic disturbances leading to altered excitability of the brain. Ion channels are therefore highly likely to be involved in the pathogenesis of more typical forms of migraine.

5.1.2 Discovery of the role of KCNK18 (TRESK) gene in migraine

To examine the role of ion channels in common types of migraines, Lafreniere et al. screened 150 ion channel genes in 110 unrelated migraine probands (Lafreniere & Rouleau, 2011). This led to the identification of a frameshift mutation (F139WfsX24) in the KCNK18 gene in one subject suffering from migraine with visual aura (Lafreniere et al., 2010). The TRESK-encoding gene KCNK18 is involved in pain pathways, mediates neuronal excitability and is activated by volatile anesthetics which is believed to inhibit CSD (Liu, Au, Zou, Cotten, & Yost, 2004). The proband with the KCNK18 mutation described the visual aura as "bilateral slowly enlarging scotoma with a scintillating edge" which lasted 20 to 30min, followed by "a throbbing lateralized or holocranial headache" that lasted 24 to 48h. The headache was triggered by "tiredness, alcohol and bright lights". A further investigation of the subject's multigenerational family revealed that 8 affected relatives also harbored the TRESK variant whereas the 8 unaffected relatives did not – resulting in a genome-wide

significant genetic linkage of KCNK18 with the trait. This was the first evidence of a direct association between a genetic mutation and a common form of migraine. Furthermore, KCNK18 expression was identified in all adult mouse spinal cord and brain regions, but with the highest expression in trigeminal ganglion (TG). In human tissues, RT-PCR showed the presence of TRESK specifically in dorsal root ganglia (DRG) and immunohistochemistry revealed a strong staining for TRESK in TG neurons. The high expression of TRESK in migraine related regions support the role of TRESK in the pathophysiology of migraine. In addition, the functional analysis of TRESK in Xenopus oocytes showed that the frameshift mutation not only caused a complete loss of channel function but also reduced the current amplitude of the wild-type channel in a dominant-negative and dose-dependent fashion.

5.1.3 TRESK, Pain and Excitability

TRESK(TWIK[tandem pore domain weak inward rectifying channel]-related spinal cord K^+ channel) is a voltage-independent K^+ channel that belongs to a family of two-pore domain K^+ channels (K2P) (Yost, 2003). Structurally, K2P channels are distinctive from other K^+ channels in possessing 4 transmembrane domains (TMDs) and 2 pore-forming domains in each subunit. In addition, TRESK is unique among the family of K2P channels with the least sequence similarity (Liu, et al., 2004) and the presence of extended intracellular regulatory loops between TMD2 and TMD3(Huang, Yu, & Fan, 2008). By outwardly rectifying K currents that generate background K^+ leak currents, K2P channels stabilize the resting membrane potential and are thus considered important in mediating cellular excitability (Kim, 2005).

Evidence from a TRESK knock-out (KO) mice study supports the role of TRESK in neuronal excitability (Dobler et al., 2007). Current-clamp recordings showed that DRG neurons of wild-type (WT) littermate were less excitable, with higher amplitude and shorter duration of after-hyperpolarization, than DRG neurons of TRESK KO mice. A subsequent study, reported increased thermal pain sensitivity and increased isoflurane sensitivity in TRESK KO mice (Chae et al., 2010). Interestingly, the DRG hyperexcitability induced by axonal injury may involve TRESK, which was found to be significantly down-regulated at the mRNA level (Tulleuda et al., 2011). Furthermore, reducing TRESK expression in lumbar DRG neurons resulted in a reduced threshold in mechanical pain sensitivity of the animals. These in vivo studies support the role of TRESK channels in pain and neuronal excitability.

5.1.4 Candidate Gene Study

There are several approaches to identifying genetic variants associated with migraine. Genome-wide association studies (GWAS) identify and compare single-nucleotide polymorphisms (SNPs) and other DNA variants between disease and control groups and are becoming an increasingly popular approach in unraveling common genetic variability associated with disease (Simon-Sanchez & Singleton, 2008). However, most GWAS require a large number of samples to achieve statistical power and reveal common low penetrance variants of disease.

An alternative approach is to identify candidate genes based upon their functions and other evidence for a role in disease pathogenesis. Its major limitation it is this very dependency on pre-existing knowledge about gene function, which is often not

available. Furthermore, statistical tests for significance may be biased and replication is often not achieved. Nevertheless it is a cost-effective approach and can provide immediate mechanistic insights.

We selected four genes (TRESK, SLC12A3, KCNG4, OPN4) for further screening of deleterious coding mutations in a study sample of 741 migraine with aura subjects and 416 headache-free controls.

5.1.4.1 SLC12A3

A recent study has revealed that the association between TRESK and migraine may be more complex than previously considered (Andres-Enguix et al., 2012). Five missense variants, R10G, A34V, C110R, S231P and A233V were identified in additional screening for KCNK18 in unrelated migraineurs and control cohorts. Importantly, some unaffected subjects harbored a defective mutation, C110R indicating that additional genetic loci may modify the penetrance of KCNK18 mutations.

SLC12A3 is a gene encoding the thiazide-sensitive sodium-chloride transporter (Simon et al., 1996). It is the key mediator of renal sodium and chloride reabsorption and its loss of function leads to an autosomal recessive disorder called Gitelman syndrome (Mastroianni et al., 1996). Further analysis of the family with the frameshift KCNK18 mutation, revealed a second genetic linkage peak overlying a region containing SLC12A3 (Dr Cader, personal communication). Whole exome sequence analysis in three affected individuals from the family identified a deleterious

heterozygous mutation in SLC12A3 genes and subsequent analysis revealed all affected migraineurs (n=8) also carry the same SLC12A3 variants. Two unaffected members also have this mutation. SLC12A3 is therefore a candidate gene for migraine and potential genetic interactor of KCNK18.

5.1.4.2 OPN4

A recent study showed that the convergence of photic signals from the melanopsin(OPN4)-containing ipRGCs and the nociceptive signals from the dura at thalamus may underlie the mechanism of migraine related photophobia(Noseda et al., 2010). However, there are no studies that have attempted to explore the genetic and molecular aspects of the role of the melanopsin encoding OPN4 gene in migraine. This despite significant evidence for the potential involvement of the hypothalamaus and circadian rhythms in migraine. For example, the periodic dysfunction of the suprachiasmastic nucleu of hypothalamus may account for the periodicity of migraine attacks(Zurak, 1997) . Indeed, attacks of migraine have been reported to occur more frequently during early morning and the night (Solomon, 1992). Another argument claims that the role of the hypothalamus in mediating homeostasis may be responsible for the premonitory symptoms such as thirst, hunger, yawning and lethargy that often seen in migraineurs preceding attacks. Finally, a positron mission tomography (PET) study revealed hypothalamic activation during attack, suggesting that hypothalamic dysfunction may be related to migraine onset(Denuelle, Fabre, Payoux, Chollet, & Geraud, 2007). Dysfunction of OPN4 leading to altered hypothalamic function and circadian entrainment is therefore a strong gene candidate in migraine.

5.1.4.3 KCNG4

KCNG4 encodes a member of the voltage-gated potassium channel, subfamily G, and has a strong expression in brain(Sano et al., 2002). It modulates channel activity by shifting the threshold and the half-maximal activation to more negative values(Ottschytsch, Raes, Timmermans, & Snyders, 2005). In a GWA study examining patients with bipolar disorder and comorbid migraine, a suggested association was found in KCNG4 on the chromosomal locus 16: 82813324 – 82830857(Oedegaard et al., 2010). In the 150 ion channels screened by Lafreniere et al., a suggestive association was found between KCNG4 and migraine [(Lafreniere & Rouleau, 2012)

5.1.5 DNA Pooling and Next Generation Sequencing

Recently, DNA pooling has also offered a practical way in reducing the costs for screening large population for common disease (Sham, Bader, Craig, O'Donovan, & Owen, 2002). It is both rapid and cost-effective for screening of linkage regions and candidate genes in a large population of samples (Norton, Williams, O'Donovan, & Owen, 2004). It was first used in a case-control association study of HLA-DR type in insulin-dependent diabetes (Arnheim, Strange, & Erlich, 1985) and has been applied to both microsatellite markers and single nucleotide polymorphisms (SNPs) (Sham, et al., 2002).

Next generation sequencing (NGS) is a revolutionary technology using massive parallel sequencing (Shendure & Ji, 2008). The reliability and cost effectiveness of NGS based on pooled DNA has been investigated and showed advantages over individual genome

sequencing (Futschik & Schlotterer, 2010) (Van Tassell et al., 2008). This is particularly the case in population studies, where the primary aim is to detect variants and their frequencies rather than identifying the source of individual variants. However, there may be high rates of sequencing errors in pooling unless the minimum number of reads required for allele calling is high(Cutler & Jensen, 2010). Sequencing large pools carries the cost of reduced detection of rare alleles and importantly, haplotype information is lost.

The accuracy of constructing equimolar pools is the most important consideration to ensure unbiased sequence coverage. Traditional ultraviolet (UV) absorbency is inadequate as inaccuracies arise from the presence of non-double stranded template DNA. PicoGreen reagent is a nucleic acid stain that quantifies double-stranded DNA (dsDNA) based on fluorimetry, with high sensitivity and accuracy (Ahn, Costa, & Emanuel, 1996) (Sham, et al., 2002). Although various methods of pooling have been proposed (Sham, et al., 2002) (Margraf, 2010), Barratt et al suggested that pools of approximately 50 individuals is superior to fewer but larger pools (Barratt et al., 2002). We adopted a pool size of 13 individuals allowing all samples to be reduced to a single 96-well plate.

5.1.6 Aims

The current study designed and prepared amplicons suitable for next-generation sequencing of these candidate genes, namely KCNK18(TRESK), SLC12A3, KCNG4 and OPN4, in a large cohort of migraineurs and controls using the DNA pooling method. It is part of a larger project of identifying rare coding genetic variants that associate with migraine.

5.2 Methods

5.2.1 Optimization of PCR conditions

5.2.1.1 Design of primers

Gene sequences were obtained from Ensembl genome brower 69 (http://www.ensembl.org/index.html). PCR primers were then designed using Primer 3 (http://frodo.wi.mit.edu/) to amplify 3 exons in KCNK18, 26 exons of SLCN12A3, 12 exons of OPN4 and 3 exons of KCNG4(Kersey et al., 2012). Since we adopted a next-generation sequencing strategy on the Illumina HiSeq platform, we aimed for large PCR fragments of 3-9kb. Hence, where possible, multiple exons were covered in a single amplicon.

The following conditions were used to select primers:

1. The primer melting temperatures (Tm) were set in the range between 55°C and 75°C.
2. The percentage of G and C in the sequences (GC contents) was between 40 and 60%.
3. Primer sizes were between 18 to 27base pairs

5.2.1.2 Genomic PCR

For genomic PCR, we used Phusion Hot Start II DNA Polymerase (2U/µl) in 25µl reaction, setup on ice. In all optimization reactions, 10ng genomic DNA template (10ng/µl) was used. Other constituents are as provided in Table 2.1 PCR Cycling parameters are given in Table 2.2. and followed manufacturer's instructions. Several parameters were altered during optimization.

Components	**Volume (µl)**
Water	15.5
5 X Phusion HF (GC) Buffer	5
2mM dNTPs	2.5
Forward primer	0.625
Reverse primer	0.625
Genomic DNA (10ng/µl)	1
Phusion Hot Start II DNA Polymerase (2U/ µl)	0.25

Table 2.1. Components of a PCR containing water, Phusion HF (GC) buffer, dNTPs, forward and reverse primers, genomic DNA and Phusion Hot Start II DNA Polymerase.

Cycling step	**Temperature**	**Time**	**Number of cycles**
Initial denaturation	98° C	30s	1
Denaturation	98° C	15s	~30
Annealing	according to Tm	30s	
Extension	72° C	15 to 30s/1 kb	
Final extension	72° C	10min	1
cooling	4° C	hold	

Table 2.2. Summary of cycling parameters in PCR optimization.

PCR products were assessed using 1% Agarose gel electrophoresis, prepared by 1:100 agarose water and a few microliters of either ethidium bromide or SYBR®Safe (Invitrogen). 2µl of 6 x dye was added into each 10µl of the PCR products and the product-dye mixture was loaded into a well of the gel. A separate well was also loaded with a 1kb reference ladder (BioLabs® cat# N3232L). After loading all the wells with the PCR products we wanted to test, electrophoresis was performed at 100v for 40min.

5.2.1.3 96well-plate genomic PCR

After optimization experiments, Genomic PCR was undertaken on the migraine samples using 50ng total DNA (Table 2.3)

Components	Volume (μl)
DNA multiplex	4.69
dNTP	5
GC buffer	10
H_2O	27.31
Forward primer	1.25
Reverse primer	1.25
Phusion enzyme	0.5

Table 2.3. 96well-plate genomic PCR. Components of 50 μl PCR reactions in one well of the 96 well-plate containing DNA multiplex, dNTP, GC buffer, water, forward and reverse primers and Phusion enzyme.

5.2.2 Quantification of DNA samples

A total of 1157 DNA samples including 741 from subjects with migraine with aura and 416 healthy controls were available. These samples were provided by Professor Jes Olesen, University of Copenhagen, as part of a larger migraine genetics study. Invitrogen Quant-iT™ PicoGreen® dsDNA Assay Kit was used for quantifying the DNA samples in 96-well plates. A dilution of stock DNA standard in TE buffer was made from 100µg/ml to 2µg/ml, then the DNA standards were prepared (Table 2.4).

STD	DNA 2ug/ml	TE buffer (x1)
Std0	0ul	1000ul
Std25	25ul	975ul
Std50	50ul	950ul
Std100	100ul	900ul
Std300	300ul	700ul
Std500	500ul	500ul
Std700	700ul	300ul
Std1000	1000ul	0ul

Table 2.4. Preparation of DNA standards. DNA standards were prepared by adding various volumes of standards to TE buffer to make final volumes of 1000µl. STD: standard

1.5µl of sample DNA was diluted with 150µl of TE and the mixture was mixed well with a multi-channel pipette. 50µl of each diluted DNA sample and 50µl of the prepared standards were pipetted in duplicate. 50µl of the diluted PicoGreen assay (25 µl stock PicoGreen, 4975µl TE) was added to each of both DNA samples and standards and well mixed. By the method of fluorescence, the plates were analysed with a Tecan SpectraFluor Plus (94848) fluorimeter.

5.2.3 Constructing DNA pools

The current study constructed pools of 13 distinct individuals, each sample at 500ng. As such, a master 96well plate with a total of 89 pools consisting of 57 MA and 32 controls was constructed after quantifing the DNA concentrations of all 1157 samples (741 migraine with aura, 416 controls), In order to avoid inaccuracies that may arise from pipetting small volumes of DNA solutions, DNA samples that were relatively high in concentration were diluted. The master plate is shown in figure 2.1. A1 to E9 contained samples from migraine subjects whereas F1 to H9 contained samples from healthy controls. The wells E10 – 12 and H9 – 12 were empty.

	1	2	3	4	5	6	7	8	9	10	11	12
A	MA	MA	MA	MA	MA	MA	MA	MA	MA	MA	MA	MA
B	MA	MA	MA	MA	MA	MA	MA	MA	MA	MA	MA	MA
C	MA	MA	MA	MA	MA	MA	MA	MA	MA	MA	MA	MA
D	MA	MA	MA	MA	MA	MA	MA	MA	MA	MA	MA	MA
E	MA	MA	MA	MA	MA	MA	MA	MA	MA	X	X	X
F	controls	controls	controls	controls	controls	controls	controls	controls	controls	controls	controls	controls
G	controls	controls	controls	controls	controls	controls	controls	controls	controls	controls	controls	controls
H	controls	controls	controls	controls	controls	controls	controls	controls	X	X	X	X

Figure 2.1. Master plate containing pooled DNA samples. A total of 89 pools consisting of 57 MA and 32 controls. Migraine samples, control samples and empty wells are presented as MA, controls and X respectively.

5.3 Results

The optimization of primer condition was challenging because PCRs were on long fragment genomic DNA. My first attempt using the standard genomic PCR protocol failed to generate the targeted products with sufficient yield or purity, highlighting the difficulties of this method and necessitating extensive optimization.

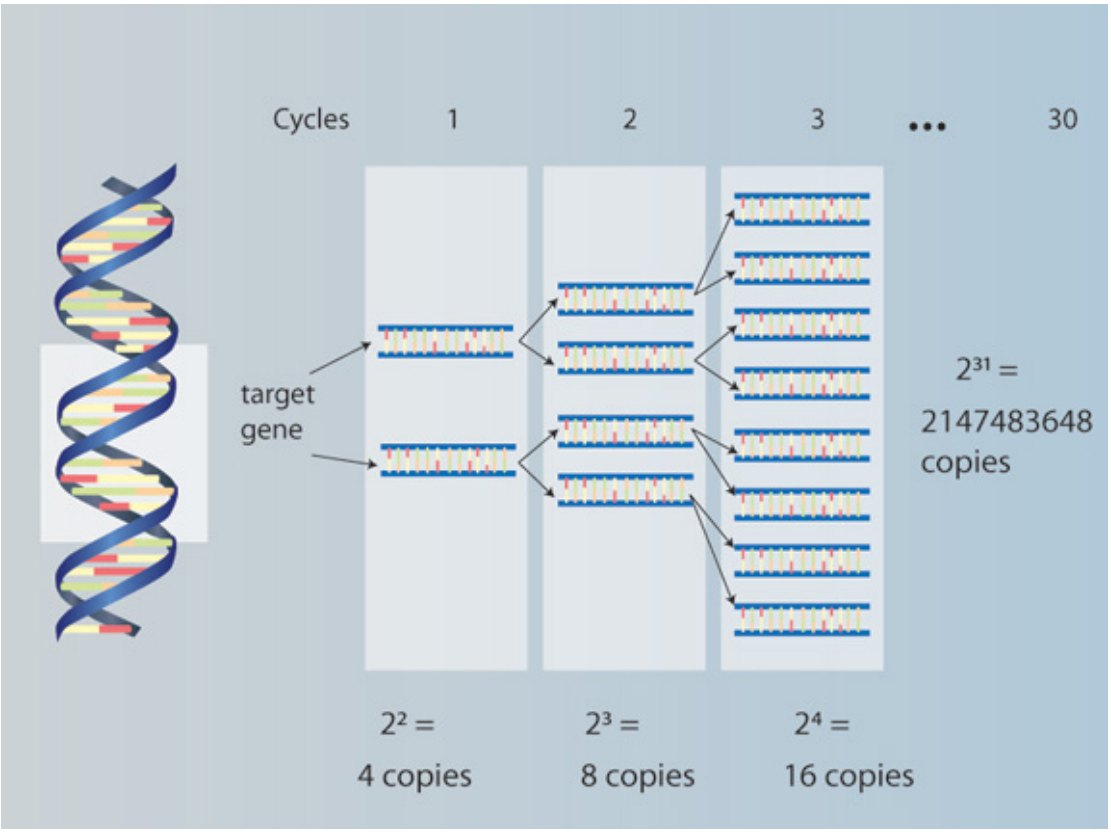

Figure 3.1. Polymerase chain reaction (PCR). PCR begins with a genomic DNA that combines with forward and reverse primers, dNTPs and DNA polymerase to undergo repeated cycles in a thermocycler. Each cycle contains the denaturation phase, annealing phase and extension phase that react at various temperatures and durations. The denature step separates the double strand DNA by heating to a high temperature. Too high a temperature would result in breaking the DNA backbone and thus yielding no DNA products. The next step is the annealing phase in which primer pairs bind to the target sequence of the denatured DNA. As such, an incorrectly designed primer set or inappropriate annealing temperature will result in the primers binding to the wrong targets and therefore yielding non-specific products. The last extension phase extends the targeted site via DNA polymerase by adding the dNTP to the annealed primers. These 3 phases complete one cycle of PCR and the cycle is then repeated for n cycles with a final product of $(2^n - (n+1))$ target fragments. Any mistakes arising from any of the phases would result in producing the incorrect product, products with low specificity or no product at all. Adapted from © 2010 *Nature Education*.

5.3.1 PCR with no product or low yield

Although increasing DNA template has been proposed as a possible method of increasing the yield of PCR products, this had no impact in my PCR. Increasing the extension time did in some cases result in a PCR product but often at the expense of non-specific bands appearing (figure 3.2A and B). Decreasing annealing temperature generally increased the yield often without the generation of non-specific bands (figure 3.2C). GC buffer, as supplied by the manufacturer, often significantly improved the performance of Phusion enzyme over the standard HF buffer, figure 3.2D. In same cases a combination of approaches was required, again illustrated in Figure 3.2D, where the buffer used was GC buffer along with a decrease of the extension time from 4.5 to 3.5min.

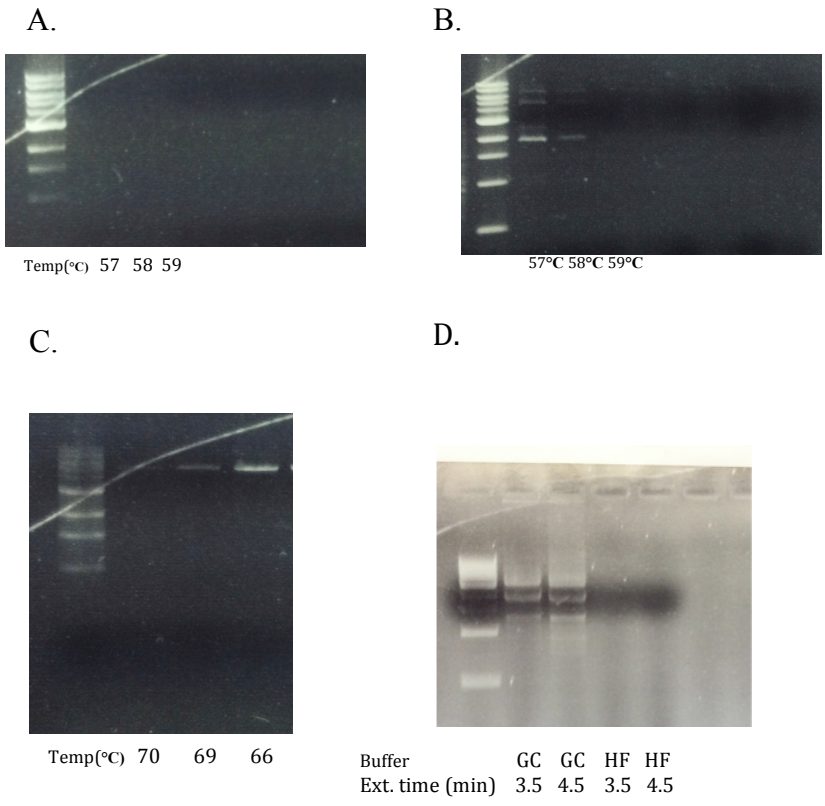

Figure 3.2. Gel electrophoresis for optimizing PCR conditions with **A.** 2.5min and **B.** 3min as extension time. Increasing the extension time results in a PCR product at the expense of non-specific products. **C.** No product and low-yield at 70°C and 69°C respectively. Decreasing the annealing temperature to 66°C gave a high-yield product. **D.** Comparing the performances of GC and HF buffers. PCRs were performed using Phusion enzyme under standardized PCR cycling conditions with primers selected for amplifying desired targets. Gel electrophoresis was run on 1% agarose gel stained with SYBR®Safe. Ext. time: extension time(min). Temp.: temperature (°C)

5.3.2 PCR with non-specific bands

These PCRs were improved by reducing extension time, reducing number of cycles, increasing annealing temperature or a combination. To assess the best annealing temperature, I used a temperature gradient, 57 to 70**°C.**

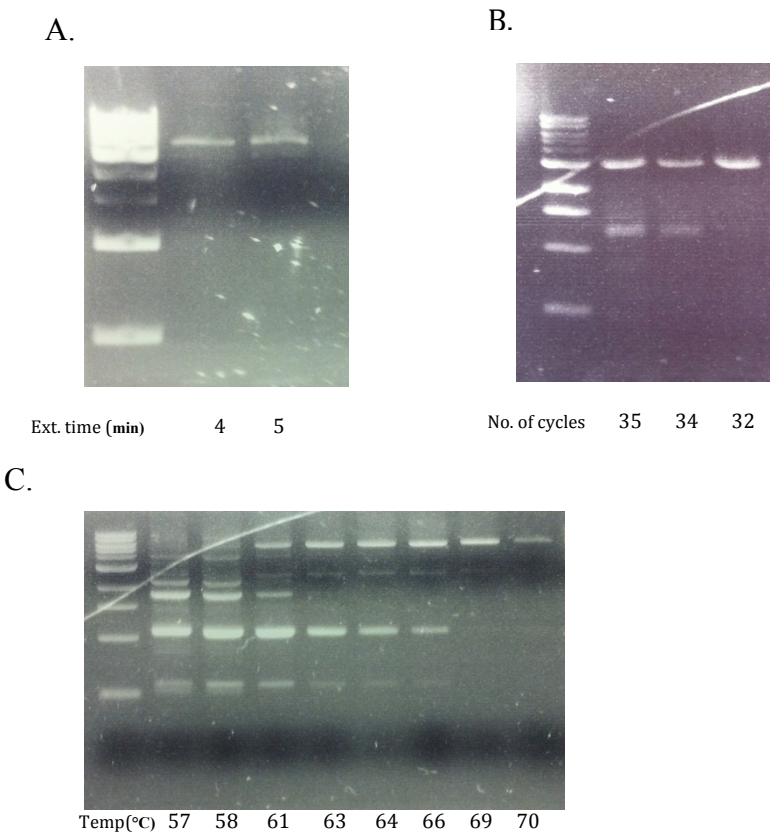

Figure 3.3. Gel electrophoresis for optimizing PCR conditions showing **A.** Decreasing extension time from 5 to 4min yielded a more specific product. **B.** decreasing the number of cycle from 35 to 32 significantly improved the specificity **C.** Increasing annealing temperature from 57 to 70°C yielded a specific product at 70°C. PCRs were performed using Phusion enzyme under standardized PCR cycling conditions with primers selected for amplifying desired targets. Gel electrophoresis was run on 1% agarose gel stained with SYBR®Safe. Ext. time: extension time(min). Temp.: temperature (°C).

5.3.3 Designing new primers

Although the above strategies helped to optimize some of the genomic PCR, in many cases, I designed new primers and optimized them with similar strategies.

5.3.4 Optimized PCR results

13 primer fragments covering all the exons in these four candidate genes (2 in KCNK18, 7 in SLC12A3, 2 in OPN4 and 2 in KCNG4) were designed and optimized (table 3.1 and 3.2). The sequences and gel electrophoresis pictures of these targeted fragments following optimization are shown as below, figure 3.4 and 3.5.

Target Fragment	Exon	Forward primer	Reverse primer
OPN4			
1	1-8	5'CTCATGGGGGCCAAACATGG3'	5'AGCCCTCAGTGGCTGGCTCA3'
2	7-12	5'AGGGGAGCCTCAGGAGACAAGG3'	5'GCCAACCCCTTCCCCAAGAA3'
KCNG4			
1	1-2	5' TGACTCCCACCCAGCGCTCA3'	5' TGAGGCCGGGGACCTTTGCA3'
2	3	5'ATGAATGAGGGGTGGTAAACAACAAAG3'	5'GTGAAGGGGCTTTCCTTGTGTCA3'
KCNK18			
1	1-2	5' GGGCACCTTTTCTCATGGCAGA 3'	5' GCCACGTCCCTTGCTGGAGA 3'
2	3	5' GCCACAGCTCCCTCCCCTACA 3'	5' GGCTGGGATTGGGCTGGTCT 3'

Table 3.1. PCR primers used to amplify regions of the human OPN4, KCNG4 and KCNK18 genes.

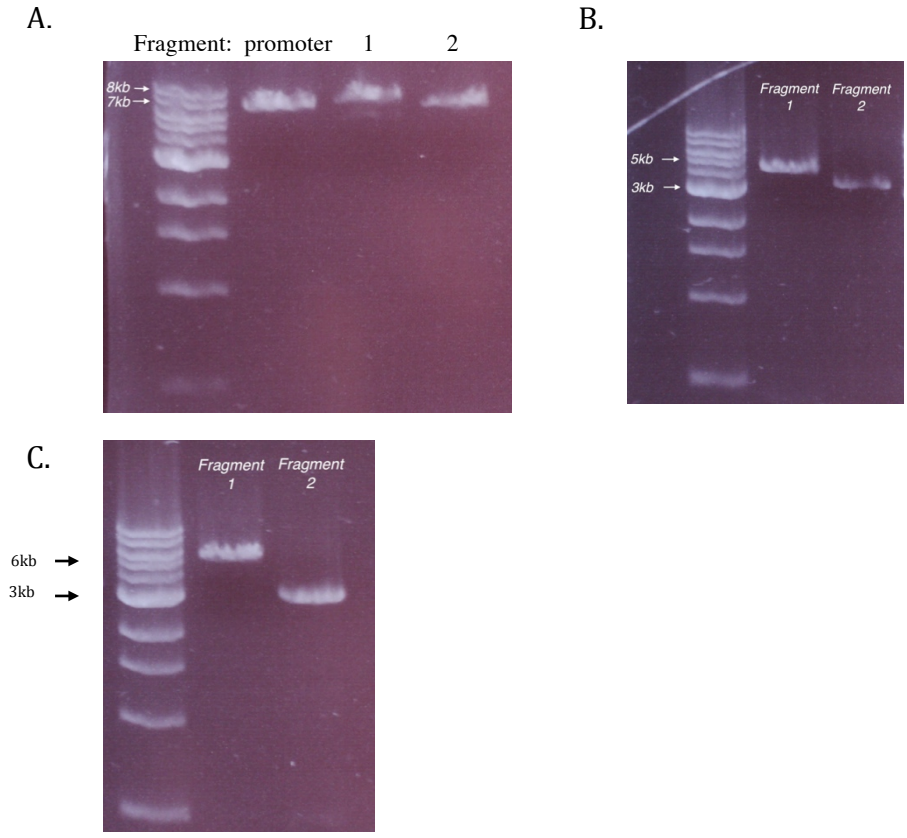

Figure 3.4. Optimized primer conditions for targeted fragments of **A**. OPN4. Fragment 1 (8kb), GC buffer, extension time 4min, 30cycles, annealing temperature 76.2° C. Fragment 2 (7kb), GC buffer, extension time 3.5min, 30cycles, annealing temperature 66° C. **B.** KCNG4. Fragment 1 (4kb), GC buffer, extension time 2min, 30cycles, annealing temperature 73° C. Fragment 2 (3.5kb), GC buffer, extension time 1.5min, 30cycles, annealing temperature 70° C. **C.** KCNK18. Fragment 1 (6kb), GC buffer, extension time 2.5min, 30cycles, annealing temperature 71° C. Fragment 2 (3kb), GC buffer, extension time 1.5min, 32cycles, annealing temperature 71° C. PCRs were performed using Phusion enzyme with gel electrophoresis run on 1% agarose gel stained with SYBR®Safe.

Target Fragment	Exon	Forward primer	Reverse primer
1	1-8	5’ CCGGCCGAATAAACCCCTTC 3’	5’ GGGAAGGGTGGCACTGGTCA 3’
2	9-15	5’ TTTCACCAACATCCCTGACA 3’	5’CAGGAGCCATCAGGAGAGAG 3’
3A	16-18	5’ ATCCTCTTCCCACCAGATCC 3’	5’ TTTGGAGTCAGCCCTGAAGT 3’
3B	19	5’ AACACGCTGAGGCTGAAGAT 3’	5’ AGGGCTCCCTTAATGCTAGG 3’
3C	20-22	5’ AGCCGTGATTGCACCACT 3’	5’ CTGAGGTGGGTGGATCACTT 3’
4	23-25	5’ CCCTGCCCCACCCGCTTT 3’	5’ GGCCTCTGTTTCTGTTGCTC 3’
5	26	5’ GCTTAATGAAATGGCCTTGG 3’	5’ CTTAACCCCCACCTCCTGAT 3’

Table 3.2. PCR primers used to amplify regions of the human SLC12A3 genes. *Fragment 3 was amplified in three separate minimally-overlapping PCR fragments.

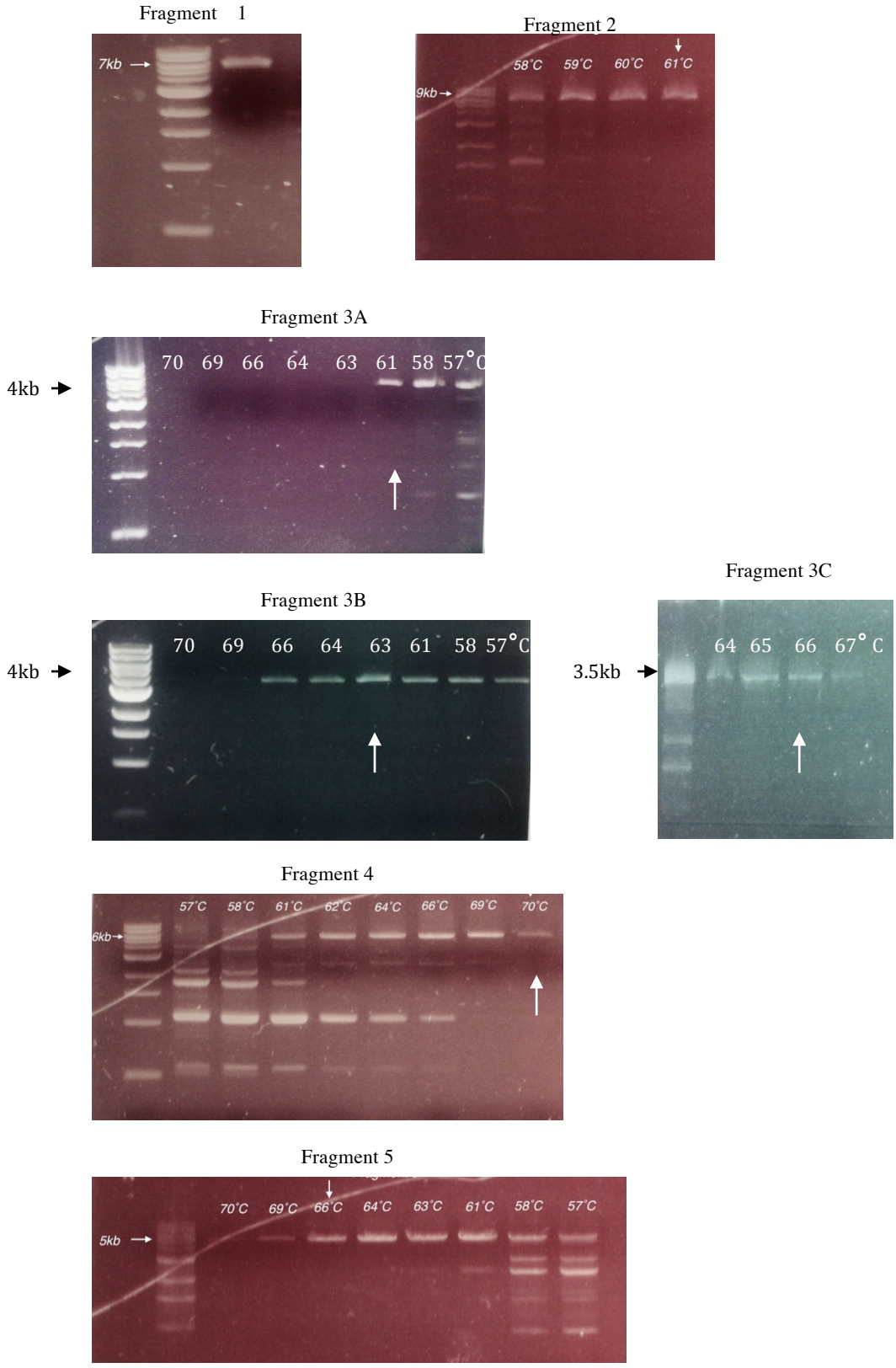

Figure 3.5. Optimized primer conditions for SLC12A3 targeted fragments.
Fragment 1 (8kb), GC buffer, extension time 4min, 30cycles, annealing temperature 66° C.
Fragment 2 (9kb), GC buffer, extension time 4.5min, 30cycles, annealing temperature 61° C.
Fragment 3A (4kb), GC buffer, extension time1.5min, 30cycles, annealing temperature 61° C.
Fragment 3B (4kb), GC buffer, extension time 2min, 30cycles, annealing temperature 63° C.
Fragment 3C (9kb), HF buffer, extension time 1.5min, 30cycles, annealing temperature 66° C.
Fragment 4(7kb), GC buffer, extension time 3.5min, 30cycles, annealing temperature 66° C.
Fragment 5(5kb), GC buffer, extension time 2.5min, 30cycles, annealing temperature 66° C.
PCRs were performed using Phusion enzyme with gel electrophoresis run on 1% agarose gel stained with SYBR®Safe.

5.3.5 PicoGreen quantification of the migraine and control DNA samples

DNA quantification results of the 1157 samples including 741migraineurs and 416 controls were recorded in Excel sheets. In all 33 reader plates, all eight points in the standard curve remained linear with $R^2 > 0.9$, indicating that the standards served as effective controls to the experimental samples.

5.3.6 Robustness of DNA pooling

As shown in figure 3.6, 10ng template DNA of individual subjects (migraine no. 1 to 13) were used to perform individual PCR reactions. The gel electrophoresis of the PCR products (10µl of 25µl) showed an approximately equivalent of product yields across 13 subjects(individual fragments not shown were not successful). The gel electrophoresis in figure 3.7 showed the robust PCR products of the KCNK18 (fragment 1 and 2), KCNG4 (fragment 1 and 2), OPN4 (fragment 1, and 2) and SLC12A3 (fragment 1, 2, 4, 6 and 7) using pooled DNA from13 migraine samples.

A. KCNK18 sequence fragment 1

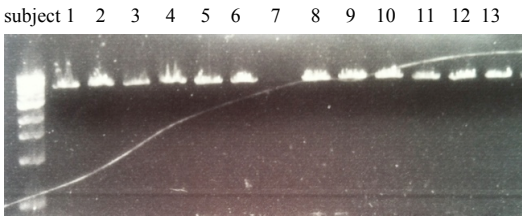

B. KCNG4 sequence fragment 1

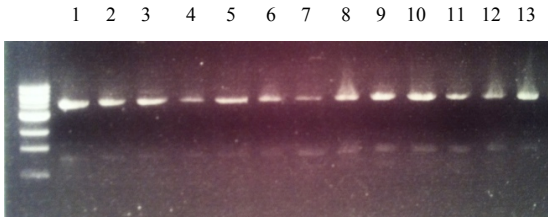

C. OPN4 sequence fragment 1

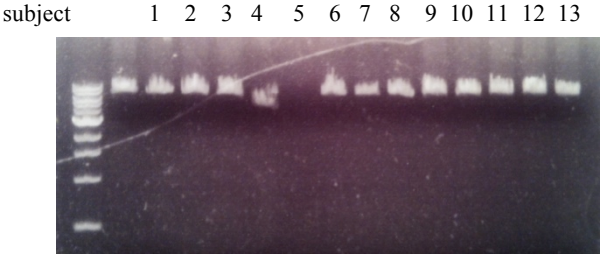

D. SLC12A3 sequence fragment 1

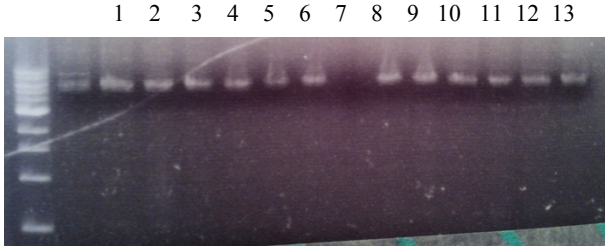

E. SLC12A3 sequence fragment 2

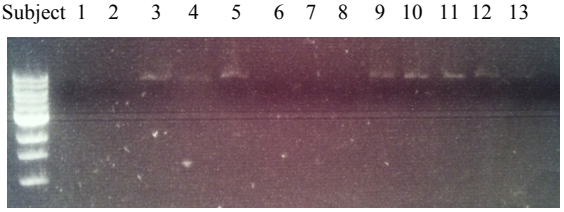

F. SLC12A3 sequence fragment 3A

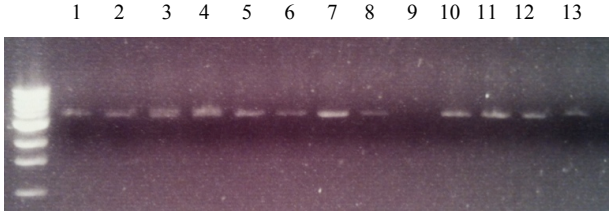

G. SLC12A3 sequence fragment 4

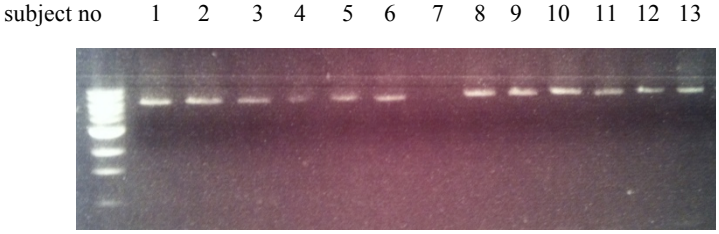

H. SLC12A3 sequence fragment 5

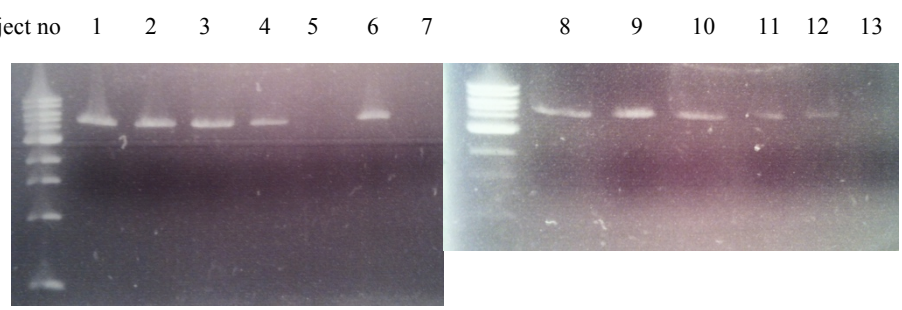

Figure 3.6 Gel electrophoresis showing the robustness of PCR using individual template DNA. **A**. KCNK18 sequence fragment 1 **B**. KCNG4 sequence fragment 1 C. OPN4 sequence fragment 1 D. SLC12A3 sequence fragment 1 **E**. SLC12A3 sequence fragment 2 **F**. SLC12A3 sequence fragment 3A **G**. SLC12A3 sequence fragment 4 **H.** SLC12A3 sequence fragment 5. Fragments not shown and missing bands were not successful. PCRs were performed using Phusion enzyme under optimized PCR cycling conditions with primers selected for amplifying desired targets. Gel electrophoresis was run on 1% agarose gel stained with SYBR®Safe.

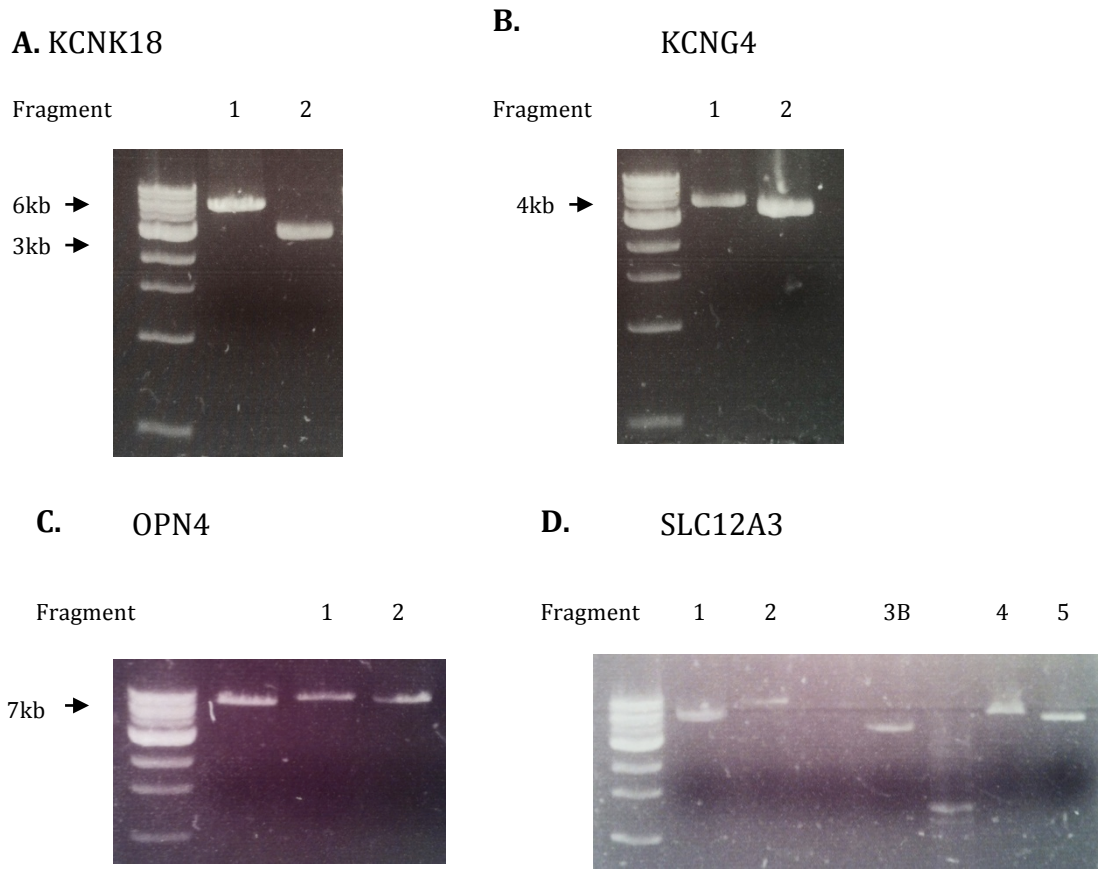

Figure 3.7. Gel electrophoresis of the PCR products of the target fragments of **A.** KCNK18 **B.** KCNG4, **C.** OPN4 and **D.** SLC12A3 using the DNA multiplex of pool A1 (migraine no. 1 to 13, please refer to figure 2.1) as DNA templates. Fragment 3 and 5 of SLC12A3 were not successful and further optimization was performed. PCRs were performed using Phusion enzyme under optimized PCR cycling conditions with primers selected for amplifying desired targets. Gel electrophoresis was run on 1% agarose gel stained with SYBR®Safe.

5.3.7 Comparison of PCR yields using 10, 50 and 130ng DNA multiplex as templates

The comparison of the PCR product concentrations using three different starting amount of DNA templates showed no significant difference, suggesting that increasing the amount of DNA template from 10, 50 to 130ng would not significantly increase the yield of the PCR products.

5.4 Discussion

The aim of the current study was to prepare amplicons of the four candidate genes KCNK18 (TRESK), KCNG4, SLC12A3 and OPN4 for next-generation sequencing using the DNA-pooling method. I successfully 1) optimized genomic PCR to amplify fragments covering these genes, 2) quantified the DNA concentration of 1157 samples including 741migraineurs and 416 controls, 3) designed and constructed a master plate containing all samples with 13 individual samples per well of equimolar and 4) performed the optimized genomic PCR on the DNA complexes(figure 4.1).

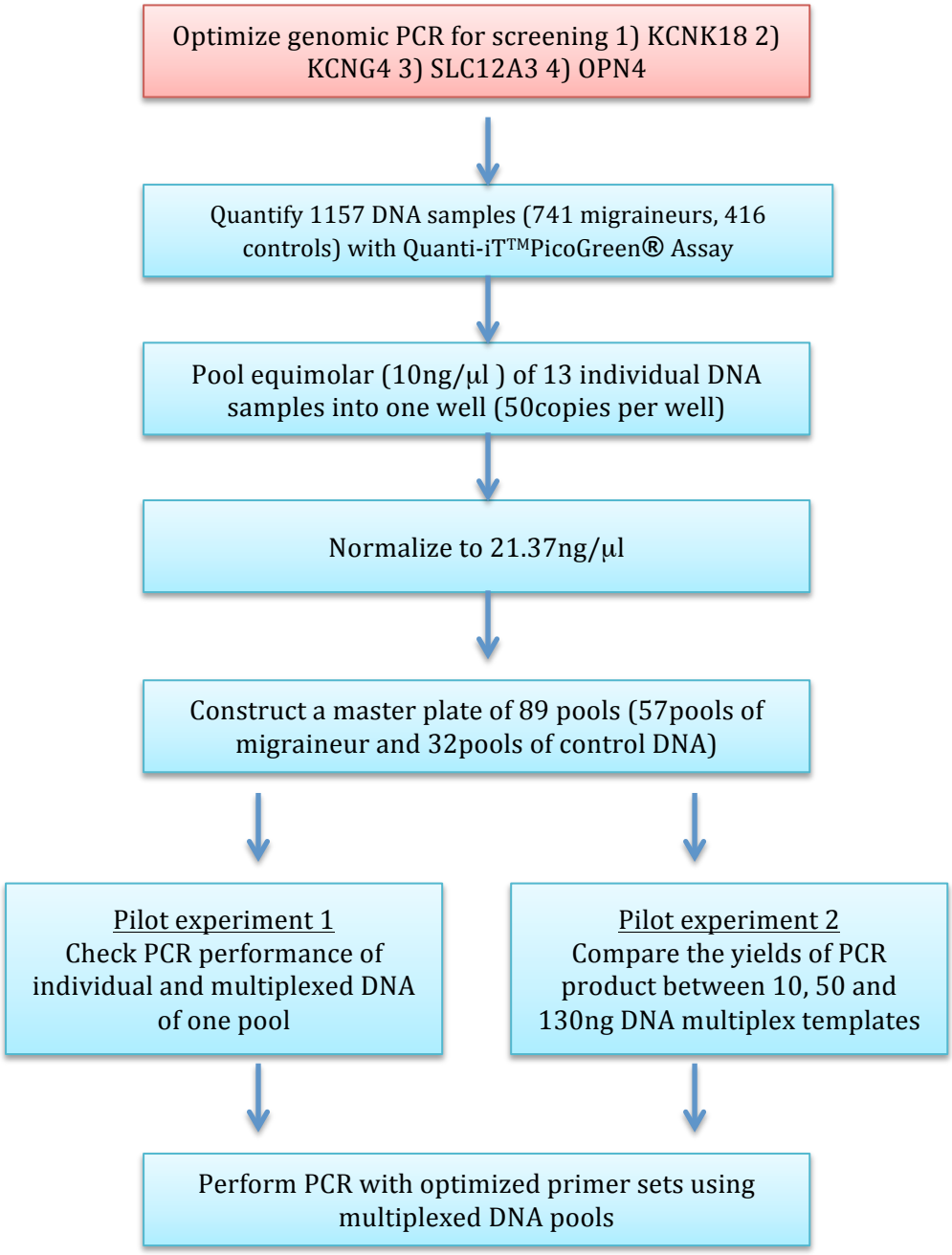

Figure 4.1 Summary of the current study.

5.4.1 Primer condition optimization

Although the above strategies helped to optimize some of the genomic PCR, many of the initially designed primer sets failed to generate the targeted products. In such cases, I designed new primers and optimized them with the same strategies. In general I found the following criteria for a successful primer design:

1) avoid selecting primers that contain long successive sequences of polypurines (adenine and guanine) or polypyrimidines (cytosine and thymine). For examples, all successful primer sets in our optimized PCR have random distributions of nucleobases and the longest sequence of repetitive nucleobases did not exceed 5, i.e. five successive cytosines in the reverse primer of SLC12A3 fragment 5 and five guanines in the forward primer of OPN4 fragment 1.
2) Where possible, I selected primers with GC contents similar to the amplified targeted sequence.
3) When designing new primers, I tried to limit the maximum 3' complementarity of the primers so as to minimize the formation of primer dimers.

5.4.2 Alternative strategies of DNA sequencing and comparison of cost-effectiveness

The initial purpose of adopting a candidate gene approach method for NGS in my study was to achieve high cost-effectiveness by reducing the labor and costs. However, I spent a considerable time in optimizing primer conditions. Alternative strategies to consider for future studies include:

5.4.2.1 Sanger sequencing

The conventional Sanger sequencing was first described by Frederick Sanger in 1977(Sanger, Nicklen, & Coulson, 1977). It is based on amplifying a DNA fragment with the integration of dideoxynucleotides (ddNTPs) that terminates the addition of further nucleotides (Shendure & Ji, 2008). It has the advantages of longer read length and lower error rates compared to the novel techniques of NGS(Robison, 2010). Moreover, since the amplicons required in Sanger sequencing can be much shorter than that in my experiment, optimization is faster. However, it is limited by low throughput which renders it uncompetitive with NGS, both in costs and labor (Mardis, 2011). The estimated cost for the study for each individual presented in this thesis, assuming a price for each sample of £5, sequencing 44 short DNA fragments is £220. To sequence all 1147 samples would cost £252,340.

5.4.2.2 Genome wide sequencing

Another strategy is whole exome sequencing, WES (Mamanova et al., 2010) or whole genome sequencing, WGS method. WES enables the sequence of all coding gene regions to be determined. WGS has the advantage of providing the complete DNA sequence of an individual including non-coding regions that may have significant contribution to liability to disease(Hobert, 2010). However whilst the cost for these technologies has been reducing exponentially in the recent years, it remains expensive. Furthermore analysis of sequencing reads is non-trivial.

5.4.3 DNA pooling

The DNA pooling method that I adopted provides a cost-effective way to employ NGS. However, there are limitations that need to be considered. First, the construction of DNA pool is a labor intensive and time-consuming process. In order to achieve equimolar pools, accurate quantification of DNA using Picogreen assay and normalization of sample concentration are required in several steps throughout the entire process of sample preparation for NGS. Second, the high quality of laboratory procedures in achieving accuracy remains a great technical challenge. For instance, errors could arise easily when pipetting small volumes over 1000 samples at the standard of accuracy within ng/μl per sample. Even when equimolar pooling is achieved, individual sample may potentially show variable PCR amplification. Sham et al. suggested validating the performance of amplification of each sample by PCR to check the robustness of product (Sham, et al., 2002). Hence, I checked the quality of PCR products by performing PCR with both multiplexed DNA and individual DNA

samples of one well on repeated experiments to ensure the robustness of the PCR reaction.

Another drawback of DNA pooling is the loss of haplotype information. By sequencing the pooled DNA with NGS, we will obtain the group variants of migraineurs and healthy subjects. Although a limited number of studies claimed the efficiency in estimating haplotype frequencies from DNA pools of various sizes (Kirkpatrick, Armendariz, Karp, & Halperin, 2007) (Zhang, Yang, & Yang, 2008), these are often simulation studies and are not supported by other studies(Kuk, Xu, & Yang, 2010). Therefore, the DNA pooling method of my study may be regarded as the preliminary screen for variants between migraine cases and controls, whereas a subsequent haplotype analysis will be required to confirm the individual genotyping. As such, a custom single nucleotide polymorphisms (SNPs) genotyping will be performed in a future step using the Sequenom platform.

5.5 Conclusion

Of note, the current study is the PCR optimization and preparation step for a larger project of NGS with the final aim of identifying rare coding genetic variants that associate with migraine. To this end, I adopted two strategies, the DNA pooling and candidate gene approach for NGS. Samples will be sent for NGS and the variants in both migraine and control groups will be identified. To recover the haplotype information on each individual, custom SNPs genotyping will be performed.

5.6 References

Ahn, S. J., Costa, J., & Emanuel, J. R. (1996). PicoGreen quantitation of DNA: effective evaluation of samples pre- or post-PCR. *Nucleic acids research, 24*(13), 2623-2625.

Andres-Enguix, I., Shang, L., Stansfeld, P. J., Morahan, J. M., Sansom, M. S., Lafreniere, R. G., . . . Tucker, S. J. (2012). Functional analysis of missense variants in the TRESK (KCNK18) K channel. *Scientific reports, 2*, 237.

Arnheim, N., Strange, C., & Erlich, H. (1985). Use of pooled DNA samples to detect linkage disequilibrium of polymorphic restriction fragments and human disease: studies of the HLA class II loci. *Proceedings of the National Academy of Sciences of the United States of America, 82*(20), 6970-6974.

Barratt, B. J., Payne, F., Rance, H. E., Nutland, S., Todd, J. A., & Clayton, D. G. (2002). Identification of the sources of error in allele frequency estimations from pooled DNA indicates an optimal experimental design. *Annals of human genetics, 66*(Pt 5-6), 393-405.

Chae, Y. J., Zhang, J., Au, P., Sabbadini, M., Xie, G. X., & Yost, C. S. (2010). Discrete change in volatile anesthetic sensitivity in mice with inactivated tandem pore potassium ion channel TRESK. *Anesthesiology, 113*(6), 1326-1337.

Cutler, D. J., & Jensen, J. D. (2010). To pool, or not to pool? *Genetics, 186*(1), 41-43.

De Fusco, M., Marconi, R., Silvestri, L., Atorino, L., Rampoldi, L., Morgante, L., . . . Casari, G. (2003). Haploinsufficiency of ATP1A2 encoding the Na+/K+ pump alpha2 subunit associated with familial hemiplegic migraine type 2. *Nature genetics, 33*(2), 192-196. doi: 10.1038/ng1081

de Vries, B., Frants, R. R., Ferrari, M. D., & van den Maagdenberg, A. M. (2009). Molecular genetics of migraine. *Human genetics, 126*(1), 115-132.

Denuelle, M., Fabre, N., Payoux, P., Chollet, F., & Geraud, G. (2007). Hypothalamic activation in spontaneous migraine attacks. *Headache, 47*(10), 1418-1426.

Dichgans, M., Freilinger, T., Eckstein, G., Babini, E., Lorenz-Depiereux, B., Biskup, S., . . . Strom, T. M. (2005). Mutation in the neuronal voltage-gated sodium channel SCN1A in familial hemiplegic migraine. *Lancet, 366*(9483), 371-377.

Dobler, T., Springauf, A., Tovornik, S., Weber, M., Schmitt, A., Sedlmeier, R., . . . Doring, F. (2007). TRESK two-pore-domain K+ channels constitute a significant component of background potassium currents in murine dorsal root ganglion neurones. *The Journal of physiology, 585*(Pt 3), 867-879.

Futschik, A., & Schlotterer, C. (2010). The next generation of molecular markers from massively parallel sequencing of pooled DNA samples. *Genetics, 186*(1), 207-218.

Hobert, O. (2010). The impact of whole genome sequencing on model system genetics: get ready for the ride. *Genetics, 184*(2), 317-319.

Huang, D. Y., Yu, B. W., & Fan, Q. W. (2008). Roles of TRESK, a novel two-pore domain K+ channel, in pain pathway and general anesthesia. *Neuroscience bulletin, 24*(3), 166-172.

Joutel, A., Bousser, M. G., Biousse, V., Labauge, P., Chabriat, H., Nibbio, A., . . . et al. (1993). A gene for familial hemiplegic migraine maps to chromosome 19. *Nature genetics, 5*(1), 40-45. doi: 10.1038/ng0993-40

Kersey, P. J., Staines, D. M., Lawson, D., Kulesha, E., Derwent, P., Humphrey, J. C., . . . Birney, E. (2012). Ensembl Genomes: an integrative resource for genome-scale data from non-vertebrate species. *Nucleic acids research, 40*(Database issue), D91-97.

Kim, D. (2005). Physiology and pharmacology of two-pore domain potassium channels. *Current pharmaceutical design, 11*(21), 2717-2736.

Kirkpatrick, B., Armendariz, C. S., Karp, R. M., & Halperin, E. (2007). HAPLOPOOL: improving haplotype frequency estimation through DNA pools and phylogenetic modeling. *Bioinformatics, 23*(22), 3048-3055.

Kuk, A. Y., Xu, J., & Yang, Y. (2010). A study of the efficiency of pooling in haplotype estimation. *Bioinformatics, 26*(20), 2556-2563.

Lafreniere, R. G., Cader, M. Z., Poulin, J. F., Andres-Enguix, I., Simoneau, M., Gupta, N., . . . Rouleau, G. A. (2010). A dominant-negative mutation in the TRESK potassium channel is linked to familial migraine with aura. *Nature medicine, 16*(10), 1157-1160.

Lafreniere, R. G., & Rouleau, G. A. (2011). Migraine: Role of the TRESK two-pore potassium channel. *The international journal of biochemistry & cell biology, 43*(11), 1533-1536.

Lafreniere, R. G., & Rouleau, G. A. (2012). Identification of novel genes involved in migraine. *Headache, 52 Suppl 2*, 107-110.

Liu, C., Au, J. D., Zou, H. L., Cotten, J. F., & Yost, C. S. (2004). Potent activation of the human tandem pore domain K channel TRESK with clinical concentrations of volatile anesthetics. *Anesthesia and analgesia, 99*(6), 1715-1722, table of contents.

Mamanova, L., Coffey, A. J., Scott, C. E., Kozarewa, I., Turner, E. H., Kumar, A., . . . Turner, D. J. (2010). Target-enrichment strategies for next-generation sequencing. *Nature methods, 7*(2), 111-118.

Mardis, E. R. (2011). A decade's perspective on DNA sequencing technology. *Nature, 470*(7333), 198-203.

Mastroianni, N., Bettinelli, A., Bianchetti, M., Colussi, G., De Fusco, M., Sereni, F., . . . Casari, G. (1996). Novel molecular variants of the Na-Cl cotransporter gene are responsible for Gitelman syndrome. *American journal of human genetics, 59*(5), 1019-1026.

Norton, N., Williams, N. M., O'Donovan, M. C., & Owen, M. J. (2004). DNA pooling as a tool for large-scale association studies in complex traits. *Annals of medicine, 36*(2), 146-152.

Noseda, R., Kainz, V., Jakubowski, M., Gooley, J. J., Saper, C. B., Digre, K., & Burstein, R. (2010). A neural mechanism for exacerbation of headache by light. *Nature neuroscience, 13*(2), 239-245.

Oedegaard, K. J., Greenwood, T. A., Johansson, S., Jacobsen, K. K., Halmoy, A., Fasmer, O. B., . . . Kelsoe, J. R. (2010). A genome-wide association study of bipolar disorder and comorbid migraine. *Genes, brain, and behavior, 9*(7), 673-680.

Ophoff, R. A., Terwindt, G. M., Vergouwe, M. N., van Eijk, R., Oefner, P. J., Hoffman, S. M., . . . Frants, R. R. (1996). Familial hemiplegic migraine and episodic ataxia type-2 are caused by mutations in the Ca2+ channel gene CACNL1A4. *Cell, 87*(3), 543-552.

Ottschytsch, N., Raes, A. L., Timmermans, J. P., & Snyders, D. J. (2005). Domain analysis of Kv6.3, an electrically silent channel. *The Journal of physiology, 568*(Pt 3), 737-747.

Robison, K. (2010). Editorial: Second-generation sequencing. *Briefings in bioinformatics, 11*(5), 455-456.

Rozen, S. and Skaletsky, H.J. (2000). Primer3 on the WWW for general users and for biologist programmers. In: Krawetz S, Misener S (eds). *Bioinformatics Methods and Protocols: Methods in Molecular Biology.* Humana Press, Totowa, NJ, pp 365-386.

Russell, M. B., Iselius, L., & Olesen, J. (1995). Inheritance of migraine investigated by complex segregation analysis. *Human genetics, 96*(6), 726-730.

Russell, M. B., & Olesen, J. (1995). Increased familial risk and evidence of genetic factor in migraine. *BMJ, 311*(7004), 541-544.

Sanger, F., Nicklen, S., & Coulson, A. R. (1977). DNA sequencing with chain-terminating inhibitors. *Proceedings of the National Academy of Sciences of the United States of America, 74*(12), 5463-5467.

Sano, Y., Mochizuki, S., Miyake, A., Kitada, C., Inamura, K., Yokoi, H., . . . Furuichi, K. (2002). Molecular cloning and characterization of Kv6.3, a novel modulatory subunit for voltage-gated K(+) channel Kv2.1. *FEBS letters, 512*(1-3), 230-234.

Sham, P., Bader, J. S., Craig, I., O'Donovan, M., & Owen, M. (2002). DNA Pooling: a tool for large-scale association studies. *Nature reviews. Genetics, 3*(11), 862-871.

Shendure, J., & Ji, H. (2008). Next-generation DNA sequencing. *Nature biotechnology, 26*(10), 1135-1145.

Simon, D. B., Nelson-Williams, C., Bia, M. J., Ellison, D., Karet, F. E., Molina, A. M., . . . Lifton, R. P. (1996). Gitelman's variant of Bartter's syndrome, inherited hypokalaemic alkalosis, is caused by mutations in the thiazide-sensitive Na-Cl cotransporter. *Nature genetics, 12*(1), 24-30.

Simon-Sanchez, J., & Singleton, A. (2008). Genome-wide association studies in neurological disorders. *Lancet neurology, 7*(11), 1067-1072.

Solomon, G. D. (1992). Circadian rhythms and migraine. *Cleveland Clinic journal of medicine, 59*(3), 326-329.

Tulleuda, A., Cokic, B., Callejo, G., Saiani, B., Serra, J., & Gasull, X. (2011). TRESK channel contribution to nociceptive sensory neurons excitability: modulation by nerve injury. *Molecular pain, 7*, 30.

van de Ven, R. C., Kaja, S., Plomp, J. J., Frants, R. R., van den Maagdenberg, A. M., & Ferrari, M. D. (2007). Genetic models of migraine. *Archives of neurology, 64*(5), 643-646.

Van Tassell, C. P., Smith, T. P., Matukumalli, L. K., Taylor, J. F., Schnabel, R. D., Lawley, C. T., . . . Sonstegard, T. S. (2008). SNP discovery and allele frequency estimation by deep sequencing of reduced representation libraries. *Nature methods, 5*(3), 247-252.

Yost, C. S. (2003). Update on tandem pore (2P) domain K+ channels.. *Current drug targets, 4*(4), 347-351.

Zhang, H., Yang, H. C., & Yang, Y. (2008). PoooL: an efficient method for estimating haplotype frequencies from large DNA pools. *Bioinformatics, 24*(17), 1942-1948.

Zurak, N. (1997). Role of the suprachiasmatic nucleus in the pathogenesis of migraine attacks. *Cephalalgia : an international journal of headache, 17*(7), 723-728.

Chapter 6

General Discussion

6.1 The role of the NIF visual system in migraine

One of the important functions of the NIF system is to reset our intrinsic circadian clock according to environmental daylight and thus regulate our sleep-awake cycle. Over the past 30 years, a growing body of evidence suggests the existence of a third photoreceptor (ipRGC) that governs the NIF visual functions of the eye. A ground-breaking discovery that supports the close relationship between the NIF visual system and migraine was found recently – the axons of nociceptive signals from the dura overlapped with those coming from ipRGCs of the NIF visual system at the thalamus. Whilst this now prompts questions over the role of the NIF in migraine, human imaging studies of SCN and its response to light in healthy subjects is very limited. My findings (Chapter 2) provided the first neuroimaging evidence showing the distinctly prolonged response of the SCN towards blue light. This is consistent with current understanding of the NIF visual system as more resistant to light adaptation in comparison to the classic IF visual system. Notably, my study was in accordance with the electrophysiological studies in animals and humans. This is important physiologically as longer maintained luminal response underpins circadian entrainment.

In clinical practice, sleep disturbance is a well-known trigger for migraine and is common among migraineurs(Kelman & Rains, 2005). Although the sleep cycle appears to be important in migraine pathophysiology, the underlying mechanism remains elusive. Having established the protocols for imaging and the normal response of the SCN, future studies can test whether the NIF visual system response is abnormal in migraine. Imaging should also be combined with a detailed evaluation of the sleep-wake cycle as well as monitoring of papillary response which are governed by the NIF system. Further investigation of the relationship between the NIF visual system and migraine would also have potential clinical impact. For example, blue-light treatment is now proved to be effective for SAD that is known to be associated with the SCN and circadian system (Glickman, Byrne, Pineda, Hauck, & Brainard, 2006). Whilst some studies suggest that migraineurs may be more sensitive to blue and grey light and the research of the NIF system in migraine has just begun, some commercial products such as glasses that filter blue light have already been launched as a "protection" for light-triggered migraine attacks.

6.2 Cortical hypo-excitability as a protective mechanism between attacks

Given that there has been a continuous debate of whether the brain of migraineurs is more or less excitable, I attempted to examine the interictal cortical excitability of MwA and TRESK migraineurs in Chapter 3. Although the cortical excitability can be assessed by various methods, I chose an approach that focused mainly on light and vision. Light and the visual cortex are considered as important components underlying the mechanism of migraine. CSD, the electrophysiological correlate of aura, originates in the visual cortex and is widely held as the cause of aura and

considered by some to be also the cause of trigeminovascular activation and headache. A strength of the current study is the careful selection of subjects – female, visually triggered migraine with visual aura subjects and patients with the frameshift TRESK mutation.

Contrary to expectation, I found that the response of the visual cortex to light onset as assessed using BOLD, was significantly reduced in migraineurs compared to controls. This is however consistent with other electrophysiological studies indicating that inter-ictal migraine subjects have hypo-excitability or reduced cortical pre-activation, presumably serving as a protective mechanism against the development of attacks(Coppola, Pierelli, & Schoenen, 2009). Interestingly, when exposed to the more flickering checkerboards, the cortical responses normalized. This suggests protective mechanisms are overwhelmed by more aversive visual stimulus, the flickering checkerboard paradigm, and thus a normal cortical response is displayed. This interpretation was further strengthened by the trend showing an inverse correlation between the frequency of migraine attacks and the response evoked by diffuse constant illumination, but not flickering checkerboards.

This interpretation was also supported by the findings in the TRESK migraineurs, which can be regarded as an extreme of the spectrum of migraine. Diffuse constant light elicited lower response in the TRESK MwA in 2 of 3 subjects compared controls. More strikingly, the hypo-excitable state evoked by diffuse light further extended towards the more aversive level of stimulation, i.e. low contrast checkerboards, but not the strongest level of stimulation, i.e. high contrast checkerboards. This suggests that the TRESK MwA with established molecular

evidence of altered neuronal excitability exhibited an even stronger level of pre-activation hypo-excitability. This part of the study is difficult to make firm conclusion as there is a clear limitation from the number of subjects that could undergo brain imaging. Nevertheless, these finding raise interesting hypotheses that future studies might address in animal models.

6.3 Total glutamate, GABA and NAA levels at interictal migraine visual cortex

Glutamate has a proposed involvement in migraine aura by acting on NMDA receptors in the initiation and propagation of CSD. Other lines of evidence including the suppression of CSD by glutamate, the altered glutamate levels in plasma, platelet and CSF, the trigger of migraine by monosodium glutamate as well as the discovery of the receptors in the trigeminovascular complex have also suggested a role of glutamate in migraine. GABA is the main inhibitory metabolite in the brain and was found only detectable in CSF after migraine attacks whereas NAA is a marker of axonal integrity found to be elevated in one ^{1}H-MRS study.

My MRS findings reveal no change in levels of these metabolites at the interictal visual cortex of either TRESK or non-TRESK MwA compared to controls. This suggests that glutaminergic or gabaergic transmission at the visual cortex do not contribute to the aetiology of migraine attacks or in compensatory mechanism. This interpretation was further supported by the lack of correlation between the levels of these metabolites neither with attack frequency nor BOLD response evoked by diffuse constant illumination. An important caveat however is that MRS measures total metabolites and not synaptic metabolites so it remains possible that glutamatergic or

gabaergic transmission are significantly altered. In the TRESK study, photic stimulation reduced the occipital glutamate and NAA in both TRESK MwA and controls. Although the magnitudes of reduction in TRESK MwA was relatively smaller than controls, again, a cautious interpretation of these data is required due to the small sample size.

Since almost all MwA subjects developed headache within 24 hours of the scans, future longitudinal studies with a follow-up MRS scan within 24 hours after the initiation of migraine symptoms would allow a more complete assessment of the role of brain metabolites in migraine. This will provide insights into the potential change of these metabolites during specific phases of migraine such as the onset of aura and headache symptoms. Furthermore, these metabolites can also be measured in a range of brain regions such as the trigeminal nucleus caudalis or the periaqueductal grey matter to clarify differential involvement of these neurotransmitters at different sites.

6.4 Insights into the molecular mechanisms of migraine

I used a DNA pooling method to prepare samples for NGS of four candidate genes that I argued may have significant role in migraine pathogenesis and may alter brain excitability. An overwhelming body of genetic epidemiological evidence indicates the substantial heritability of migraine(Montagna, 2008). I selected four candidate genes based upon pre-existing evidence from genetic or physiological studies. KCNK18 and SLC12A3 appear to be interacting genes in a single migraine family and are predicted to increase neuronal excitability. It is therefore important to establish if variants in the genes are also found in sporadic migraine subjects. There is also preliminary evidence of a genetic association of KCNG4 with migraine. As an accessory ion channel

subunit it is well placed to modulate activity of partner potassium channels and again affect neuronal excitability. Finally OPN4 is the gene encoding the key photopigment of the NIF system – melanopsin. Deleterious variants in OPN4 would therefore have major implications for migraine aetiology.

I found that whilst DNA pooling to prepare samples for NGS was cost-effective, it did require considerable effort to optimize the PCR. I successfully achieved optimization of PCR and the samples are now ready for NGS. It is important to note that whilst variants can now be identified in the migraine group as a whole compared to controls, haplotype information is lost and the reliability of the variant calls is unclear. It will therefore be necessary to undertake custom SNP genotyping, based upon the variants identified through NGS.

6.5 Conclusions

The aim of this thesis was to explore the brain response to light in health controls and migraineurs and to develop resources to understand the genetic underpinnings of such responses. Hence my work began by the assessment of the response of the non-image forming pathway to light of different wavelengths. I found a distinct sustained response of the SCN elicited by blue light in comparison to other wavelengths in healthy controls. I next tested the response of migraineurs and controls to light and visual stimuli and found migraine subjects had hypoexcitable visual cortical responses when presented with diffuse continuous light. The response normalized when exposed to a more aversive stimulus, namely the flickering checkerboards, suggesting that the initial hypo-excitability of visual cortex may represent a protective mechanism. Surprisingly, I found this reduced visual cortical pre-activation was not mediated by alterations in total glutamate or GABA, which were comparable between migraineurs and controls. Finally, to understand how genes may alter brain excitability, I optimized PCR samples from 741 migraineurs and 416 controls in order to sequence four candidate genes including TRESK and OPN4. This body of work therefore establishes a solid foundation for future studies including the response of migraineurs to light of specific wavelength as well as variants in candidate genes that may be involved in modulating visual responsiveness in migraine.

6.6 References

Andres-Enguix, I., Shang, L., Stansfeld, P. J., Morahan, J. M., Sansom, M. S., Lafreniere, R. G., . . . Tucker, S. J. (2012). Functional analysis of missense variants in the TRESK (KCNK18) K channel. *Scientific reports, 2*, 237.

Coppola, G., Pierelli, F., & Schoenen, J. (2009). Habituation and migraine. *Neurobiology of learning and memory, 92*(2), 249-259.

Devoto, M., Lozito, A., Staffa, G., D'Alessandro, R., Sacquegna, T., & Romeo, G. (1986). Segregation analysis of migraine in 128 families. *Cephalalgia : an international journal of headache, 6*(2), 101-105.

Di Lorenzo, C., Grieco, G. S., & Santorelli, F. M. (2012). Migraine headache: a review of the molecular genetics of a common disorder. *The journal of headache and pain, 13*(7), 571-580.

Edgar, D. M., Dement, W. C., & Fuller, C. A. (1993). Effect of SCN lesions on sleep in squirrel monkeys: evidence for opponent processes in sleep-wake regulation. *The Journal of neuroscience : the official journal of the Society for Neuroscience, 13*(3), 1065-1079.

Glickman, G., Byrne, B., Pineda, C., Hauck, W. W., & Brainard, G. C. (2006). Light therapy for seasonal affective disorder with blue narrow-band light-emitting diodes (LEDs). *Biological psychiatry, 59*(6), 502-507.

Kelman, L., & Rains, J. C. (2005). Headache and sleep: examination of sleep patterns and complaints in a large clinical sample of migraineurs. *Headache, 45*(7), 904-910.

Lafreniere, R. G., Cader, M. Z., Poulin, J. F., Andres-Enguix, I., Simoneau, M., Gupta, N., . . . Rouleau, G. A. (2010). A dominant-negative mutation in the TRESK potassium channel is linked to familial migraine with aura. [*Nature medicine, 16*(10), 1157-1160.

Lafreniere, R. G., & Rouleau, G. A. (2011). Migraine: Role of the TRESK two-pore potassium channel. *The international journal of biochemistry & cell biology, 43*(11), 1533-1536.

Montagna, P. (2008). Migraine: a genetic disease? *Neurological sciences : official journal of the Italian Neurological Society and of the Italian Society of Clinical Neurophysiology, 29 Suppl 1*, S47-51.

Moore, R. Y., & Eichler, V. B. (1972). Loss of a circadian adrenal corticosterone rhythm following suprachiasmatic lesions in the rat. *Brain research, 42*(1), 201-206.

Refinetti, R., Kaufman, C. M., & Menaker, M. (1994). Complete suprachiasmatic lesions eliminate circadian rhythmicity of body temperature and locomotor activity in golden hamsters. *Journal of comparative physiology. A, Sensory, neural, and behavioral physiology, 175*(2), 223-232.

Stewart, W. F., Staffa, J., Lipton, R. B., & Ottman, R. (1997). Familial risk of migraine: a population-based study. *Annals of neurology, 41*(2), 166-172.

Wehr, T. A., Duncan, W. C., Jr., Sher, L., Aeschbach, D., Schwartz, P. J., Turner, E. H., . . . Rosenthal, N. E. (2001). A circadian signal of change of season in patients with seasonal affective disorder. *Archives of general psychiatry, 58*(12), 1108-1114.

Weir, G. A., & Cader, M. Z. (2011). New directions in migraine. *BMC medicine, 9*, 116.